INVESTIGATIONS ON COPPER(II) AND COBALT(III) COMPLEXES WITH POTENTIALLY DINUCLEATING LIGANDS

A Thesis
Submitted for the Degree of
Doctor of Philosophy

By
SWAMY MALOTH

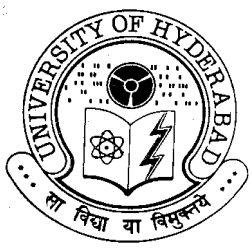

School of Chemistry
University of Hyderabad
Hyderabad 500 046
India

October 2012

To
Amma and Naanna

CONTENTS

STATEMENT i

CERTIFICATE ii

ACKNOWLEDGEMENT iii

CHAPTER 1 Introduction

1.1. Abstract 1

1.2. Overview 1

1.3. Diazine ligands and their modes of coordination 2

1.4. Diamine and aroylhydrazide based Schiff bases and their metal complexes. 11

1.5. About the present investigation 19

1.6. References 21

CHAPTER 2 Copper(II) complexes with 2-[(2-pyridin-2-yl-ethylimino) methyl]-phenol and its substituted derivatives

2.1. Abstract 30

2.2. Introduction 31

2.3. Experimental 32

2.4. Results and discussion 42

2.5. Conclusion 55

2.6. References 56

CHAPTER 3 A tetracopper(II) complex with N,N′-bis(picolinoyl)hydrazine

3.1. Abstract 60

3.2. Introduction 61

3.3. Experimental 62

3.4. Results and discussion 67
3.5. Conclusion 79
3.6. References 80
CHAPTER 4 Dicopper(II) complexes with 2-hydroxy-5-methylbenzene-1,3-dicarbaldehyde bis(benzoylhydrazone)
4.1. Abstract 84
4.2. Introduction 85
4.3. Experimental 86
4.4. Results and discussion 96
4.5. Conclusion 113
4.6. References 114
CHAPTER 5 A Pentacobalt(III) Complex with a paramagnetic Octahedral Metal Center Exhibiting Thermal Spin Transition
5.1. Abstract 118
5.2. Introduction 118
5.3. Experimental 120
5.4. Results and discussion 128
5.5. Conclusion 138
5.6. References 139

List of Publications 142

STATEMENT

I hereby declare that the matter embodied in this thesis entitled "***Investigations on Copper(II) and Cobalt(III) Complexes with Potentially Dinucleating Ligands"*** is the result of the investigations carried out by me in the School of Chemistry, University of Hyderabad, under the supervision of **Prof. Samudranil Pal**.

In keeping the general practice of reporting scientific observations, due acknowledgement has been made wherever the work is described is based on findings of other investigators. Any omission, which might have occurred by oversight or error, is regretted.

October 2012 **Swamy Maloth**

PROF. SAMUDRANIL PAL

SCHOOL OF CHEMISTRY

UNIVERSITY OF HYDERABAD

HYDERABAD-500 046, INDIA

Phone: +91-40-23134756 (office)

Fax: +91-4023012460

Email: spsc@uohyd.ernet.in

---

th October, 2012

CERTIFICATE

Certified that the work embodied in the thesis entitled "***Investigations on Copper(II) and Cobalt(III) Complexes with Potentially Dinucleating Ligands"*** has been carried out by **Mr. Swamy Maloth** under my supervision and the same has not been submitted elsewhere for any degree.

Prof. Samudranil Pal

(Thesis supervisor)

Dean

School of Chemistry

University of Hyderabad

Acknowledgement

I express my deep sense of gratitude and profound respect to my research supervisor ***Prof. Samudranil Pal*** *for his invaluable guidance, support and constant encouragement. I have learned a great deal from him and consider my association with him to be a rewarding experience. Any discussion with him has been always very enriching. He has allowed me to grow as a chemist by letting me work on my own ideas and having me learn from my own mistakes. I am quite lucky to get such a person as my supervisor.*

I would like to thank Prof. M. V. Rajasekharan, Dean, School of Chemistry and former Deans, for their kind co-operation and providing available facilities and infrastructure. I am extremely thankful individually to all the faculty members of the school for their help, cooperation and encouragement at various stages of my stay in the school.

I thank all the non-teaching staff of the school for their cooperation; Dr. Raghavaiah for his efforts for mounting the tiny crystals, Mr. Suresh, Mr. Kumar and Mr. Satyanarayana for collecting EPR and NMR spectra respectively, Mr. B. Rao for LCMS,I thank Prof. Kaul and his students Ugendhar, Uma shanker, Ravi, Pavan, Allu Naik for measurement of variable temperature magnetic data at CIL and Ms. Asia for IR spectra. I am thankful to IGM library for providing excellent collection of books and journals.

Financial assistance from UGC-CAS, New Delhi and CSIR, New Delhi are gratefully acknowledged.

I am extremely thankful to my all teachers for their admirable teaching and priceless suggestions in different stages of my life. I would like to extend my

thanks to all Professors of Kakatiya University and Osmania University, for their excellent guidance and teaching.

Each of the members of our group has helped me to enrich my experience in their own way. I thank all my seniors in the lab: Dr. R. Raveendran, Dr. Anindita Sarkar and Dr. Tulika Ghosh, Nagaraju with whom I am associated at various stages of my stay in the lab. I thank my juniors Balaverdhan Rao, Sathish Kumar and Narendra Babu for their support and in maintaining a lively atmosphere in the lab.

I am very thankful to my entire School, B.Sc. and M.sc. friends, especially Sathish Kumar his care and being there with me through all difficulties.

I am thankful to Miss. Bhargavi for her help in calculation of magnetic data fit.

I thank my friends Dr. Mallesh, M. Shivaprasad (chintu), Naveen kumar (gadda), Madhavachary (Bhai), Sathish kumar, Gangaram, venkanna (potya), Krishnachary, Praveen for their help.

All the research scholars of the school of chemistry have been extremely helpful and I thank them all. Dr. Phani pavan, santhosh, satpal, Ramsuresh, Anji, Ramesh, Srinu, Nagrajuna Reddy, Gangader, yasin, shasi,Sudhir, Viji, S. Ramesh, Ramesh Reddy, Shekar reddy, Sai, Chandu, Lings, Mallikarjun, Venky, Sivaprasad, Madhavachary, Srinivasa reddy, Shashank, Murali, Ravindrababu, Ramana, Naveen, Manojveer, Sheshadri, Venukumar, Anesh, Praveen, Satish, Obaiah, Brijesh, Nandakishore, Kishore, Anand, Nagarjuna, Bharat, Srinu, Kishore, Krishna, Mallesh, Ramuyadav,Bhanu,Ghosh, Sanathan ,Rajesh, Naba, Babu, Mahaboob, Maddileti, Karunakar, Balaswamy, Hariprasad, Gupta,

Thirupathireddy, Ashok, Chandu, Rajagopal Reddy, Dinesh, A……Z are to mention.

My special thanks to my sister Mayuri, brother-in-law Srinivas, brothers Narsimha and Yakub with whom I grew up, for their love, care and affection.

I am at a loss of words to express gratitude to my parents. The tireless support and encouragement of my parents needs a special mention. Without my parents relentless support, love, care and blessing I cannot be whatever I am today. I owe everything to them. I am grateful to all my relatives for their encouragement.

I convey my profound regards to all my teachers who taught me throughout my student life. I end by thanking each and everyone who helped me to reach here.

Swamy Maloth

Chapter 1

Introduction

1.1. Abstract

A brief survey of copper and cobalt coordination chemistry with diazine ligands and Schiff bases derived from diamines and aroylhydrazides is described. With this background the objectives of the present investigation have been stated.

1.2. Overview

1.2.1. Schiff base coordination chemistry: A brief survey

Coordination chemistry was established as an important branch of chemistry due to the outstanding efforts of Alfred Werner in the late 19th century. The influence of organic ligands on electrochemical, magnetic and catalytic properties of coordinated metal ions, when they are coordinated is very impressive.[1] The molecular structures of these coordination complexes and the supramolecular structures supported by various intermolecular noncovalent interactions have drawn considerable attention of the chemists in recent times due to their potential applications as functional materials.

Schiff bases originated by Hugo Schiff in 1864, can easily be prepared by condensation of carbonyl compounds and amines in various conditions. A Schiff base derived from substituted aliphatic, aromatic and hetero aromatic aldehydes and amines can act as a flexidentate ligand.

The importance of Schiff bases as ligands is significant, because of their potential capability to form stable complexes with metal ions,[2] which show excellent catalytic activity at high temperature even in the presence of moisture.

Over the past few years many Schiff base complexes have been used as homogeneous and heterogeneous catalysts with a wide range of applications.[3,4]

Polydentate Schiff bases offer various coordination modes and they can produce supramolecular structures by coordinating various types of metal ions. Such structures are able to provide binding sites and cavities for various cations, anions and organic molecules.[5,6,7]

Bioinorganic and medicinal chemistry aspects of the Schiff base coordination complexes are reflected in their applications as metalloproteins/enzymes mimics, DNA binding and cleavage agents, tools for DNA finger printing, therapeutics, diagnosis agents and biocidals.[8,9,10]

1.3. Diazine ligands and their modes of coordination

The coordination chemistry of diazine based ligands has emerged as a new field over the past few decades. Thompson and others worked especially on open chain diazine (N-N) coordination chemistry.[11,12,13] These ligands can be synthesized by condensing two identical/different aldehydes/ketones/esters with one mole equivalent of hydrazine to yield symmetrical and unsymmetrical systems. The diazine fragments also found in conjugated aromatic heterocyclic polyfunctional systems, such as pyrazole, triazole, pyridazine and pthalazines, but they are rigidly fixed. New (N-N) bridged complexes can readily be produced by using rotationally flexible diazine ligands. These complexes are subjected to a number of studies related to their magnetic and structural features.

Aromatic heterocyclic compounds containing 1, 2-diazine (N–N) fragment are handful (Figur1.1). The examples are pyridazine and its 3,6-disubstituted derivatives (Type 1), phthalazine, condensed phthalazines and their substituted derivatives (Type 2), and other compounds such as pyrazole, triazole, thiadiazole,

tetrazole, indazole, 1,2,4-triazine, 1,2,4,5-tetrazine, and thiadiazepines. Alternatively, the 1, 2-diazine (N–N) moiety also exists as an open-chain entity in some related compounds, e.g., N-substituted-amide hydrazonimidates (Type3), N-substituted-amide hydrazonidates (Type4), N-substituted hydrazides (Type5), N-substituted amidrazones (Type 6), and N-substituted hydrazidates (Type7) and mixed type containing both aromatic and open chain diazines (Type 8).[13k]

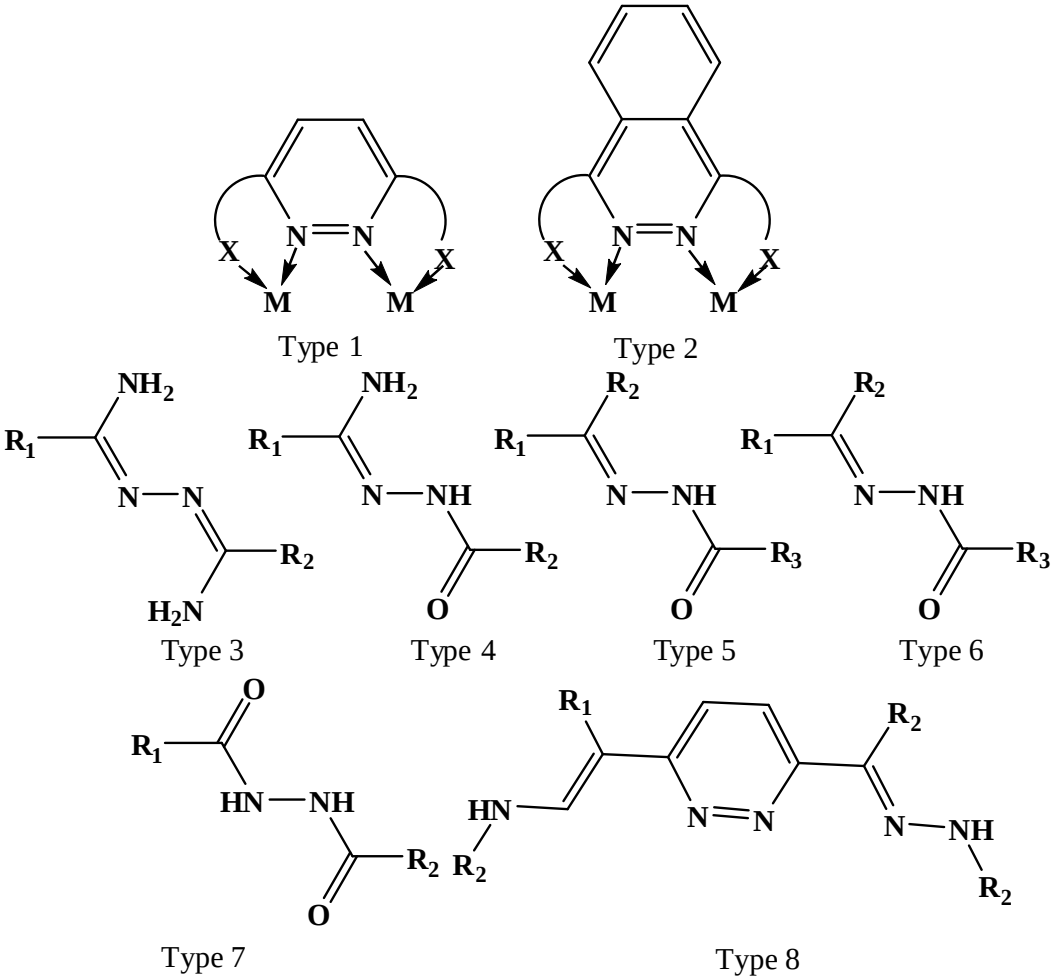

Figure 1.1

Open chain Polydentate diazine ligands based on single N-N bond fragments (Figure 1.2) displays several possible mononucleating, and dinucleating coordination modes due to the flexibility of the ligand around the N-N single bond. Ligands in this class have been found to produce mononuclear, dinuclear, trinuclear and tetranuclear metal complexes Figure 1.3.

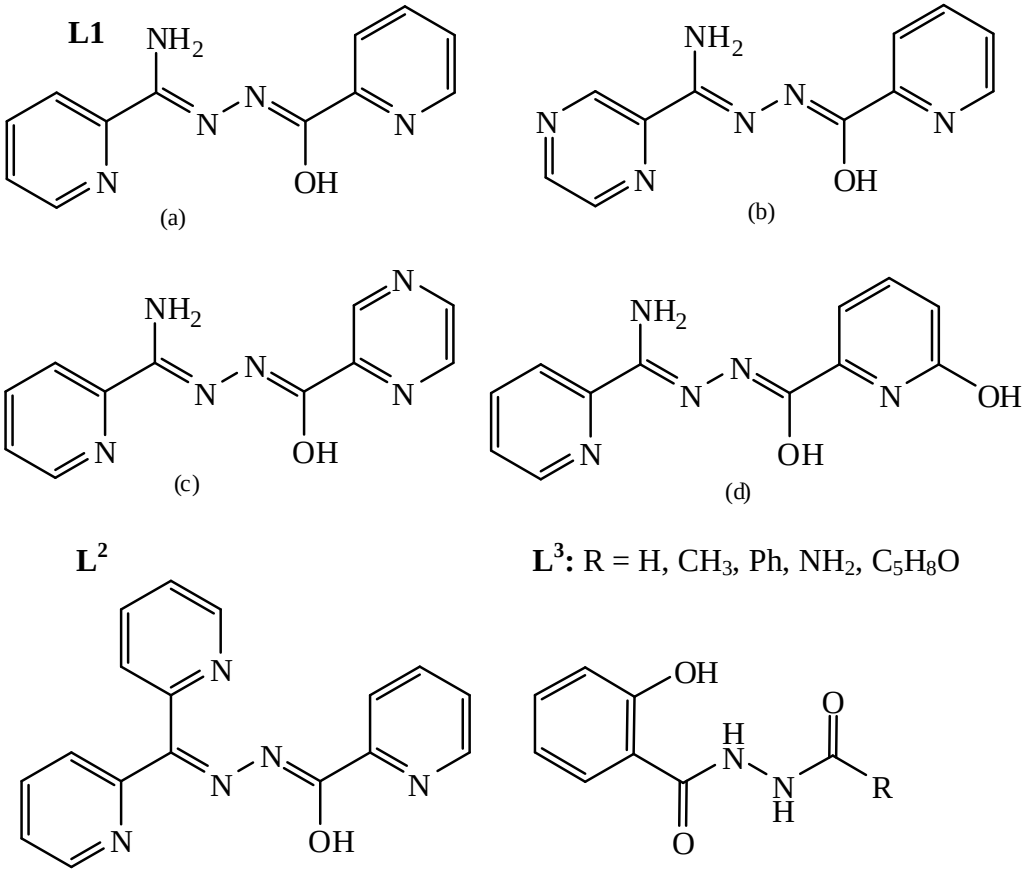

L^4

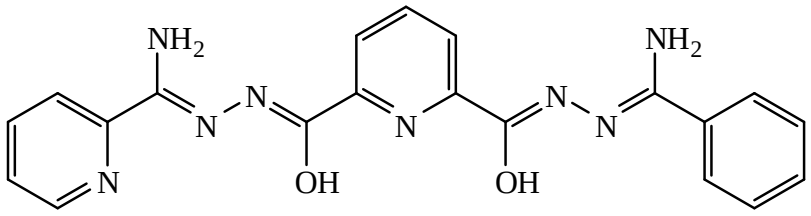

Figure 1.2

Depending on the terminal chelating sites, the diazine based ligands can exhibit various coordination modes, e.g., N,N'-bis(picolinoyl)hydrazine can act as bis-bidentate, bidentate/tridentate[14] or bis-tridentate[15] ligand (Figure 1.3). The ligand having alkoxide group can provide alkoxide bridge in addition to μ(N-N) bridge between the metal ions[17] Figure 1.3.

A: bis (N, O):[16]

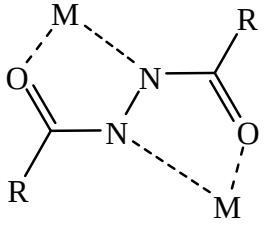

B: bis(N,N',O):

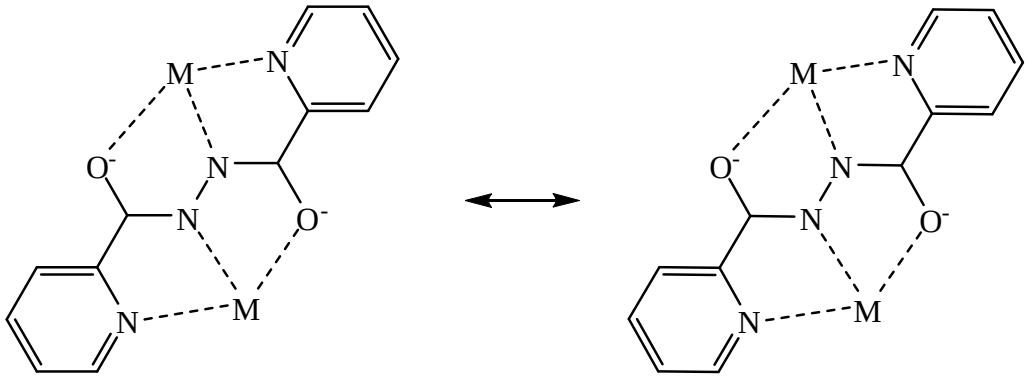

C: bis (N, N'):

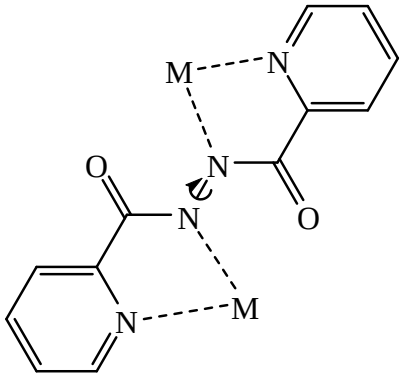

D: (N, N', N, N', O):[14]

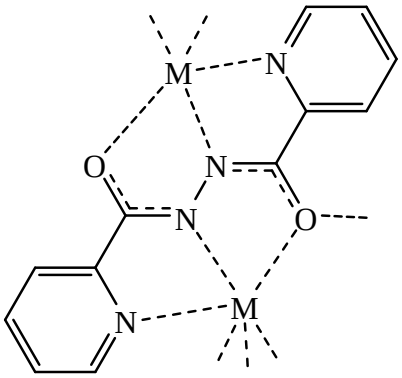

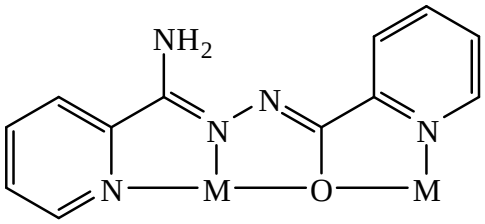

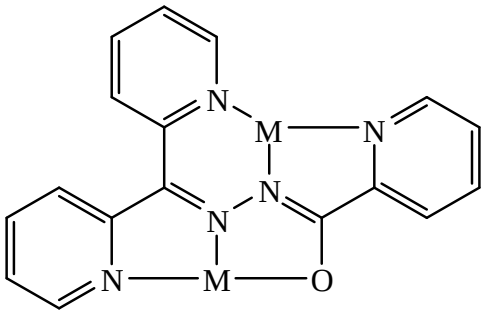

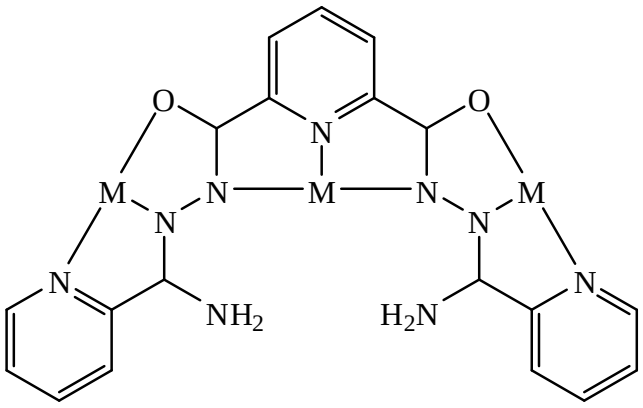

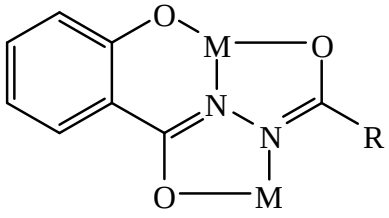

Figure 1.3

1.3.1. Supramolecular species

(a) Self-assembled Grids and clusters

Self assembled supramolecular architectures such as helicates, grids, cylinders and boxes[18,19,20] are produced *via* metal coordination to ligands, utilizing the unique features such as donor site arrangement and high flexibility of polydentate diazines. These species have attracted lot of attention owing to their potential applications in magnetism, molecular selection, ion exchange, catalysis, medicine, electrical conductivity and enantioselectivity.[21]

Polydentate diazines with adjacent coordination pockets allow the metal ions to coordinate in a linear fashion.[22] Methews et al. reported self assembled [2x2], [3x3] and [4x4] square grid complexes[22b,23a] and hetero metallic[25b] grid complexes with flexible diazine ligands and M(II) salts [M = Cu, Ni, Mn and Co].

The [2x2] tetra nuclear Cu(II) square grid structure is shown in Figure 1.4a. The symmetrical arrangement of four Cu(II) centers in a pseudo-square plane is assisted by two pairs of parallel ligands leading to a 2-fold rotational symmetry.

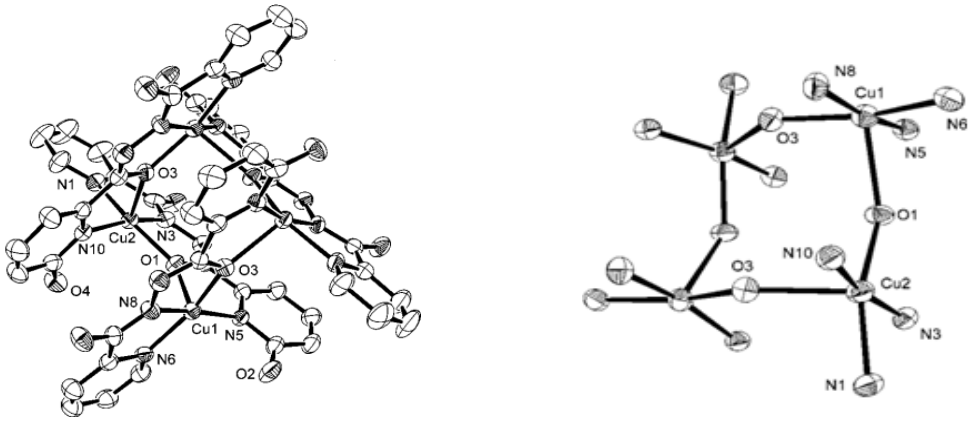

(a) **(b)**

Figure 1.4

(From *Inorg. Chem.*, **1999**, *38*, 5266)

The [3x3] nonacopper(II) (Cu_9O_{12}) square grid[13b] structure is shown in Figure 1.5. The nine Cu(II) centers arranged in a metal pseudo-plane (Figure 1.5b) assisted by two groups of three parallel ligands. The metal pseudo-plane (Cu_9O_{12}) consists four fused (Cu_4O_4) square chambers and each square chamber exists in boat like conformation. The nine Cu(II) centers can be classified into three groups: the central Cu(II) atom having *trans*-N_2O_4, four corner Cu(II) atoms having *cis*-N_4O_2 and four edge centered Cu(II) atoms having *mer*-N_3O_3 pseudo-octahedral coordination spheres.

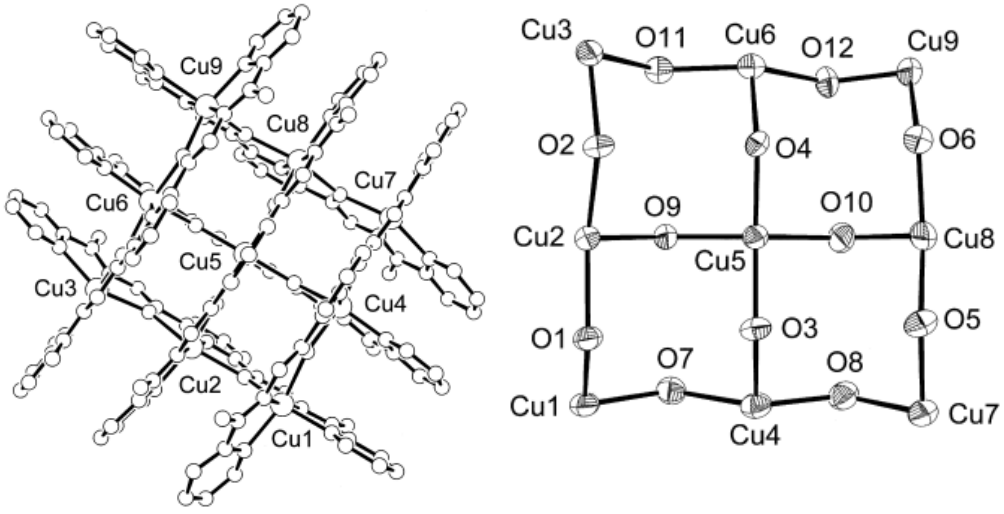

(a) **(b)**

Figure 1.5

(From *Angew. Chem. Int. Ed.*, **2000**, *39*, 17)

In the structure of trinuclear[24] Cu(II) complex shown in Figure 1.6, the three Cu(II) atoms are connected through (N-N) bridges offered by two similar ligands. The central Cu(II) center coordinated with two ligands via a tridentate

N_2O coordination pocket of each ligand in a tetragonally elongated manner. One of the two terminal copper centers bonded to three N-atoms of one ligand has tetragonally distorted octahedral geometry, while another coordinated to three N-atom of the second ligand has distorted square pyramidal geometry.

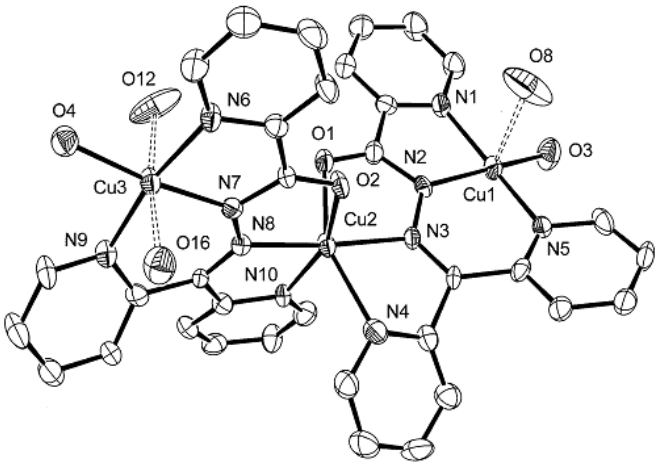

Figure 1.6

(From *J. Chem. Soc., Dalton.Trans.*, **2001**, 1706)

In the pentanuclear homoleptic (Figure 1.7) cobalt(II) cluster the five cobalt(II) centers are arranged at the apexes of a trigonal bipyramid, and each apical cobalt(II) ion connected to each equatorial cobalt ion through an alkoxide bridge from each of the six tetradentate ligands L^1 (Figure 1.2). Each cobalt center of the trigonal bipyramidal core Figure 1.7(b) have pseudo-octahedral geometry. The apical cobalt centers have *fac*-N_3O_3 chromophores and equatorial cobalt centers have *cis*-N_4O_2 chromophores.

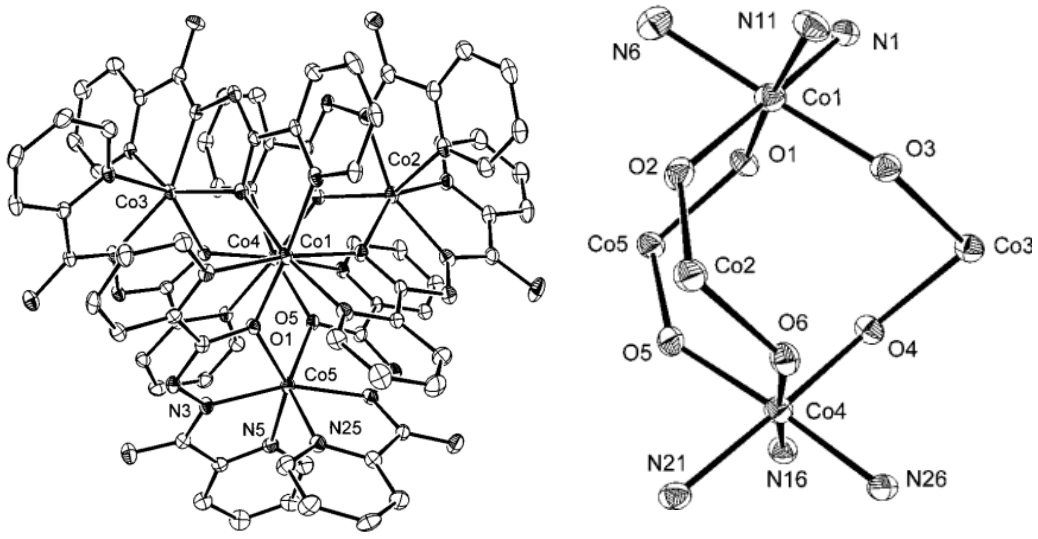

(a) **(b)**

Figure 1.7

(From *Inorg. Chem.*, **2001**, *40*, 17)

(b) Metallacrowns compounds

Metallacrowns are new class of coordination complexes that are analogous to crown ethers in their structure and function.[26] with respect to crown ethers, the metallacrowns consist metal-ligand alternating bridges instead of oxygen atoms and methylene groups. Metallacrowns acquired considerable interest owing to their "host-guest" chemistry, and applications such as chemically modified electrodes, ion-selective separation agents, liquid-crystal precursors and magnetic materials.[26c,d.] Pecoraro and coworkers reported the first metallacrown in 1989, using a metal salt and a bifunctional hydroxamic acid.[26a] Latter a variety of structural types, e.g., [9]metallacrown-3, [12]metallacrown-4, [15]metallacrown-5 and [18]metallacrown-6 were reported with a $[M\text{-}N\text{-}O]_n$ repeat unit.[26b,c,27] The

structure of [30]mettalacrowns-10 is displayed[27] with $[M\text{-}N\text{-}N]_{10}$ repeating units in Figure 1.8. The ligand plays an important role in self assembly of this supramolecular structure by projecting phenolate-O, carbonyl–O and two hydrazide-N donar sites towards unique directions (Figure 1.8).

.

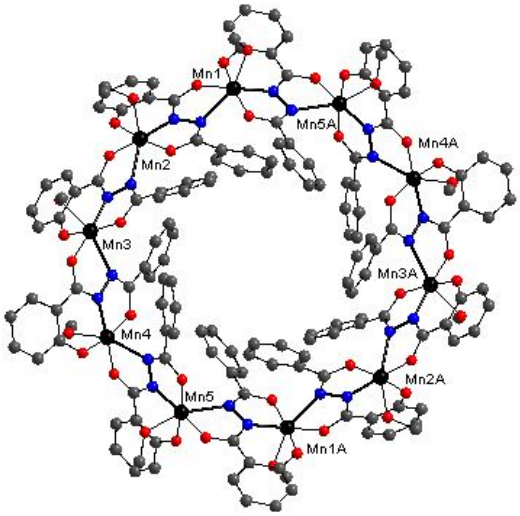

Figure 1.8
(From *Angew.chem.Int.Ed.*, **2001**, *40*, 6)

1.4. Diamine and aroylhydrazide based Schiff bases and their metal complexes.

In the previous section, we have discussed about different types of diazines and their coordinaton modes in their complexes. In this following section, the structures and properties of different diamine and aroylhydrazine based Schiff base complexes are discussed. Mononuclear copper(II) complexes are of interest for their coordination geometry and spectroscopic properties. In dinuclear complexes, two metals are connected through single atomic bridge, such

as endogenous phenoxide and exogenous hydroxide, alkoxide, halide, pseudo halide, carboxylate etc. These complexes are very interesting with respect to their structural features, spin-exchange interactions, as models for metalloenzymes[33] and electron transfer and catalytic[34] activities.

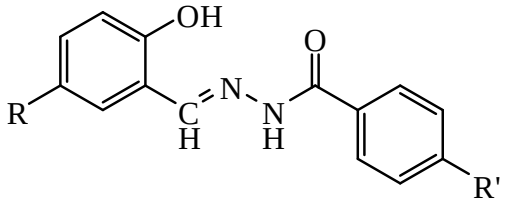

(L^1)

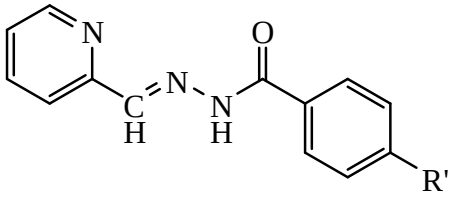

(L^2)

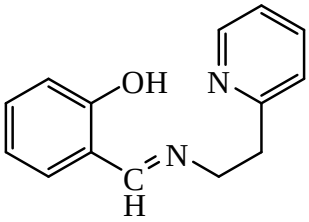

(L^3)

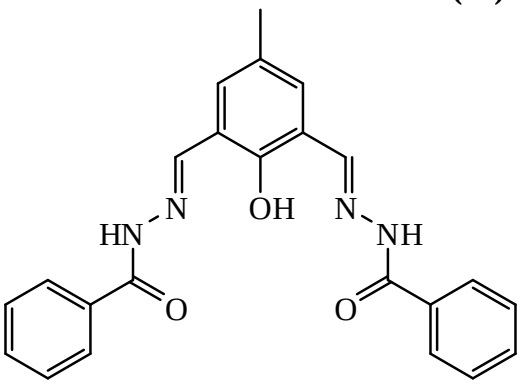

(L^4)

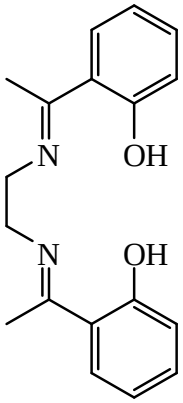

(L^5)

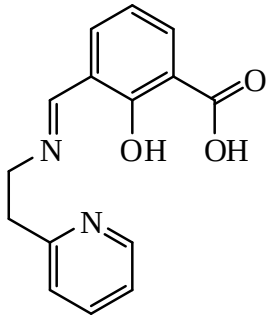

(L^6)

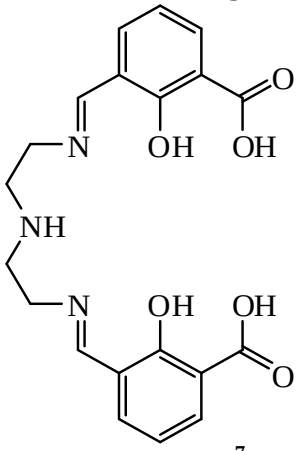

(L^7)

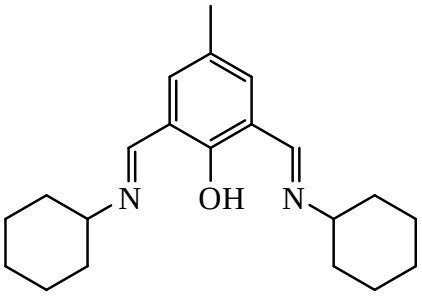

(L^8)

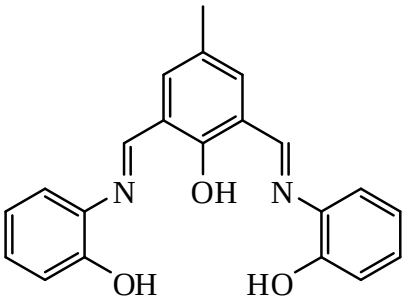

(L^9)

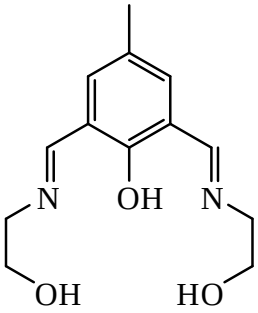

(L^{10})

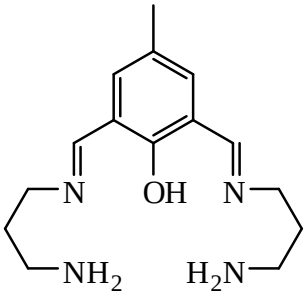

(L^{11})

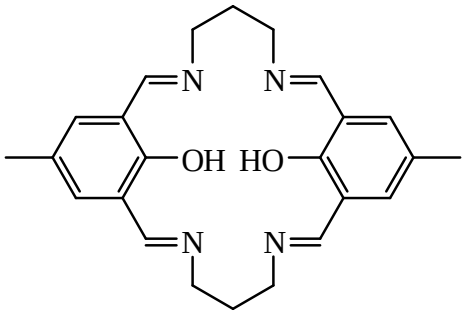

(L^{12})

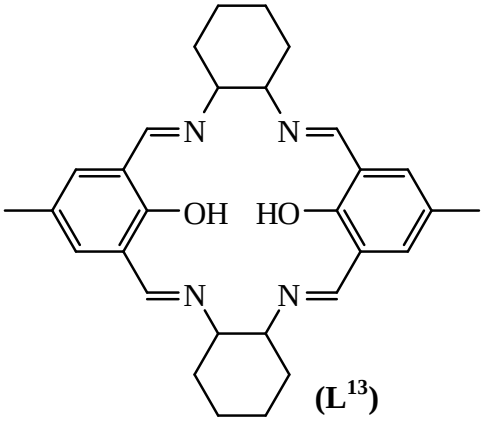

(L^{13})

Figure 1.9

1.4.1. Mononuclear copper(II)

In hexacoordinated copper(II) complexes, the Jahn–Teller distortion causes tetragonal distortion from the octahedral symmetry. Such complexes with different types of ligands are attractive mainly for their coordination geometies and the spectral features.[35,36] Schiff bases (L^2) derived from 2-pyridine-carboxaldehyde and aroylhydrazines provide the pyridine-N, the imine-N and the amide-O as the metal coordinating atoms and form two five-membered chelate rings upon complexation with a metal ion. Two of such deprotonated meridionally spanning ligands produce a neutral copper(II) complex containing a CuN_4O_2 coordination sphere (figure 1.10).

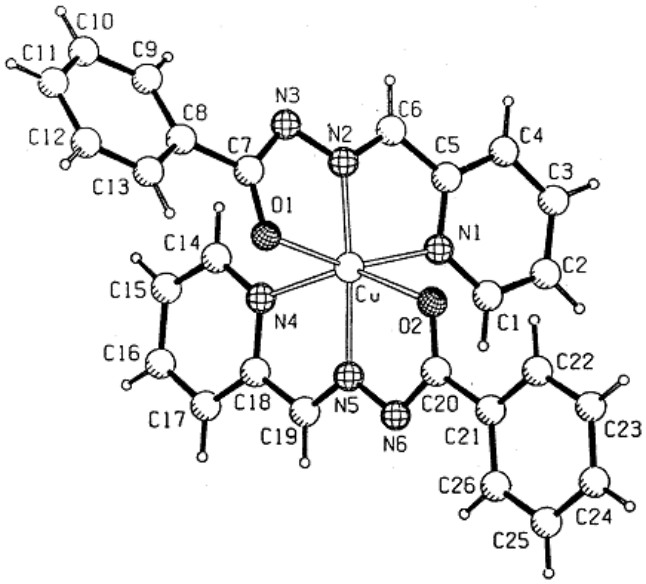

Figure 1.10

(From *Proc. Indian Acad.Sci. (Chem. Sci)*, **2002**, *114*, 417)

1.4.2. Dinuclear copper(II) complex

The ligand (L^1) is planar and binds the metal ion via deprotonated amide-O, imine-N, and two bridging phenolate-O atoms forming a five- and six-membered chelate ring. Each copper(II) centre is square pyramidal. The amide-O, imine-N and the two bridging phenolate-O atoms form the square plane and the axial coordination site of each copper(II) is occupied by the oxygen atom of a water molecule(Figure 1.11).

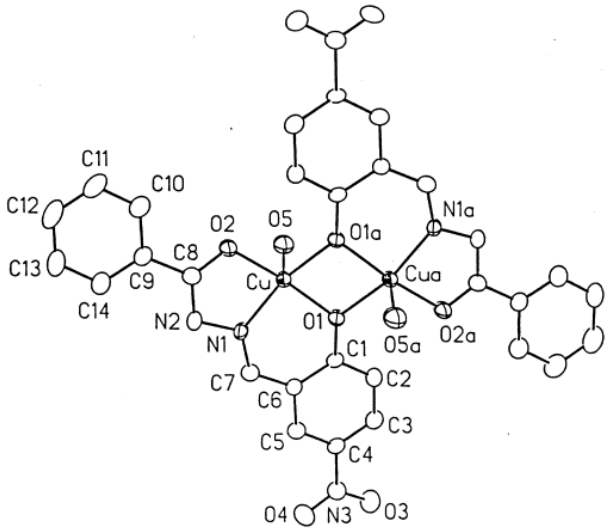

Figure 1.11

(From *Proc. Indian Acad.Sci. (Chem. Sci)*, **2002**, *114*, 417)

1.4.3. Polynuclear complexes.

The chemistry of polynuclear transition metal complexes is a growing subject because of their effective applications as magnetic materials, bioinorganic model compounds and catalysts. The dinuclear phenoxide bridged fragments have been widely studied as chemical models and building units for tetra and polynuclear species with interesting magnetic exchange properties.[32,33,34] Variety of [Cu_4] aggregates such as Cubanes, tetrahedrons, stepped Cubanes, rhomboids and double-Cubanes can be obtained depending on secondary bridging groups.

The tetranulear complex[35] [$Cu_4(\mu\text{-}L^8)_2(\mu_4\text{-}O)(\mu_{1,3}\text{-}O_2CPh)_4$].2$CH_3OH$ (Figure 1.12) consists two Cu_2-phenoxide bridged fragments connected by four benzoate and one μ_4-O^{2-} ancillary ligands. In this complex the ligand (L^8) exists in two numbers in its deprotonated form and offers N_2O coordination sites to distorted tetrahedral Cu_4(μ_4-O) core.

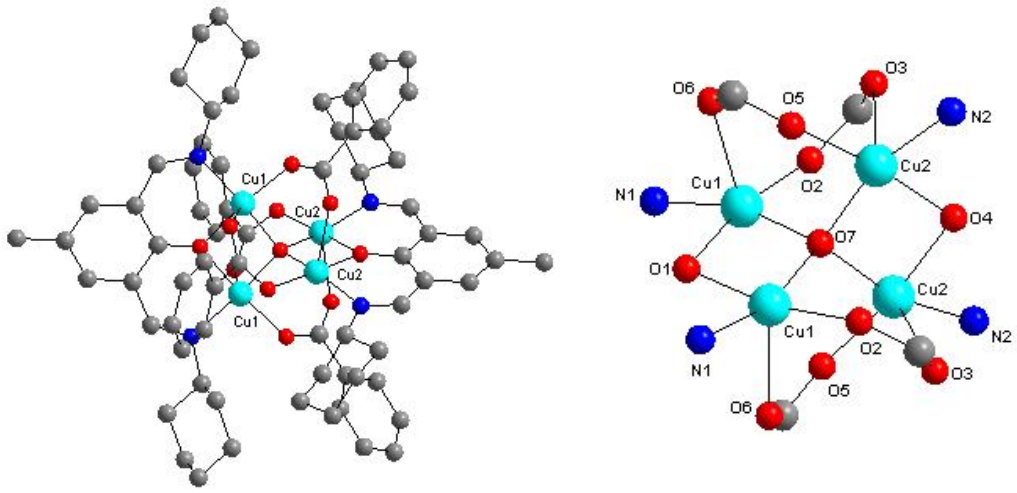

Figure 1.12

(From *Inorg. Chem.*, **2011**, *50*, 3922)

The tetranuclear Co(III) complex[36] $[Co_4(\mu_3\text{-}OMe)_2(\mu\text{-}L^{11})_2(N_3)_2(OH_2)_2](ClO_4)_2.4H_2O\{1.(ClO_4)_2.4H_2O\}$ (Figure 1.13) consists of two Co_2-phenoxide bridged fragments connected by two μ_3-methoxo and two μ_2-alkoxo bridges. The remaining primary and secondary valences are satisfied by two N_3^-, two water ligands and two ClO_4^- ions. In this complex the ligand (L^{11}) exists in two numbers in its deprotonated form and offers N_2O_3 coordination sites to a tetrameric Co(III) cubane.

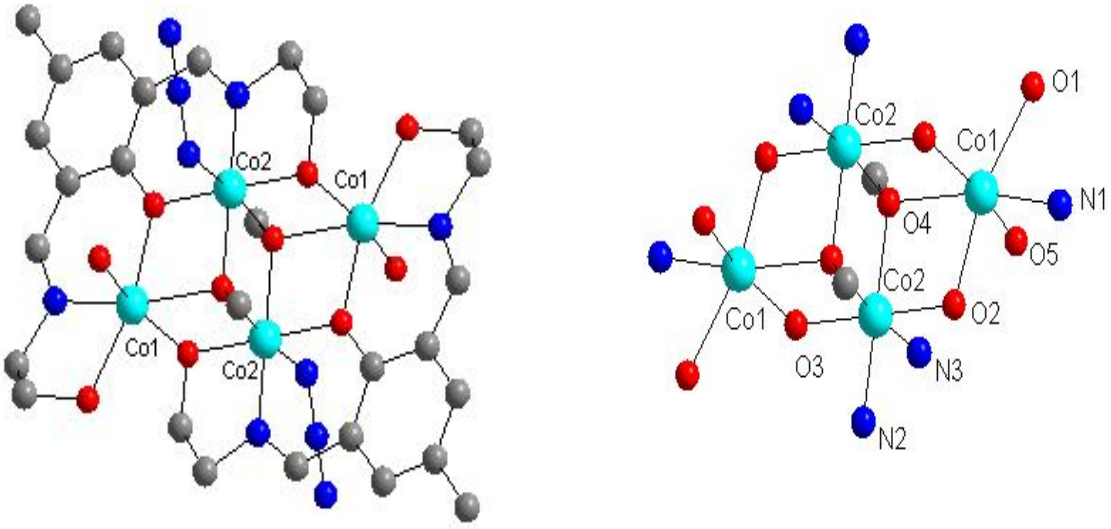

Figure 1.13

(From *Inorganic Chemistry Communications.,* **2007,** *10,* 1202)

1.4.4. Catalytic properties of Cu(II) complexes

The Cu(II) mono, di, tri or multinuclear complexes are known to serve as promising catalysts for oxidative conversions of various hydrocarbons such as cycloalkanes, alkenes, alcohols, aromatic-hydrocarbons, acids etc.[37,38] The oxidized products of cyclohexane such as cyclohexanol, cyclohexanone etc are important with regard to their usage in industrial synthesis of adipic acid, nylon-6,6′, soaps and detergents, rubber chemicals, pesticides etc.[39]

Controlled oxidation of toluene is still a challenging subject to the chemists. The oxidized products of toluene such as benzyl alcohol, benzaldehyde and benzoic acid[40] are industrially very significant. The catalytic activity of Cu-peroxo species with toluene to produce benzaldehyde and benzyl alcohol,[41] has been described in some recent reports.

The tetranuclear complexes containing $\{Cu_4(\mu_4\text{-}O)\}$ core are also catalytically active in the oxidation reactions of cyclohexane and cycloheptane through a Cu-peroxo intermediate.[38b,42,43]

1.4.5. Copper(II) in biology

Copper has been recognized as an essential element in various biological systems, because of its occurrence in a vast number of metalloproteins/enzymes such as hemocyanin, cytochrome-*c* oxidase, Cu-Zn superoxide dismutase, tyrosinase, Catechol oxidase, monoamine oxidase etc., and its role in fulfilling the biological functions such as electron transfer, oxygen carriage, oxidative decorboxylation etc.[44,45,46] In the biological systems the proteins that bind with Cu(II)/(I) ions are known as copper proteins and are classified into three types.

(i) Blue copper proteins in which Cu is coordinated to two histidine nitrogen atoms ,one cystien sulphur atom and one sulphur atom from methionine or oxygen atom from glutamine or the water molecules., e.g., azurin, plastocyanin, laccase, phytocyanins, ceruloplasmin.

(ii) In non-blue copper proteins in which Cu is coordinated to one nitrogen atom from histdine, one sulphur atom from methionine or oxygen atom from carboxylate. Examples are Non-blue oxidases, nitrite reductase, dioxygenase, monooxygenase and Cu-Zn superoxide dismutase.

(iii) Dimeric copper proteins contain dinuclear μ-η_2:η_2 peroxo copper active sites, e.g., haemocyanins, tyrosinase, catechol oxidase etc.

Multicopper complexes are also profound in molecular biology and medicinal biochemistry. These multinuclear Cu(II) species bind double helix DNA preferentially at N_7 guanine site and promotes oxidative/hydrolytic cleavage under physiological conditions.[47,48,49,50,51] Due to the selective binding and efficient DNA cleavage properties, these species have potential to be used in artificial DNA cleaving agents, cancer chemotherapeutics etc.[52,53]

1.5. About the present investigation

In the present investigation, we have explored the coordination chemistry of Cu and Co with 2-[(2-pyridin-2-yl-ethylimino)-methyl]-phenol (HL^1,1), N,N'-bis(picolinoyl)hydrazine (H_2L^2,2), aroylhydrazone of 2-hydroxy-5-methyl-benzene-1,3-dicarbaldehyde bis(benzoylhydrazone) (H_3L^3, 3), and 2,6-bis((3-aminopropylimino)methyl)-4-methylphenola-te) (HL^4, 4). The primary objectives were to synthesize dinuclear complexes and to study their structures and physical properties.

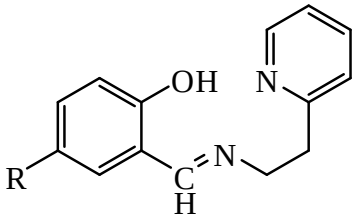

(HL^1, 1)

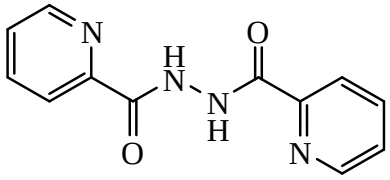

(H_2L^2, 2)

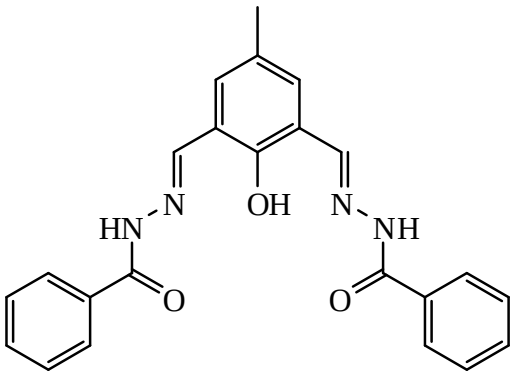

(H_3L^3, 3)

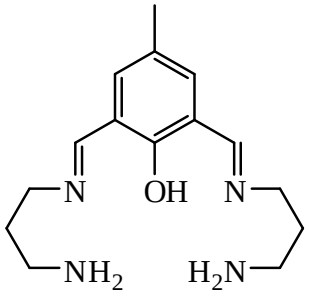

(HL^4, 4)

The complexes have been characterized with the help of elemental analysis, various spectroscopic and electrochemical measurements. Molecular structures of several complexes have been confirmed by X-ray crystallography. Self-assembly patterns via non-covalent intermolecular interactions have been also investigated. In the following chapters, we have described all these observations.

1.6. References

1. L.K. Thompson, *Coord. Chem. Rev*., **2002**, *233*, 193.
2. P. Souza, J.A. Garcia-Vazquez and J.R. Masaguer, *Transition Met. Chem*., **1985**, *10*, 410.
3. H. Naeimi, J. Safari and A. Heidarnezhad, Dyes Pigments. **2007**, *73.* 251.
4. (a) S.J. Lippard and J.M. Berg, Principles of bioinorganic chemistry, University Science books, California, **1994**. (b) R.I. Kureshy, N.H. Khan, S.H.R. Abdi, S.T. Patel and P. Iyer, *J. Mol. Catal*., **1999**, *150*, 175. (c) Y. Aoyama, J.T. Kujisawa, T. Walanawe, A. Toi and H. Ogashi, *J. Am. Chem. Soc*., **1986**, *108*, 943. (d) R.S. Sdrawn, M. Zamakani and J.L. Coho, *J. Am. Chem. Soc*., **1986**, *108*, 3510.
5. N.Dixit, L.Mishra, S.M. Mustafi, K.V.R. Chary and H.Houjou, *Spectrochimica Acta Part A*: *Molecular and Biomolecular Spectroscopy*., **2009**, *73*, 29.
6. N.E. Borisova, M.D. Reshetova and Y.A. Ustynyuk, *Chem. Rev*., **2007**, *46*, 107.
7. W.R. Paryzek, V. Patroniak and J. Lisowski, *Coord. Chem. Rev*., **2005**, *249*, 2156.
8. A.G. Quiroga and C.N. Ranninger, *Coord. Chem. Rev*., **2004**, *248*, 119.
9. L. Yet, *Chem. Rev*., **2003**, *103*, 4283.
10. P. Sengupta, S. Ghosh and T.C.W. Mak, *Polyhedron*., **2001**, *20*, 975.
11. (a) Steel, P. J. *Coord. Chem. Rev*., **1990**, *106*, 227–265. (b) Thompson, L. K.; Chacko, V. T.; Elvidge, J. A.; Lever, A. B. P.; Parish, R. V. *Can. J. Chem.*, **1969**, *47*, 4141–4152. (c) Ball, P. W.; Blake, A. B. *J. Chem. Soc., A* **1969**, 1415–1422. (d) Lever, A. B. P.; Thompson, L. K.; Reiff, W. M. *Inorg. Chem*., **1972**, *11*, 104–109. (e) Thompson, L. K.; Hanson, A. W.; Ramaswamy, B. S. *Inorg. Chem*., **1984**, *23*, 2459–2465. (f) Thompson, L.

K.; Mandal, S. K.; Gabe, E. J.; Charland, J.-P. J. *Chem. Soc., Chem. Commun.*, **1986**, 1537–1539.

12. (a) Woon, T. C.; McDonald, R.; Mandal, S. K.; Thompson, L. K. *J. Chem. Soc., Dalton Trans*., **1986**, 2381–2386. (b) Thompson, L. K.; Lee, F. L.; Gabe, E. J. *Inorg. Chem.*, **1988**, *27*, 39–46. (c) Thompson, L. K.; Mandal, S. K.; Charland, J.-P.; Gabe, E. J. *Can. J. Chem*., **1988**, *66*, 348–354. (d) Chen, L.; Thompson, L. K.; Bridson, J. N. *Can. J. Chem*., **1992**, *70*, 1886–1896. (e) Tandon, S. S.; Thompson, L. K.; Miller, D. O. *J. Chem. Soc., Chem. Commun.*, **1995**, 1907–1908. (f) Brooker, S.; Kelly, R. J.; Sheldrick, G. M. *J. Chem. Soc., Chem. Commun*., **1994**, 487–488. (g) Rosen, W. *Inorg. Chem.*, **1971**, *10*, 1832–1835. (h) Yeager, E. *Electrochim. Acta*., **1984**, *29*, 1527–1537.

13. (a) Xu, Z.; Thompson, L. K.; Miller, D. O. *J. Chem. Soc., Chem. Commun*., **2001**, 1170–1171. (b) Zhao, L.; Xu, Z.; Thompson, L. K.; Heath, S. L.; Miller, D. O.; Ohba, M. *Angew. Chem. Int. Ed. Engl*., **2000**, *39*, 3114–3117. (c) Matthews, C. J.; Xu, Z.; Mandal, S. K.; Thompson, L. K.; Biradha, K.; Poirier, K.; Zaworotko, M. J. *J. Chem. Soc., Chem. Commun*. **1999**, 347–348. (d) Milway, V. A.; Zhao, L.; Abedin, T. A. M.; Thompson, L.K.; Xu, Z. *Polyhedron*., **2003**, *22*, 1271–1279. (e) Xu, Z.; Thompson, L. K.; Miller, D. O. *J. Chem. Soc., Dalton Trans*., **2002**, 2462–2466. (f) Thompson, L. K. *Coord. Chem. Rev*., **2002**, *233–234*, 193–206. (g) Duan, C.-Y.; Liu, Z.-H.; You, L.-Z.; Xue, F.; Mak, T. C. *J. Chem. Soc., Chem. Commun*., **1997**, 381–382. (h) Moubaraki, B.; Murray, K. S.; Ranford, J. D.; Wang, L.; Xu, Y. *J. Chem. Soc., Chem. Commun*., **1998**, 353–354. (i) Xu, Z.; Thompson, L. K.; Miller, D. O.; Ruiz, E.; Alvaez, S. *Inorg. Chem.*, **2003**, *42*, 1107–1111. (j) Liu, S.-L.; Lin, S.; Lin, B. Z.; Lin, C.-C.; Huang, J. Q. *Angew. Chem. Int. Ed. Engl*., **2001**, *40*, 1084–1087.

(k) Z. Xu, L. K. Thompson, *Comprehensive Coordination Chemistry II*, *vol. 1*, 63.

14. (a) X.H. Bu, H. Liu,M. Du, L. Zhang, Y.-M. Guo,M. Shionoya, J. Ribas, *Inorg. Chem*., **2002**, *41*, 1855, and 5634; (b) J.P. Wignacourt, S. Sueur, M. Lagrenée, *Acta Crystallogr., Sect. C*., **1990**, *46*, 394;(c) M. Lagrenée, S. Sueur, J.P. Wignacourt, *Acta Crystallogr., Sect. C*., **1991**, *47*, 1158.
15. S. Patra, T.A. Miller, B. Sarkar, M. Niemeyer, M.D. Ward, G.K. Lahiri, *Inorg. Chem*., **2003**, *42*, 4707.
16. (a) V. Kasack, W. Kaim, H. Binder, J. Jordanov, E. Roth, *Inorg. Chem*., **1995**, *14*, 1924. (b) M. Moscherosch, J.S. Field, W. Kaim, S. Kohlmann, M. Krejcik, *J. Chem. Soc., Dalton Trans*., 1993, 211.
17. (a) Z. Xu, L. K. Thompson, D. O. Miller, *Inorg. Chem*., **1997**, *36*, 3985. (b) L. Zhao, C. J. metthews L. K. Thompson. *J. Chem. Soc., Chem. Com*., **2001**, 1170.
18. J. –M. Lehn, *Supramolecular chemistry – Concepts and perspectives*, **1995**, VCH, Weinheim.
19. (a) M. Elhabiri, R. Scopelliti, J. C. G. Bunzil, C. Piguet, *J. Chem. Soc., Chem. Commun*., **1998**, 2347. (b) G. Rapenne, B. T. Patterson, J. p. Sauvage, F. R. Keene, *J. Chem. Soc., Chem. Commun*., **1999**, 1853. (c) C. Y. Duan, Z. H. Liu, X. Z. You, F. Xue, T. C. W. Mak, *J. Che. Soc., Chem. Commun*., **1997**, 381. (d) D. M. Bassani, J. –M. Lehn, K. Fromm, D. Fenske, *Angew. Chem.,Int. Ed*., **1998**, *37*, 236.
20. (a) C. Piguet, G. Bernardinelli, G. Hopfgartner, *Chem. Rev*., **1997**, *97*, 2005. (b) M. Albrecht, J. Inclusion phenom., *macrocyclic Chem*., **2000**, *36*, 127. (c) A. f. Williams, *pure Appl. Chem*., 1**996**, *68*, 1285. (d) M. Fujita, *Acc. Chem. Res*., **1999**, *32*, 53. (e) B. Olenyuk, A. Fechtenkotter, P.

J. Stang, *J. Chem. Soc., Dalton Trans*., **1998**, 1707. (f) K. N. Raymond, *Acc. Chem. Res*., **1999**, *32*, 975.

21. (a) S. I. Stupp, P. V. Braun, *Science*, **1997**, *277*, 1242. (b) D. Philp, J. F. Stoddart, *Angew. Chem., Int. Ed. Engl*., **1996**, *35*, 1154. (c) Z. Guo, P. J. Sadler, *Angew. Chem., Int. Ed. Engl*., **1999**, *38*, 1512. (d) P. D. Smith, D. A. Slizys, G. N. George, C. G. Young, *J. Am. Chem. Soc*., **2000**, *122*, 2946.

22. (a) L. Zhao, V. Niel, L. K. Thompson, Z. Xu, V. A. Milway, R. G. Harvey, D. O. Miller, C. Wilson, M. Leech, J. A.K. Howard, and S. L. Heath, *J. Chem. Soc., Dalton Trans*., **2004**, 1446. (b) C. J. Matthews, K. Avery, Z. Xu, L. K. Thompson, L. Zhao, D. O. Miller, K. Biradha, K. Poirier, M. J. Zaworotko, C. Wilson, A. E. Goeta, J. A. K. Howard, *Inorg. Chem*., **1999**, *38*, 5271. (c) L. Zhao, C. J. Matthews, L. K. Thompson, S. L. Heath, *J. Chem. Soc., Chem. Commun*., **2000**, 265. (d) O. Waldmann, R. Koch, S. Schromm, P. Müller, L. Zhao, L. K. Thompson, *Chem. Phys. Lett*., **2000**, *332*, 73. (e) L. K. Thompson, L. Zhao, Z. Xu, D. O. Miller, W. M. Reiff, *Inorg. Chem*., **2003**, *42*, 128. (f) L. Zhao, Z. Xu, L. K. Thompson, S. L. Heath, D. O. Miller, M. Ohba, *Angew. Chem., Int. Ed.*, **2000**, *39*, 3114.

23. (a) L. K. Thompson, C. J. Matthews, L. Zhao, Z. Xu, D. O. Miller, C. Wilson, M. Leech, J. A.K. Howard, S. L. Heath, A. G. Whittaker, R. E. P. Winpenny, *J. Solid State Chem*., **2001**, *159*, 308. (b) Z. Xu, L. K. Thompson, C. J. Matthews, D. O. Miller, A. E. Geota, J. A. K. Howard, *Inorg. Chem*., **2001**, *40*, 2446.

24. L. Zhao, L. K. Thompson, Z. Xu, D. O. Miller and D. R. Stirling, *J. Chem. Soc., Dalton Trans*., **2001**, 1706–1710.

25. C. J. Matthews, L. K. Thompson, S. R. Parsons, Z. Xu, D. O. Miller, and S. L. Heath, *Inorg. Chem*., **2001**, *40*, 4448.

26. (a) M. S. Lah, V. L. Pecoraro, J. *Am. Chem. Soc*., **1989**, *111*, 7258. (b) V. L. Pecoraro, A. J. Stemmler, B. R. Gibney, J. J. Bodwin, H. Wang, J. W. Kampf and A. Barwinski, Progress in Inorganic Chemistry, 1997, 45, 83. (c) M. S. Lah, V. L. Pecoraro, *Comments Inorg. Chem*., **1990**, *11*, 59. (d) M. S. Lah, M. L. Kirk, W. Hatfield, V. L. Pecoraro, *J. Chem. Soc*., *Chem. Commun*., **1989**, 1606.

27. (a) B. Kurzak, E. Farkas, T. Glowiak, H. Kozlowski, *J. Chem. Soc., Dalton Trans*., **1991**, 163. (b) B. R.Gibney, A. J. Stemmler, S. Pilotek, J. W. Kampf, V. L. Pecoraro, *Inorg. Chem*., **1993**, *32*, 6008. (c) B. R. Gibney, D. P. Kessissoglou, J. W. Kampf, V. L. Pecoraro, *Inorg. Chem*., **1994**, *33*, 4840. (d) A. J. Stemmler, J. W. Kampf, V. L. Pecoraro, *Inorg. Chem*., **1995**, *34*, 2271. (e) B. R. Gibney, H. Wang, J. W. Kampf, V. L. Pecoraro, *Inorg. Chem*., **1996**, *35*, 6184. (f) J. A. Halfen, J. J. Bodwin, V. L. Pecoraro, *Inorg. Chem*., **1998**, *37*, 5416.

28. (a) D.J. Hodgson, Prog. *Inorg. Chem*., **1975**, *19*, 173. (b) C. Creutz, Prog. *Inorg. Chem*., **1983**, *30*, 1. (c) O. Kahn, Angew. Chem. Intl. Ed. Engl., **1985**, *24*, 834.

29. (a) P. Zanello, S. Tamburini, P.A. Vigato, G.A. Mazzocchin, *Coord. Chem. Rev*., **1987**, *77*, 165. (b) D.E. Fenton, in: A.G. Sykes (Ed.), *Advances in Inorganic and Bio-organic Mechanisms*, Academic, London, **1983**, *2*, 187. (c) L. Que Jr (Ed.), *Metal Clusters in Proteins*, ACS, Washington, DC, **1988**.

30. (a) D. Reinen, C. Friebel, *Struct. Bonding*., **1979**, *37*, 1. (b) B. J. Hathaway, *Struct. Bonding*., **1984**, *57*, 55. (c) M. A. Hitchman, W. Maasicant, J. van der Plas, C. J. Simmons, H. Stratemeier, *J. Am. Chem. Soc*., **1999**, *121*, 1488.

31. (a) G. D. Storrier, S. B. Colbran, D. C. Craig., *J. Chem. Soc., Dalton Trans*., **1997**, 3011. (b) J. V. Folgado, W. Henke, R. Allman, H.

Stratemeier, D. Beltran-Porter, T. Rojo, D. Reinen, *Inorg. Chem.*, **1990**, *29*, 2035; (c) A. J. Blake, A. J. Lavery, M. Schroder, *Acta. Crystallogr. C.*, **1996**, *52*, 37.

32. (a) E. Coronado, K. R. Dunbar, *Inorg. Chem.*, **2009**, *48*, 3293–3295. (b) D.Maiti, J. S. Woertink, R. A. Ghiladi, E. I. Solomon, K. D. Karlin, *Inorg. Chem.*, **2009**, *48*, 8342–8356. (c) A. B. Alemayehu, E. Gonzalez, L. K. Hansen, A.Ghosh, *Inorg. Chem.*, **2009**, *48*, 7794–7799.

33. (a) A. R. Paital, D. Mandal, X. Huang, J. Li, G. Aromí, D. Ray, *Dalton Trans.*, **2009**, 1352–1362. (b) A. R. Paital, V. Bertolasi, G. Aromí,; J. Ribas-Ariñno, D. Ray, *Dalton Trans.*, **2008**, 861–864. (c) A. R. Paital, C. S. Hong, H. C. Kim, D. Ray, *Eur. J. Inorg. Chem.*, **2007**, 1644–1653. (d) P. K. Nanda, G. Aromí, D. Ray, *Chem. Commun.*, **2006**, 3181–3183. (e) A. R. Paital, P. K. Nanda, S. Das, G. Aromí, D. Ray, *Inorg. Chem.*, **2006**, *45*, 505–507. (f) P. K. Nanda, G. Aromí, D. Ray, *Inorg. Chem.*, **2006**, *45*, 3143–3145.40.

34. (a) A. R. Paital, A. -Q. Wu, G. -C. Guo, G. Aromí, J. Ribas-Ariñno, D. Ray, *Inorg. Chem.*, **2007**, *46*, 2947–2949. (b) A. Banerjee, S. Sarkar, D. Chopra, E.Colacio, K. K. Rajak, *Inorg. Chem.*, **2008**, *47*, 4023–4031. (c) A. R. Paital, T. Mitra, D. Ray, W. T. Wong, J. Ribas-Ariñno, J. J. Novoa, J. Ribas, G. Aromí, *Chem. Commun.*, **2005**, 5172–5174.

35. M. Sarkar, R. Clérac, C. Mathonière, N. G. R. Hearns, V. Bertolasi, D. Ray, *Inorg. Chem.*, **2011**, *50*, 3922–3933.

36. D. Mandal, D. Ray, *Inorganic Chemistry Communications.*, **2007**, *10*, 1202–1205.

37. (a) M. Ayala, E. Torres, *Appl. Catal., A*, **2004**, *272*, 1–13. (b) R. L. Lieberman, A. C. Rosenzweig, *Nature.*, **2005**, *434*, 177–182. (c) P. Roy, K.Dhara, M.Manassero, P.Banerjee, *Inorg. Chem. Commun.*, **2008**, *11*,

265–269. (d) P. Gamez, P. G. Aubel, W. L. Driessen, J. Reedijk, *Chem. Soc. Rev*., **2001**, 30, 376–385.

38. (a) A. M.Kirillov, M. N. Kopylovich, M. V. Kirillova, M. Haukka, M. F. C. Guedes da Silva, A. J. L. Pombeiro, *Angew. Chem., Int. Ed*., **2005**, *44*, 4345–4349. (b) P. Roy, K. Dhara,M.Manassero, P. Banerjee, *Eur. J. Inorg. Chem*., **2008**, 4404–4412. (c) M. Thirumavalavan, P. Akilan, M. Kandaswamy, K. Chinnakali, G. S. Kumar, H. K. Fun, *Inorg. Chem*., **2003**, *42*, 3308–3317. (d) A. Panja, S. Goswami, N. Shaikh, P. Roy, M.Manassero, R. J. Butcher, P. Banerjee, *Polyhedron*, **2005**, *24*, 2921–2932. (e) M. Scarpa, F. Vianello, L. Signor, L. Zennaro, A. Rigo, *Inorg. Chem*., **1996**, *35*, 5201–5206.

39. A. E. Shilov, G. B. Shul'pin, *Activation and Catalytic Reactions of Saturated Hydrocarbons in the Presence of Metal Complexes*, Kluwer Academic Publishers, Dordrecht, The Netherlands, 2000.

40. (a) S. Velusamy, T. Punniyamurthy, *Tetrahedron Lett*., **2003**, *44*, 8955–8957. (b) W. B. Li, M. Zhuang, T. C. Xiao, M. L. H. Green, *J. Phys. Chem. B*., **2006**, *110*, 21568–21571.

41. (a) C. Würtele, O. Sander, V. Lutz, T. Waitz, F. Tuczek, S. Schindler, *J. Am. Chem. Soc*., **2009**, *131*, 7544–7545. (b) H. R. Lucas, L. Li, A. A. Narducci Sarjeant, M. A.Vance, E. I. Solomon, K. D. Karlin, J. *Am. Chem. Soc*., **2009**, *131*, 3230–3245.

42. (a) S. Teipel, K. Griesar, W. Haase, B. Krebs, *Inorg. Chem*., **1994**, *33*, 456–464. (b) J. Reim, K. Griesar, W. Haase, B. Krebs, *J. Chem. Soc., Dalton. Trans.*, **1995**, 2649–2656. (c) S. Mukherjee, T. Weyhermüller, E. Bothe, K. Wieghardt, P. Chaudhuri, *Eur. J. Inorg. Chem*., **2003**, 863–875. (d) L. Chen, S. R. Breeze, R. J. Rousseau, S. Wang, L. K. Thompson, *Inorg. Chem*., **1995**, *34*, 454–465. (e) S. R. Breeze, S.Wang, L. Chen, *J. Chem. Soc., Dalton Trans*., **1996**, 1341–1349. (f) J. Reim, R. Werner, W.

Haase, B. Krebs, *Chem.–Eur. J.*, **1998**, *4*, 289–298. (g) M. Bera, W. Tak Wong, G. Aromi, J. Ribas, D. Ray, *Inorg. Chem*., **2004**, *43*, 4787–4789. (h) A. R. Paital, P. K. Nanda, S. Das, G. Aromi, D. Ray, *Inorg. Chem*., **2006**, *45*, 505–507.

43. (a) P. Roy, M. Nandi, M. Manassero, M. Riccó, M. Mazzani, A. Bhaumik, P. Banerjee, *Dalton Trans*., **2009**, 9543–9554. (b) S. Thakurta, P. Roy, R. J. Butcher, M. Salah El Fallah, J. Tercero, E. Garribba, S. Mitra, *Eur. J. Inorg. Chem*., **2009**, 4385–4395.

44. (a) M. C. Linder, C. Goode, *Biochemistry of Copper*; Plenum Press: New York, **1991**. (b) W. Kaim, J. Rall. *Angew. Chem. Int. Ed. Engl*., **1996**, *35*, 43–60.

45. (a) K. Selmeczi, M. Reglier, M. Giorgi, G. Speier, *Coord. Chem. Rev*., **2003**, *245*, 191–201. (b) L. I. Simàndi, Elsevier: Amsterdam, **1991**. (c) Y. Wang, J. L. DuBois, B. Hedman, K. O. Hodgson, T. D. P. Stack, *Science* **1998**, *279*, 537–540. (d) S. Dhar, D. Senapati, P. K. Das, P. Chattopadhyay, M. Nethaji, A. R. Chakravarty. *J. Am. Chem. Soc*., **2003**, *125*, 12118–12124.

46. (a) M. Gonzalez-Alvarez, G. Alzuet, J. Borras, M. Pitie, B. Meunier, J. *Bio. Inorg., Chem*., **2003**, *8*, 644–652. (b) S. Dhar, M. Nethaji,; A. R. Chakravarty, *Inorg. Chim. Acta*., **2005**, *358*, 2437–2444.

47. (a) T. Rasmussen, T. Brittain, B. C. Berks, N. J. Watmough, A. J. Thomson, *Dalton Trans*., *2005*, 3501. (b) T. Tsukihara, H. Aoyama, E. Yamashita, T. Tomizaki, H. Yamaguchi, K. Shinzawa-Itoh, R. Nakashima, R. Yaono, S. Yoshikawa, *Science*., **1996**, *272*, 1136. (c) S. Iwata, C. Ostermeier, B. Ludwig, H. Michel, *Nature*., **1995**, *376*, 660 (d) T. Tsukihara, H. Aoyama, E. Yamashita, T. Tomizaki, H. Yamaguchi, K. Shinzawa-Itoh, R. Nakashima, R. Yaono, S. Yoshikawa, *Science*., **1995**,

269, 1069. (e) M.Wilmanns, P. Lappalainen, M. Kelly, E. Sauer-Eriksson, M. Saraste, *Proc. Natl. Acad. Sci., U. S. A.*, **1995**, *92*, 11955.

48. (a) (a) J. Qian, W. Gu, H. Liu, F. Gao, L. Feng, S. Yan, D. Liao and P. Cheng, *Dalton. Trans.*, **2007**, 1060. (b) R.A.Peralta, A. Neves, A. J. Bortoluzzi, A. d. Anjos, F. R. Xavier, B. Szpoganicz, H. Terenzi, M. C. B. de Oliveira, E. Castellano, G. R. Friedermann, A. S. Mangrich, M. A. Novak, *J. Inorg. Biochem.*, **2006**, *100*, 992. (c) M. C. B. Oliveira, M. S. R. Couto, P. C. Severino, T. Foppa, G. T. S. Martins, B. Szpoganicz, R. A. Peralta, A. Neves, H. Terenzi, *Polyhedron*, **2005**, *24*, 495. (d)M.Gonzâlez-Álvarez, G. Alzuet, J. Borrâs, B. Macías, A. Castíñeiras, *Inorg. Chem.*, **2003**, *42*,2992.

49. D. S. Sigman, A. Mazumder, D. M. Perrin, *Chem. Rev.*, **1993**, *93*, 2295.

50. (a) B. Lippert, *Coord. Chem. Rev.*, **2000**, *200–202*, 487. (b) S. Thayagarajan, N. N. Murthy, Narducci, A. A. Sarjeant, K. D. Karlin, S. E. Rokita, *J. Am. Chem. Soc.*, **2006**, *128*, 710.

51. K. J. Humphreys, K. D. Karlin, S. E. Rokita, *J. Am. Chem. Soc.*, **2002**, *124*, 6009.

52. K. J. Humphreys, K. D. Karlin, S. E. Rokita, *J. Am. Chem. Soc.*, **2002**, *124*, 8055.

53. (a) K. Dhara, J. Ratha, M. Manassero, X.-Y. Wang, S. Gao, P. Banerjee, *J. Inorg. Biochem.*, **2007**, *101*, 95. (b) K. Dhara, S. Karan, J. Ratha, P. Roy, G. Chandra, M. Manassero, B. Mallik, P. Banerjee, *Chem.–Asian J.*, **2007**, *2*, 1091.

Chapter 2

Copper(II) complexes with 2-[(2-pyridin-2-yl-ethylimino)-methyl]-phenol and its substituted derivatives

2.1. Abstract

This chapter describes synthesis, characterization, physical properties and x-ray structures of five new complexes of copper(II) having the general formula [CuL(OAc)], where HL and OAc^- represent the N,N,O-donor 4-*R*-2-[(2-pyridin-2-yl-ethylimino)-methyl]-phenol (*R* = H, Br, NO_2 and OMe) or 5-methoxy-2-[(2-pyridin-2-yl-ethylimino)-methyl]-phenol and acetate, respectively. The solid state effective magnetic moments of the complexes at 298 K are within 1.79–1.97 μ_B. The electronic spectra of these species display a weak ligand-field band within 640–615 nm and several strong charge transfer bands in the range 410–235 nm. The complexes are EPR active. The frozen (120 K) solution spectral parameters are $g_{\|}$ = 2.22–2.23, $A_{\|}$ = 189–191 x 10^{-4} cm^{-1}, $g_{\perp}$ = 2.06–2.07, and $A_{\perp(N)}$ = 10–16 x 10^{-4} cm^{-1}. X-ray structures show that the ligand L^- binds the metal via the phenolate-O, the imine-N and the pyridine-N and forms two six-membered chelate rings. The acetate is bidentate but asymmetric with respect to the Cu–O as well as C–O bond lengths. Only the complex where *R* = Br dimerises due to two reciprocal Cu---Br interactions.

2.2. Introduction

Dicopper(II) complexes are of immense interest primarily for their structural, magnetic and catalytic properties.[1–6] Such complexes are also very appealing for their relevance with respect to several biological processes. Simple chelating ligands having one terminal phenolate-O coordinating site are well known to bridge two copper(II) centres and form dinuclear species where the metal ions are in edge-shared square-based coordination geometry. Very often mononuclear square-planar or square-pyramidal copper(II) complexes form dimeric species in the solid state due to apical-equatorial sharing of metal coordinated atoms. Our group has been working with such copper(II) complexes with Schiff bases and reduced Schiff bases for the past several years.[7–23] In the present chapter, we have explored the coordination chemistry of copper(II) with the O,N,N-donor Schiff bases n-*R*-2-[(2-pyridin-2-yl-ethylimino)-methyl]-phenol (HL, where *R* = H, Br, NO_2 and OCH_3 when n = 4 and *R* = OCH_3, when n = 5). In addition to the synthesis of dicopper(II) species with this Schiff base system, we have also intended to scrutinize the effect of the flexibility of its $-(CH_2)_2C_5H_5N$ arm on the coordination geometry around the metal centre. We have been able to isolate five new ternary copper(II) complexes (**1**–**5**) of the empirical formula [CuL(OAc)] using $Cu(OAc)_2 \cdot H_2O$ as the metal ion source.

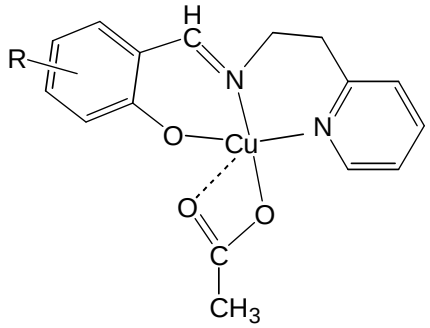

[CuL(OAc)]
1 (R = 4-H), **2** (R = 4-Br), **3** (R = 4-NO_2),
4 (R = 4-OMe), **5** (R = 5-OMe)

Molecular structures of all five complexes have been determined by X-ray crystallography. However, except one none of the complexes form any dimeric species in the solid state. Even the dimer with the bromo substituted ligand is unusual because, the dimerisation is not due to bridging by O-atom but by weak apical coordination of the Br-atom. In the following sections, we have described the synthesis, physical properties and X-ray structures of these complexes.

2.3. Experimental section

2.3.1. Materials

All chemicals and solvents used in this work were of analytical grade available commercially and were used without further purification.

2.3.2. Physical measurements

Elemental (C, H, N) analysis data were obtained with the help of a Thermo Finnigan Flash EA1112 series elemental analyzer. A Digisun DI-909 conductivity meter was used to measure the solution electrical conductivities. Magnetic susceptibilities with powdered samples of the complexes were measured with a Sherwood Scientific balance. Diamagnetic corrections calculated from Pascal's constants[24] were used to obtain the molar paramagnetic susceptibilities. Infrared spectra were recorded by using KBr pellets on a Jasco-5300 FT-IR spectrophotometer. A Cary 100 Bio UV/vis spectrophotometer was used to collect the electronic spectra. X-band EPR measurements were performed on a Jeol JES-FA200 spectrometer.

2.3.3. Synthesis of (acetato)(2-[(2-pyridin-2-yl-ethylimino)-methyl]-phenolato)copper(II) (1)

A methanol solution (15 ml) of $Cu(OAc)_2 \cdot H_2O$ (50 mg, 0.25 mmol) was added to a methanol solution of salicylaldehyde (28 mg, 0.25 mmol) and 2-(2-aminoethyl)pyridine (30 mg, 0.25 mmol). The mixture was stirred in air at room temperature for about ½ h. The initial pale yellow color of the mixture slowly changed to dark green. This green solution was then refluxed for 3 h. After cooling to room temperature it was allowed to evaporate slowly. The complex separated as green crystalline material was collected by filtration, washed with little ice-cold methanol and finally dried in air. The yield was 45 mg (52%).

The other four complexes (**2**–**5**) were synthesized in 65–80% yields using $Cu(OAc)_2 \cdot H_2O$, the appropriate substituted salicylaldehyde and 2-(2-aminoethyl)pyridine in 1:1:1 mole ratio by following the same procedure as described for **1**.

2.3.4. X-ray crystallography

Single crystals of **1**–**5** were collected directly from the products obtained during their syntheses. Except for **3**, the unit cell parameters and the intensity data at 298 K for the other four complexes were obtained on an Oxford Diffraction Xcalibur Gemini single crystal X-ray diffractometer using graphite monochromated Mo Kα radiation (λ = 0.71073 Å). The CrysAlisPro software [25] was used for data collection, reduction and absorption correction. A Bruker-Nonius SMART APEX CCD single crystal diffractometer, equipped with a graphite monochromator and a Mo Kα fine-focus sealed tube (λ = 0.71073 Å) was used to determine the unit cell parameters and data collection for **3** at 100 K.

The SMART software was used for data acquisition and the SAINT-Plus software was used for data extraction.[26] An absorption correction was performed with the help of SADABS program.[27] Each of the five structures was solved by direct methods and refined on F^2 by full-matrix least-squares procedures. All non-hydrogen atoms were refined anisotropically. Hydrogen atoms were included in the structure factor calculation at idealized positions by using a riding model. The SHELX-97[28] programs available in the WinGx[29] package were used for structure solution and refinement. The ORTEX6a[30] and Platon[31] packages were used for molecular graphics. Significant crystallographic data are summarized in Table 2.1 and 2.2. Atomic coordinates and equivalent isotropic displacement parameters for **1-5** are provided in Tables 2.3-2.7, respectively.

Table 2.1. Crystallographic data for **1**, **2** and **3**.

Complex	**1**	**2**	**3**
Chemical formula	$CuC_{16}H_{16}N_2O_3$	$CuC_{16}H_{15}N_2O_3Br$	$CuC_{16}H_{15}N_3O_5$
Formula weight	347.85	426.75	392.85
Crystal system	Monoclinic	Monoclinic	Monoclinic
Space group	*C*2/c	$P2_1/n$	$P2_1/c$
Temperature (K)	298	298	100
a (Å)	21.757(4)	11.420(2)	16.9724(17)
b (Å)	10.479(2)	9.3221(19)	5.9896(6)
c (Å)	18.166(4)	16.630(3)	15.5197(15)
β (^{o})	131.67(3)	109.90(3)	100.767(2)
V (Å^3)	3093.7(11)	1664.7(6)	1549.9(3)
Z	8	4	4
ρ (g cm^3)	1.494	1.703	1.684
μ (mm^{-1})	1.425	3.727	1.444
Reflections collected	5651	6165	13831
Reflections unique	2728	2771	2732
Reflections ($I \geq 2\sigma(I)$)	1894	1655	2590
Parameters	200	209	227
*R*1, *wR*2 ($I \geq 2\sigma(I)$)	0.0408, 0.0936	0.0378, 0.0644	0.0491, 0.0954
*R*1, *wR*2 (all data)	0.0615, 0.0985	0.0750, 0.0690	0.0530, 0.0969
GOF (F^2)	0.926	0.827	1.279
Largest peak & hole (*e* Å^{-3})	0.478, − 0.697	0.351, –0.333	0.415, – 0.441

Table 2.2. Crystallographic data for **4** and **5.**

Complex	**4**	**5**
Chemical formula	$CuC_{17}H_{18}N_2O_4$	$CuC_{17}H_{18}N_2O_4$
Formula weight	377.87	377.87
Crystal system	Monoclinic	Monoclinic
Space group	*C*2/c	$P2_1/n$
Temperature (K)	298	298
a (Å)	20.727(4)	11.1586(11)
b (Å)	12.110(2)	9.5983(7)
c (Å)	16.045(3)	15.6148(15)
β (°)	122.49(3)	103.348(10)
V (Å^3)	3397.0(12)	1627.2(3)
Z	8	4
ρ (g cm^3)	1.478	1.542
μ (mm^{-1})	1.308	1.366
Reflections collected	5471	6302
Reflections unique	2985	2866
Reflections ($I \geq 2\sigma(I)$)	2215	2168
Parameters	219	219
*R*1, *wR*2 ($I \geq 2\sigma(I)$)	0.0637, 0.1748	0.0295, 0.0703
*R*1, *wR*2 (all data)	0.0797, 0.1870	0.0429, 0.0728
GOF (F^2)	1.028	0.955
Largest peak and hole (*e* Å^{-3})	1.018, – 0.953	0.293, –0.365

Table 2.3. Atomic coordinates (x 10^4) and equivalent isotropic displacement parameters ($Å^2$ x 10^3) for **1**.

Atom	x	y	z	U(eq)
Cu	1227(1)	9427(1)	3678(1)	46(1)
O(1)	536(1)	8768(2)	3884(2)	55(1)
O(2)	1115(1)	11160(2)	4011(2)	54(1)
O(3)	2287(2)	10422(2)	5358(2)	68(1)
N(1)	1620(2)	7743(3)	3683(2)	46(1)
N(2)	1392(2)	10144(2)	2797(2)	45(1)
C(1)	331(2)	7580(3)	3837(2)	43(1)
C(2)	-269(2)	7304(3)	3898(2)	54(1)
C(3)	-506(2)	6077(4)	3862(3)	67(1)
C(4)	-164(3)	5061(4)	3750(3)	76(1)
C(5)	421(2)	5297(3)	3694(3)	64(1)
C(6)	684(2)	6541(3)	3732(2)	46(1)
C(7)	1305(2)	6687(3)	3673(2)	50(1)
C(8)	2275(2)	7616(3)	3643(2)	54(1)
C(9)	2623(2)	8883(3)	3677(2)	56(1)
C(10)	1981(2)	9708(3)	2813(2)	50(1)
C(11)	1969(2)	9989(4)	2055(3)	59(1)
C(12)	1329(3)	10717(3)	1271(3)	65(1)
C(13)	746(2)	11188(3)	1284(3)	62(1)
C(14)	794(2)	10884(3)	2048(2)	53(1)
C(15)	1756(2)	11259(3)	4913(3)	49(1)
C(16)	1857(3)	12472(3)	5430(3)	75(1)

Table 2.4. Atomic coordinates (x 10^4) and equivalent isotropic displacement parameters ($Å^2$ x 10^3) for **2**.

Atom	x	y	z	U(eq)
Cu	9943(1)	3625(1)	2457(1)	35(1)
Br	11887(1)	3346(1)	-1342(1)	71(1)
O(1)	9639(2)	2637(3)	1413(2)	49(1)
O(2)	9136(2)	1997(3)	2833(2)	42(1)
O(3)	11148(2)	1821(3)	3523(2)	61(1)
N(1)	11180(3)	4920(4)	2269(2)	37(1)
N(2)	9617(3)	4914(3)	3317(2)	33(1)
C(1)	10131(3)	2857(4)	828(3)	34(1)
C(2)	9754(4)	1993(5)	88(3)	51(1)
C(3)	10255(4)	2152(5)	-548(3)	52(1)
C(4)	11150(4)	3186(5)	-483(3)	47(1)
C(5)	11537(3)	4069(5)	218(3)	41(1)
C(6)	11042(3)	3925(4)	885(3)	30(1)
C(7)	11507(3)	4874(4)	1610(3)	37(1)
C(8)	11789(4)	6002(5)	2924(3)	53(1)
C(9)	11793(3)	5559(5)	3794(3)	46(1)
C(10)	10525(4)	5686(4)	3881(3)	38(1)
C(11)	10267(4)	6549(5)	4469(3)	48(1)
C(12)	9086(5)	6697(5)	4467(3)	58(1)
C(13)	8157(4)	5945(5)	3884(3)	55(1)
C(14)	8449(4)	5053(5)	3327(3)	43(1)
C(15)	10081(4)	1329(5)	3322(3)	45(1)
C(16)	9849(4)	-110(5)	3654(4)	89(2)

Table 2.5. Atomic coordinates (x 10^4) and equivalent isotropic displacement parameters ($Å^2$ x 10^3) for **3**.

Atom	x	y	z	U(eq)
Cu	2881(1)	4805(1)	6781(1)	13(1)
O(1)	2313(2)	3356(4)	5736(2)	16(1)
O(2)	3783(1)	2776(4)	6799(2)	16(1)
O(3)	4130(2)	6086(5)	6384(2)	25(1)
O(4)	-648(2)	4734(5)	2773(2)	26(1)
O(5)	-609(2)	7991(5)	3383(2)	26(1)
N(1)	2218(2)	7447(5)	6584(2)	12(1)
N(2)	3114(2)	5108(5)	8120(2)	15(1)
N(3)	-344(2)	6089(6)	3336(2)	18(1)
C(1)	1696(2)	4064(6)	5194(2)	13(1)
C(2)	1344(2)	2666(6)	4486(2)	18(1)
C(3)	689(2)	3297(6)	3893(2)	17(1)
C(4)	357(2)	5413(6)	3962(2)	15(1)
C(5)	678(2)	6854(6)	4625(2)	15(1)
C(6)	1339(2)	6200(6)	5252(2)	13(1)
C(7)	1637(2)	7794(6)	5937(2)	14(1)
C(8)	2440(2)	9233(6)	7227(2)	16(1)
C(9)	2297(2)	8506(6)	8122(2)	17(1)
C(10)	2859(2)	6773(6)	8586(2)	14(1)
C(11)	3095(2)	6868(6)	9496(2)	19(1)
C(12)	3557(3)	5206(7)	9943(2)	25(1)
C(13)	3794(3)	3462(7)	9468(2)	25(1)
C(14)	3580(2)	3494(6)	8567(3)	21(1)
C(15)	4299(2)	4108(6)	6567(2)	17(1)
C(16)	5112(2)	3158(7)	6554(3)	26(1)

Table 2.6. Atomic coordinates (x 10^4) and equivalent isotropic displacement parameters ($Å^2$ x 10^3) for **4**.

Atom	x	y	z	U(eq)
Cu	108(1)	6900(1)	1292(1)	46(1)
O(1)	-839(2)	6340(2)	1062(2)	52(1)
O(2)	-337(2)	8409(3)	949(3)	60(1)
O(3)	-408(2)	7872(3)	-421(3)	77(1)
O(4)	-1710(2)	2100(3)	1360(3)	78(1)
N(1)	507(2)	5413(3)	1292(2)	42(1)
N(2)	1170(2)	7493(3)	2190(3)	47(1)
C(1)	-1002(2)	5311(4)	1136(3)	42(1)
C(2)	-1700(2)	5075(4)	1095(3)	49(1)
C(3)	-1909(3)	4023(4)	1155(3)	54(1)
C(4)	-1440(3)	3122(4)	1288(4)	54(1)
C(5)	-763(3)	3305(4)	1324(3)	50(1)
C(6)	-537(2)	4400(3)	1255(3)	41(1)
C(7)	184(2)	4507(4)	1295(3)	44(1)
C(8)	1233(2)	5292(4)	1311(3)	51(1)
C(9)	1556(3)	6420(5)	1257(4)	59(1)
C(10)	1769(3)	7134(4)	2138(3)	47(1)
C(11)	2517(3)	7377(4)	2877(4)	62(1)
C(12)	2655(3)	7983(4)	3702(4)	65(2)
C(13)	2039(3)	8352(4)	3738(4)	64(1)
C(14)	1302(3)	8109(4)	2968(4)	56(1)
C(15)	-540(3)	8551(4)	52(4)	56(1)
C(16)	-969(3)	9620(4)	-439(4)	77(2)
C(17)	-1187(4)	1223(5)	1736(7)	110(2)

Table 2.7. Atomic coordinates (x 10^4) and equivalent isotropic displacement parameters (A^2 x 10^3) for **5**.

Atom	x	y	z	U(eq)
Cu	-64(1)	8751(1)	2424(1)	33(1)
O(1)	-222(2)	7799(2)	1338(1)	44(1)
O(2)	-987(2)	7196(2)	2820(1)	41(1)
O(3)	952(2)	6910(2)	3487(1)	53(1)
O(4)	397(2)	6676(2)	-1493(1)	48(1)
N(1)	1181(2)	10045(2)	2206(1)	35(1)
N(2)	-535(2)	9990(2)	3331(1)	38(1)
C(1)	349(2)	8058(2)	712(2)	32(1)
C(2)	54(2)	7249(2)	-59(2)	36(1)
C(3)	639(2)	7429(2)	-730(2)	37(1)
C(4)	1558(2)	8446(3)	-665(2)	46(1)
C(5)	1843(2)	9252(3)	67(2)	43(1)
C(6)	1264(2)	9098(2)	772(2)	34(1)
C(7)	1611(2)	10021(2)	1507(2)	35(1)
C(8)	1678(2)	11137(2)	2864(2)	42(1)
C(9)	1593(2)	10711(3)	3780(2)	43(1)
C(10)	290(2)	10796(2)	3883(2)	37(1)
C(11)	-70(3)	11650(3)	4483(2)	48(1)
C(12)	-1291(3)	11731(3)	4503(2)	56(1)
C(13)	-2130(3)	10937(3)	3936(2)	57(1)
C(14)	-1716(2)	10053(3)	3372(2)	48(1)
C(15)	-136(3)	6518(2)	3315(2)	38(1)
C(16)	-484(3)	5171(3)	3698(2)	62(1)
C(17)	-599(3)	5714(3)	-1621(2)	56(1)

2.4. Results and discussion

2.4.1. Synthesis and characterization

The complexes **1**–**5** have been synthesized in moderate-to-good yields by reacting one mole equivalent each of $Cu(OAc)_2 \cdot H_2O$, the appropriate substituted salicylaldehyde and 2-(2-aminoethyl)pyridine in methanol. Most likely the complexes were formed by template reactions. The elemental analyses data (Table 2.8) are satisfactory with the empirical molecular formula [CuL(OAc)]. All the complexes are electrically non-conducting in dichloromethane solution. The effective magnetic moments of **1**–**5** at room temperature (298 K) are within 1.79–1.97 μ_B (Table 2.8). These values are consistent with the S = ½ spin ground state expected for mononuclear copper(II) complexes.

Table 2.8. Elemental analysis, magnetic moment.[a]

Complex	Found (calc.) (%)			$\mu_{eff.}$
	C	H	N	(μ_B)
1	55.13 (55.25)	4.45 (4.64)	7.92 (8.05)	1.92
2	44.82 (45.03)	3.31 (3.54)	6.34 (6.56)	1.79
3	48.67 (48.92)	3.56 (3.85)	10.48 (10.70)	1.80
4	53.75 (54.03)	4.59 (4.80)	7.23 (7.41)	1.92
5	53.88 (54.03)	4.63 (4.80)	7.29 (7.41)	1.97

[a] In powder phase at 298 K.

2.4.2. Spectroscopic properties

Infrared spectra of the complexes were collected in KBr disks. Spectra of **1** and **3** are shown in Figure 2.1 and 2.2. All the spectra display a strong band within 1616–1635 cm^{-1}. The origin of this band is most likely the C=N stretch of L^-. Two strong bands observed in the ranges 1570–1580 and 1390–1415 cm^{-1} are attributed to the acetate γ_{asym} and γ_{sym} stretches, respectively[32]. Complex **3** shows two additional strong bands at 1605 and 1330 cm^{-1}. The higher energy band is assigned to the γ_{asym} stretch and the lower energy band is assigned to the γ_{sym} stretch of the NO_2 group[33] attached to the salicylaldimine fragment of L^-.

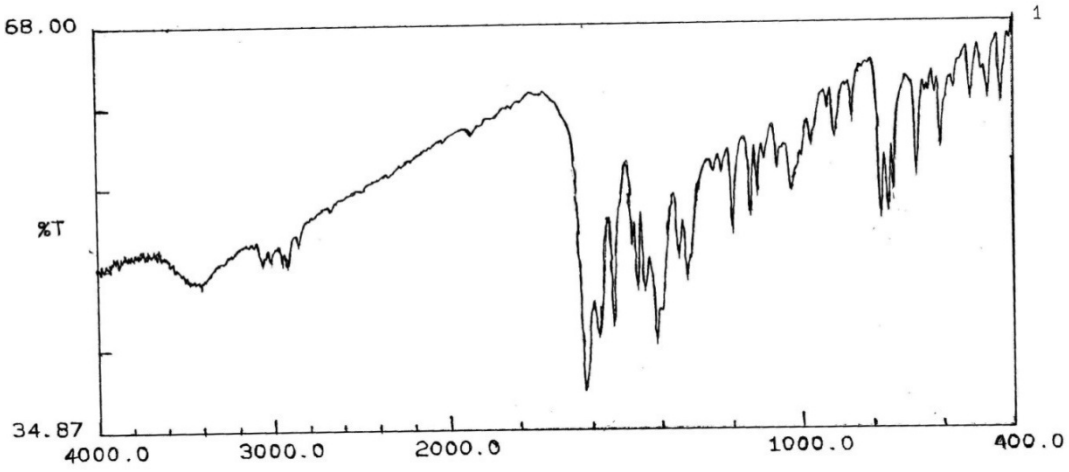

Figure 2.1. Infrared spectrum of **1.**

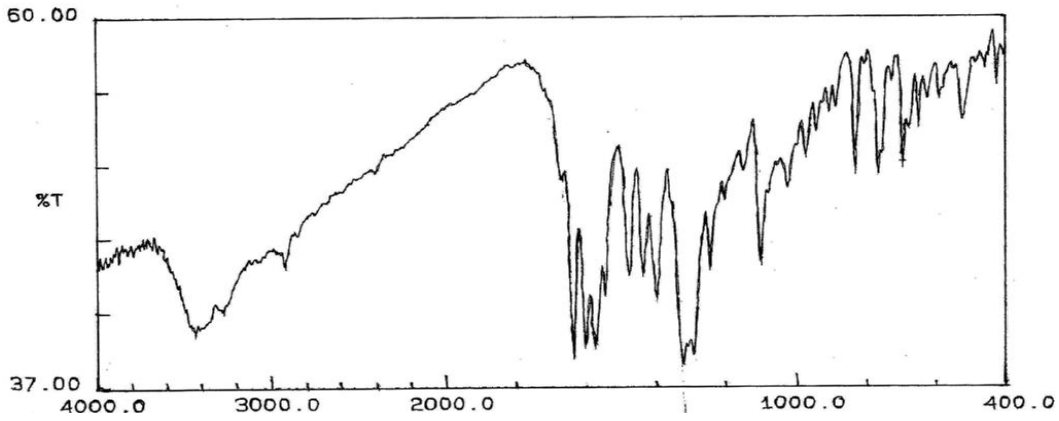

Figure 2.2. Infrared spectrum of **3.**

Dichloromethane solutions **1-5** were used to record the electronic spectra. The spectral data are listed in Table 2.9. The spectra of **3** and **4** are depicted in Figure 2.3. All the five complexes display a weak absorption in the visible region (615–640 nm). Similar weak absorptions for copper(II) complexes are known to be due to d-d transition.[34–41] Below 500 nm except for **3** the spectral profiles of the remaining four complexes are very similar. Complex **3** displays three bands, while the other complexes display four bands in the range 235–410 nm (Table 2.9). These absorptions are most likely due to charge transfer and ligand centred transitions.[38–41]

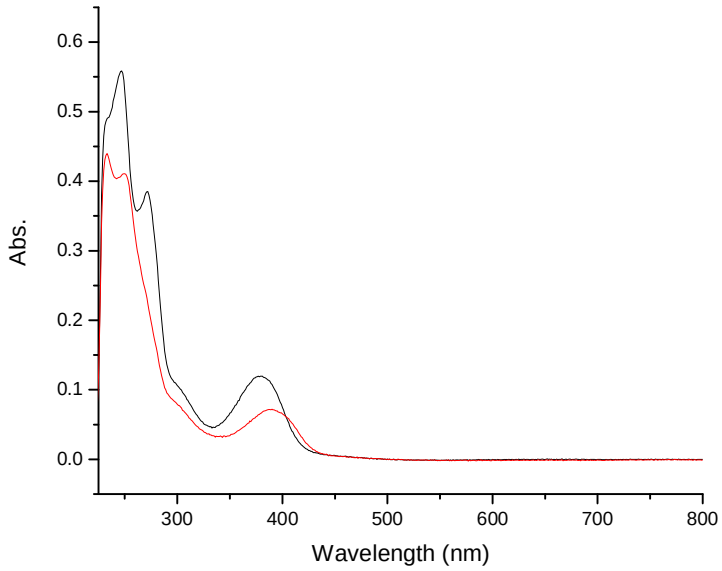

Figure 2.3a. Electronic spectra of **3** and **4** in dichloromethane.

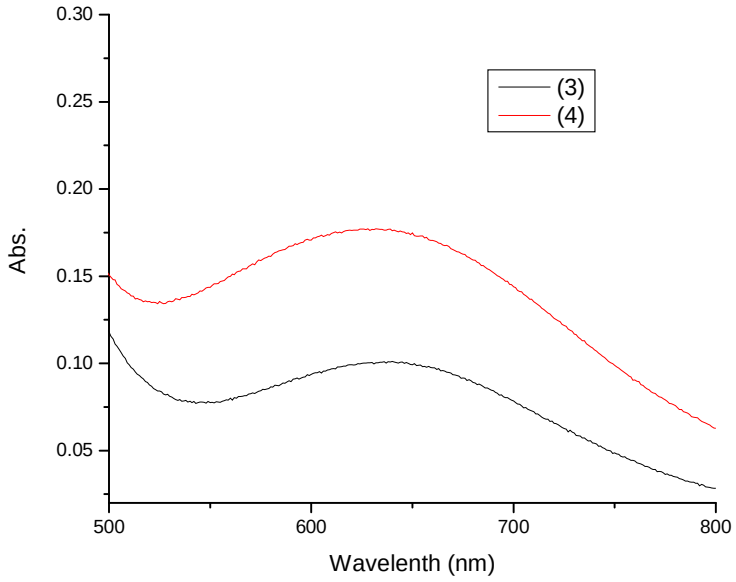

Figure 2.3b. The d-d transitions observed for **3** and **4**.

Table 2.9. Electronic spectral data

Complex	λ_{max} (nm) (10^{-2} x ε (M^{-1} cm^{-1}))
1	634 (2.0), 380 (124), 305[d] (105), 270 (395), 250 (571)
2	630[d] (1.9), 390 (72.8), 307[d] (72.8), 250 (418), 235 (445)
3	615 (202), 365 (334), 255 (445), 237 (376)
4	640[d] (1.5), 410 (90.7), 306[d] (73.4), 254 (386), 235 (381)
5	640 (1.6), 365 (153), 288 (394), 256 (496), 235 (396)

The EPR spectra of **1**–**5** in dichloromethane-toluene (1:1) were collected both at room temperature (298 K) as well as at frozen (120 K) condition. The spectral data are summarized in table 2.10. The spectra of **1** are shown in Figure 2.4. The room temperature spectra display an isotropic signal with clear four line ^{63}Cu (I = 3/2) hyperfine structure. The g_{iso} values are same (2.13) for all the complexes, while the A_{iso} values are within 79–83 x 10^{-4} cm^{-1}. In frozen solution, the complexes display axial spectra expected for copper(II) species having square-based or tetragonally elongated octahedral coordination geometry where the unpaired electron resides in the $d_{x}2_{-y}2$ orbital.[41–43] The $g_{\|}$ (2.22–2.23), $A_{\|}$ (189–191 x 10^{-4} cm^{-1}) and $g_{\perp}$ (2.06–2.07) values for all the complexes are very similar (Table 2.10). The perpendicular component of each spectrum shows a superhyperfine structure due to coupling of the metal unpaired electron with the pyridine-N and the imine-N of L^{-} (Figure 2.4). Out of nine superhyperfine lines expected seven to eight lines are clearly seen for the present series of complexes. The average coupling constants are in the range 10–16 x 10^{-4} cm^{-1}. These values of $A_{\perp(N)}$ are comparable with that reported in literature.[44]

Table 2.10. EPR[c] spectral data.

Complex	$g_{iso}(A_{iso}(cm^{-1}))$	$g_{\parallel}$ ($A_{\parallel}$ (cm^{-1})), $g_{\perp}$ (A_N (cm^{-1}))
1	2.13 (79 x 10-^{4})	2.22 (191 x 10^{-4}), 2.07 (14 x 10^{-4})
2	2.13 (80 x 10^{-4})	2.22 (190 x 10^{-4}), 2.06 (10 x 10^{-4})
3	2.13 (79 x 10^{-4})	2.23 (191 x 10^{-4}), 2.07 (16 x 10^{-4})
4	2.13 (83 x 10^{-4})	2.23 (190 x 10^{-4}), 2.06 (15 x 10^{-4})
5	2.13 (81 x 10^{-4})	2.22 (189 x 10^{-4}), 2.07 (12 x 10^{-4})

[c] In dichloromethane-toluene (1:1) at 120 K

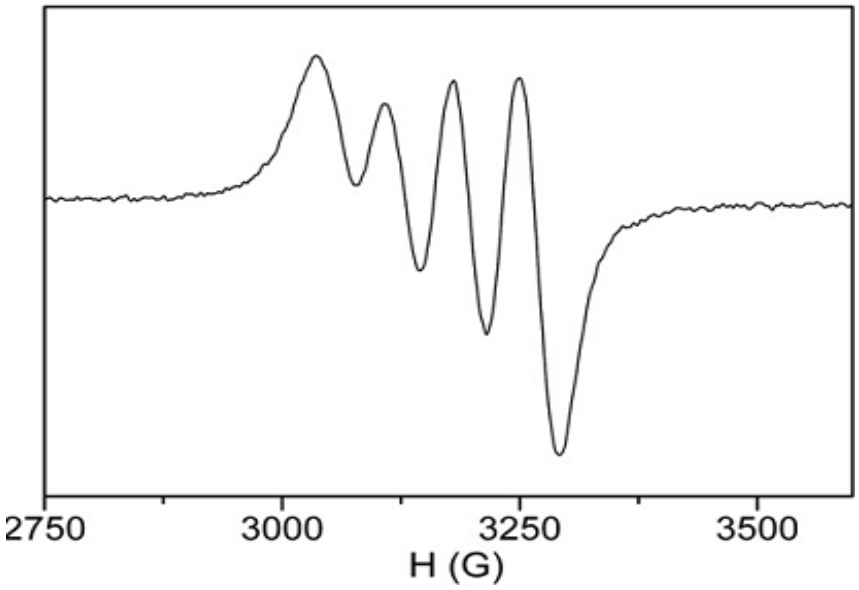

(a)

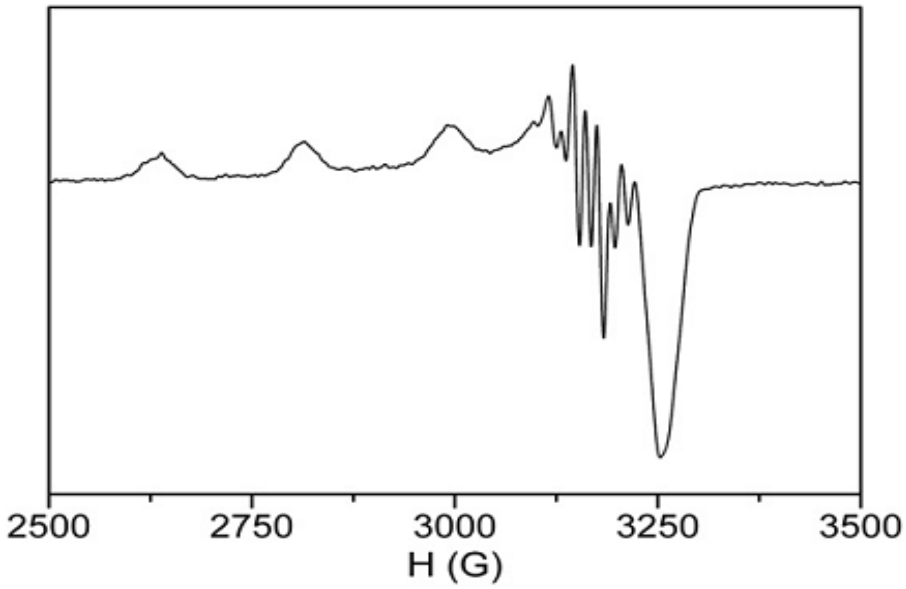

(b)

Figure 2.4. EPR spectra of **1** in dichloromethane–toluene (1:1) at 298 K (a) and at 120 K (b).

2.4.3. Description of molecular structures

Complexes **1**–**5** crystallize in *C*2/c, $P2_1/n$ or $P2_1/c$ space groups. In each case, the asymmetric unit contains a single complex molecule [CuL(OAc)]. Complex **2** is dimeric, while complexes **1**, **3**, **4** and **5** are monomeric. The monomeric structures of **1** and **3**–**5** are illustrated in Figures 2.5 and 2.6.

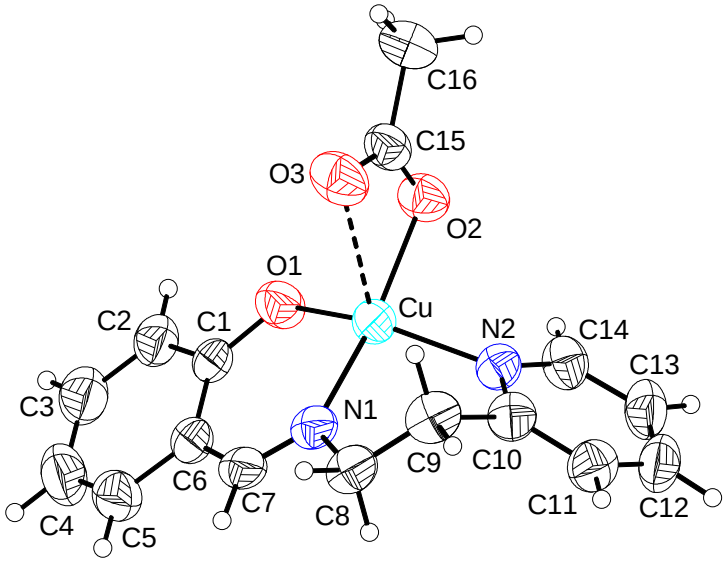

(1)

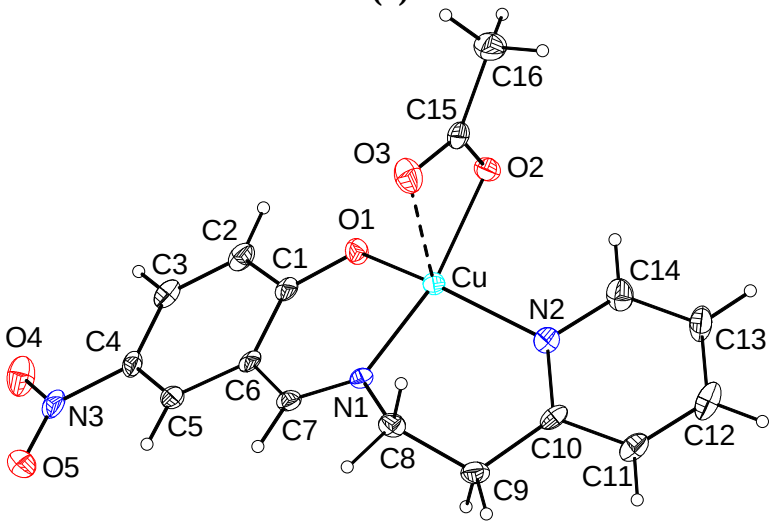

(3)

Figure 2.5. The molecular structures of **1** and **3** with the atom lebeling schemes. All non-hydrogen atoms are represented by their 50% probability thermal ellipsoids.

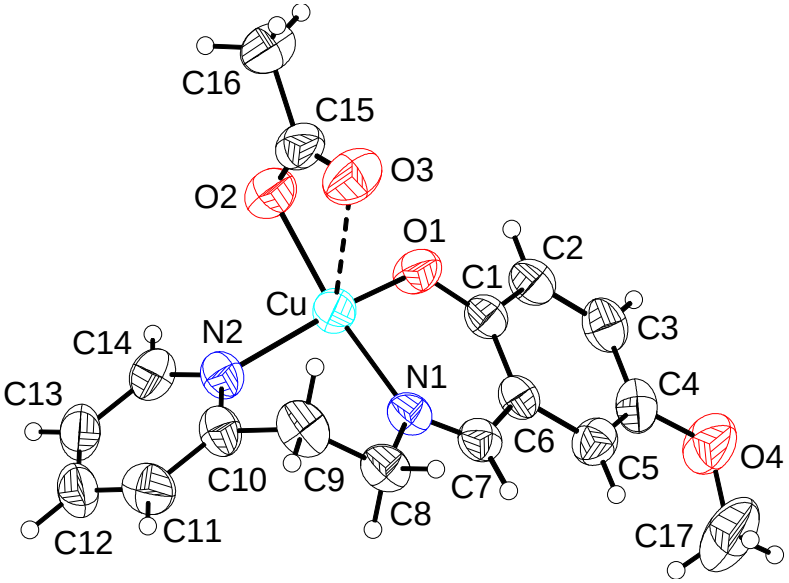

(4)

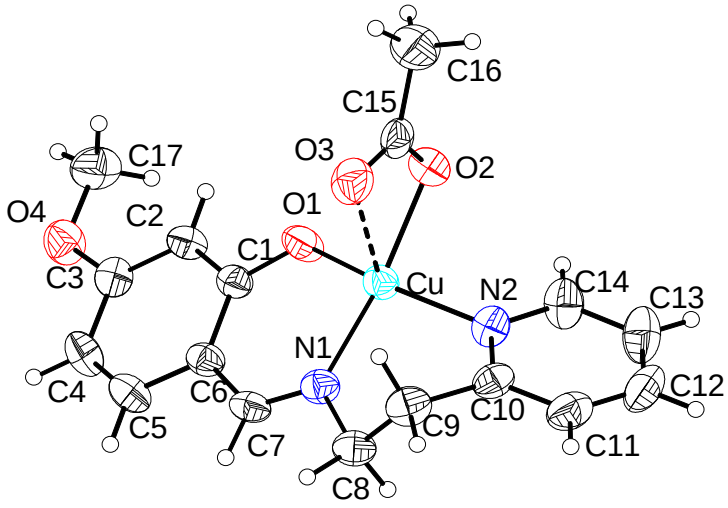

(5)

Figure 2.6. The molecular structures of **4** and **5** with the atom lebeling schemes. All non-hydrogen atoms are represented by their 50% probability thermal ellipsoids.

The structure of the only dimeric species **2** is illustrated in Figure 2.7. Here the metal atoms of two adjacent [CuL(OAc)] units are weakly coordinated in a reciprocal manner to the Br-substituents on the salicylaldimine rings. The Cu---Br distance (3.625(1) Å) in **2** is comparable with the values reported before for such interaction.[45,46] Selected bond parameters of **1**–**5** are listed in Table 2.11. The bond lengths associated with the metal centres are very similar and within the ranges observed for copper(II) complexes having the same coordinating atoms [7–23,40–43,45–51].

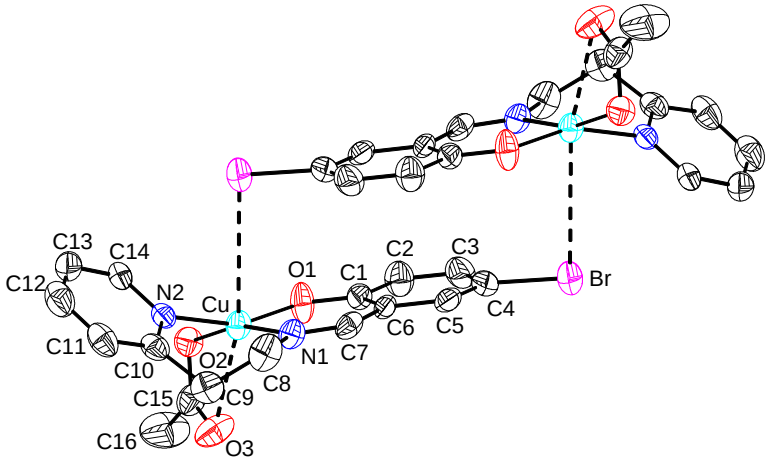

Figure 2.7. The dimeric structure of **2** with the atom lebeling scheme. All non-hydrogen atoms are represented by their 50% probability thermal ellipsoids and hydrogen atoms are omitted for clarity.

Table 2.11. Selected bond parameters for **1**, **2**, **3**, **4** and **5**

Complex	**1**	**2**	**3**	**4**	**5**
Cu–O1	1.904(2)	1.889(3)	1.932(2)	1.916(3)	1.899(2)
Cu–O2	1.980(2)	1.984(3)	1.951(2)	1.986(3)	1.991(2)
Cu–O3	2.523(3)	2.491(3)	2.440(3)	2.632(4)	2.509(2)
Cu–N1	1.957(3)	1.963(3)	1.933(3)	1.981(4)	1.951(2)
Cu–N2	2.004(3)	1.998(3)	2.049(3)	2.008(4)	2.010(2)
C15–O2	1.265(4)	1.270(4)	1.285(4)	1.276(6)	1.259(3)
C15–O3	1.231(4)	1.237(4)	1.240(5)	1.245(6)	1.240(3)
O1–Cu–O2	89.92(10)	87.55(12)	89.94(10)	89.86(13)	88.22(7)
O1–Cu–O3	96.77(10)	102.07(12)	104.43(10)	99.09(13)	100.74(7)
O1–Cu–N1	94.08(11)	94.07(14)	92.87(11)	93.60(13)	94.22(7)
O1–Cu–N2	151.27(11)	158.43(12)	149.69(11)	151.65(14)	158.26(8)
O2–Cu–O3	56.62(9)	57.47(10)	58.84(10)	55.38(14)	56.88(7)
O2–Cu–N1	165.28(10)	163.22(12)	160.78(12)	165.36(15)	166.24(7)
O2–Cu–N2	91.39(11)	90.82(12)	92.20(11)	92.09(15)	89.23(7)
O3–Cu–N1	108.78(10)	105.97(11)	102.11(11)	109.99(13)	109.39(7)
O3–Cu–N2	107.82(10)	95.10(11)	102.48(11)	105.25(14)	95.88(7)
N1–Cu–N2	91.88(12)	93.64(14)	94.89(12)	91.59(15)	93.37(8)
O2–C15–O3	122.5(3)	122.3(4)	121.1(3)	123.5(5)	122.5(2)

Except for few conformational differences the overall structures of [CuL(OAc)] units in **1**–**5** are very similar. In each structure, L^- coordinates the metal centre through the pyridine-N, the imine-N and the phenolate-O atoms forming two six-membered chelate rings. One of the two acetate-O (O2) atoms completes a tetrahedrally distorted N_2O_2 square-plane around the metal centre. The dihedral angle between the planes containing Cu, N1 and O1 and Cu, N2 and O2 reflects this distortion and it spans the range 25.0–35.2°. The distances between the metal centre and the second O-atom (O3) of the acetate are within 2.440(3)–2.632(4) Å (Table 2.11). These distances clearly indicate a relatively weak coordination of O3.[49–51] The strong coordination of O2 and weak coordination of O3 or in other words the asymmetric bidentate coordination of the acetate suggests the localization of the negative charge predominantly on O2. This is also reflected in the longer C15–O2 bond lengths (1.259(3)–1.285(4) Å) than the C15–O3 bond lengths (1.231(4)–1.245(6) Å). Due to this bidentate acetate the metal ion in each of **1**, **3**, **4** and **5** is in irregular N_2O_3 coordination sphere, while that in **2** is in irregular N_2O_3Br coordination sphere (Figures. 2.5, 2.6 and 2.7). The six-membered chelate ring formed by the salicylaldimine fragment of L^- is planar (rms deviation 0.01–0.02 Å) in **2**, **3** and **5**. However, the metal ion is displaced by 0.20(1) and 0.23(1) Å from the plane constituted by the remaining five atoms (rms deviations 0.01 and 0.02 Å) in **1** and **4**, respectively. Thus in these two complexes, the chelate ring is folded along the O1, N1 line and it has a half-chair like conformation. As expected the second six-membered chelate ring formed by the $py(CH_2)_2N=$ arm of L^- is not planar due to the two methylene groups in all five complexes. Interestingly, this chelate ring has a half-chair conformation in **3**, while it is in boat conformation in the other four

complexes (Figure 2.8). In the half-chair conformation, one of the methylene C-atoms (C8) is displaced by 0.71(1) Å from the mean plane constituted by Cu, N1, C9, C10 and N2 (rms deviation 0.02 Å). In contrast, the metal centre and the diagonally opposite methylene C-atom (C9) are displaced from the plane constituted by N1, C8, C10 and N2 (rms deviations 0.01–0.08 Å) in the boat conformation. Here the displacements of Cu and C9 are in the ranges 0.51(1)–0.70(1) and 0.70(1)–0.73(1) Å, respectively.

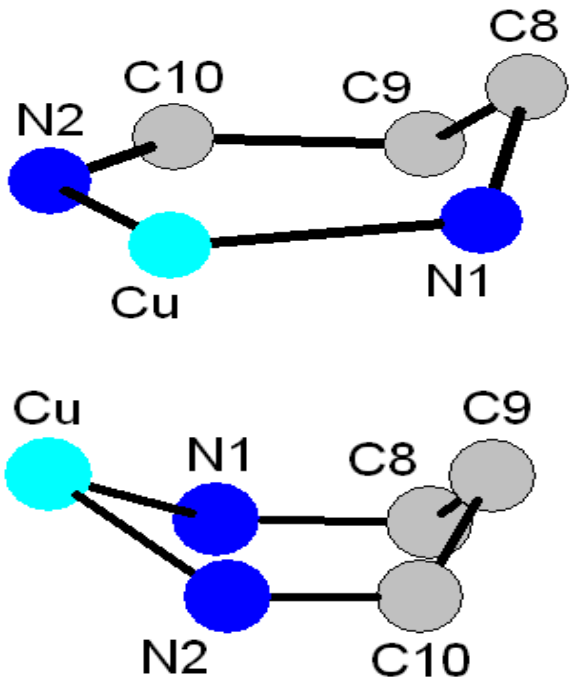

Figure 2.8. The half-chair (top) and the boat (bottom) conformations of the chelate rings formed by the py(CH2)2N= arm of L^- in **3** and **4**, respectively.

Interestingly none of **1**–**5** forms dimer via sharing of either phenolate- or acetate-O atom commonly observed in similar species. One of the reasons for this lack of dimerisation is perhaps some steric barrier for coordination of any of the O-atoms due to the non-planarity of the chelate ring formed by the py$(CH_2)_2$N= arm of L^-. On the other hand, in the case of **2** the Br-atom is at the periphery of the molecule and it is much larger than the O-atom. Consequently it has overcome the steric barrier and it interacts with the metal centre of a neighbouring molecule. As a result, a different type of discrete dimeric units are formed in the solid state via two complementary weak Cu---Br interactions between two adjacent molecules (Figure 2.7).

2.5. Conclusion

In search of dicopper(II) species with n-*R*-2-[(2-pyridin-2-yl-ethylimino)-methyl]-phenol (n = 4, *R* = H, Br, NO_2 and OMe; and n = 5, *R* = OMe) (HL), a series of ternary complexes of formula [CuL(OAc)] has been synthesized. The complexes have been characterized elemental analysis, magnetic susceptibility, various spectroscopic and X-ray crystallographic measurements. The N,N,O-coordinating L^- and the asymmetric bidentate acetate form an irregular N_2O_3 coordination sphere in these complexes. No dimer formation due to sharing of O-atom is observed. However, the complex having the Br-substituent on L^- forms an atypical dimer due to two complementary weak Cu---Br interactions.

2.6. References

1. K. Selmeczi, M. Réglier, M. Giorgi, G. Speier, *Coord. Chem. Rev*., **2003**,*245*, 191-201.
2. C. Liu, M. Wang, T. Zhang, H. Sun, *Coord. Chem. Rev*., **2004**, *248*, 147-168.
3. L. M. Mirica, X. Ottenwaelder, T.D.P. Stack, *Chem. Rev*., **2004**, *104*, 1013-1046.
4. E.J. O'Neil, B.D. Smith, *Coord. Chem. Rev*., **2006**, *250*, 3068-3080.
5. P.A. Vigato, S. Tamburini, *Coord. Chem. Rev*., **2008**, *252*, 1871-1995.
6. D. Venegas-Yazigi, D. Aravena, E. Spodine, E. Ruiz,S. Alvarez, *Coord.Chem. Rev*., **2010**, *254*, 2086-2095.
7. N.R. Sangeetha, K. Baradi, R. Gupta, C.K. Pal, V. Manivannan, S. Pal, *Polyhedron*., **1999**, *18*, 1425-1429.
8. N.R. Sangeetha, S. Pal, *J. Chem. Crystallogr*., **1999**, *29*, 287-293.
9. N.R. Sangeetha, S.N. Pal, C.E. Anson, A.K. Powell, S. Pal, *Inorg. Chem. Commun*., **2000**, *3*, 415-419.
10. N.R. Sangeetha, S. Pal, *Polyhedron*., **2000**, *19*, 1593-1600.
11. N.R. Sangeetha, S.N. Pal, S. Pal, *Polyhedron*., **2000**, *19*, 2713-2717.
12. S. Pal, *Proc. Indian Acad. Sci., (Chem. Sci*.)., **2002**, *114*, 417-430.
13. S. Das, G.P. Muthukumaragopal, S.N. Pal, S. Pal, *New J. Chem*., **2003**, *27*, 1102-1107.
14. S. Das, S. Pal, *J. Mol. Struct*., **2005**, *741*, 183-192.
15. S. Das, S. Pal, *J. Mol. Struct*., **2005**, *753*, 68-79.
16. V.K. Muppidi, P.S. Zacharias, S. Pal, *Chem. Commun*., **2005**, 2515-2517.

17. V.K. Muppidi, S. Pal, *Eur. J. Inorg. Chem*., **2006**, 2871-2877.
18. S. Das, S.A. Maloor, S.N. Pal, S. Pal, *Cryst. Growth .Des.*, **2006**, *6*, 2103-2108.
19. V.K. Muppidi, P.S. Zacharias, S. Pal, *J. Solid State Chem*., **2007**, *180*, 132-137.
20. V.K. Muppidi, S. Das, P. Raghavaiah, S. Pal, *Inorg. Chem. Commun*., **2007**, *10*, 234-238.
21. S. Pal, *Rev. Inorg. Chem*., **2009**, *29*, 111-130.
22. T. Ghosh, A. Mukhopadhyay, K.S.C. Dargaiah, S. Pal, *Struct. Chem*., **2010**, *21*, 147-152.
23. S. Das, S. Pal, *Inorg. Chim. Acta* in press.
24. W.E. Hatfield, in: E.A. Boudreaux, L.N. Mulay (Eds.), *Theory and Applications of Molecular Paramagnetism*, *Wiley*, New York, **1976**, p. 491.
25. CrysAlisPro version 1.171.33, Oxford Diffraction Ltd., Abingdon, Oxfordshire, UK, **2007**.
26. SMART version 5.630 and SAINT-plus version 6.45, Bruker-Nonius Analytical X-ray Systems Inc., Madison, WI, USA, **2003**.
27. G.M. Sheldrick, SADABS, Program for Area Detector Absorption Correction, University of Göttingen, Göttingen, Germany, **1997**.
28. G.M. Sheldrick, XHELX-97, Structure Determination Software, University of Göttingen, Göttingen, Germany, **1997**.
29. L.J. Farrugia, *J. Appl. Crystallogr*., **1999**, *32*, 837-838.
30. P. McArdle, *J. Appl. Crystallogr*., **1995**, *28*, 65.

31. A.L. Spek, Platon, A Multipurpose Crystallographic Tool, Utrecht University, Utrecht, The Netherlands, **2002**.
32. K. Nakamoto, *Infrared and Raman Spectra of Inorganic and Coordination Compounds*, Wiley, New York, **1986**, p. 233.
33. W. Kemp, *Organic Spectroscopy, Macmillan, Hampshire*, **1987**, pp. 47-52.
34. A. Taha, *Spectrochim. Acta A.*, **2003**, *59*, 1611-1620.
35. A.K. Patra, M. Nethaji, A.R. Chakravarty, *Dalton Trans*., **2005**, 2798-2804.
36. P. Sarmah, R.K. Barman, P. Purkayastha, S.J. Bora, P. Phukan, B.K. Das, *Indian J. Chem. Sect. A.*, **2009**, *48*, 637-644.
37. Z. Lu, T. Ladrak, O. Roubeau, J. van der Toorn, S. J. Teat, C. Massera, P. Gamez, J. Reedijk, *Dalton Trans*., **2009**, 3559-3570.
38. A. Paulovicova, U. El-Ayaan, K. Shibayama, T. Morita, Y. Fukuda, *Eur. J. Inorg. Chem.*, **2001**, 2641-2646.
39. R. Srivastava, T.H. Bennur, D. Srinivas, *J. Mol. Catal. A*., **2005**, *226*, 199-205.
40. C.P. Pradeep, P.S. Zacharias, S.K. Das, *J. Chem. Sci*., **2005**, *117*, 133-137.
41 T. Ghosh, S. Das, S. Pal, *Polyhedron*, **2010**, *29*, 3074-3080.
42. A.W. Addison, T.N. Rao, J. Reedijk, J. van Rijn, G.C. Verschoor, *J. Chem. Soc., Dalton Trans*., **1984**, 1349-1356.
43. Z. Liu, C. Duan, Y. Tian, X. You, *Inorg. Chem*., **1996**, *35*, 2253-2258.
44. P. Basu, *J. Chem. Ed*., **2001**, *78*, 666-669.
45. H. Endres, I.N. Andoseh, M. Mégnamisi-Belombé, *Acta Cryst. B.*, **1981**, *37*, 681-683.

46. J. Costamagna, F. Caruso, J. Vargas, V. Manriquez, *Inorg. Chim. Acta*., **1998**, *267*, 151-158.

47. R. Kannappan, S. Tanase, I. Mutikainen, U. Turpeinen, J. Reedijk, *Inorg. Chim. Acta*., **2005**, *358*, 383-388.

48. W.-K. Dong, J.-H. Feng, L. Xu, J.-K. Zhong, Y.-X. Sun, X.-Q. Yang, *Indian J. Chem.*, **2008**, *47A*, 1343-1347.

49. B.K. Koo, *Bull. Korean Chem. Soc*., **2001**, *22*, 113-116.

50. C.R. Warthen, C.J. Carrano, *J. Inorg. Biochem*., **2003**, *94*, 197-199.

51. L. Gomes, J.N. Low, M.A.D.C. Valente, C. Freire, B. Castro, *Acta Cryst. C*., **2007**, *63*, m293-m296.

Chapter 3

A tetracopper(II) complex with N,N′-bis(picolinoyl)hydrazine

3.1. Abstract

Synthesis, physical properties and X-ray structure of a hydrated tetranuclear copper(II) complex $[Cu_4(\mu\text{-diph})_2(\mu\text{-}H_2O)_2(O_2CCH_3)_4(H_2O)_2]\cdot 4H_2O$ with N,N′-bis(picolinoyl)hydrazine (H_2diph) are reported. The centrosymmetric complex has two types of copper(II) centres with distorted square-pyramidal N_2O_3 coordination spheres. The dinucleating *trans* planar $diph^{2-}$ ligands are parallel to each other and act as N_2O-donor to one metal centre and N_2-donor to the other metal centre. The complex has a rectangular $\{Cu_4(\mu\text{-N–N})_2(\mu\text{-}OH_2)_2\}$ core with Cu···Cu distances as 4.834(1) and 3.762(1) Å. Solid state as well as solution electronic spectra show several transitions in the wavelength range 700 to 280 nm. The room temperature (298 K) solid state magnetic moment is 3.55 μ_B. The powder EPR spectra at 298 and 130 K are very similar and axial ($g_{\|}$ = 2.25 and $g_{\perp}$ = 2.08) in character.

3.2. Introduction

Helical coordination complexes have attracted considerable attention during the last two decades not only due to their elegant structures but also for their applications in a wide variety of research areas such as enantioselective processes, optical and magnetic phenomena, probing of DNA structure and understanding helical self-organization processes.[1–14] Ligands with two or more chelating sites connected by flexible spacers are very efficient in assembling helical coordination complexes. The most simple in this family of ligands are the diazines where two chelating sites are linked by an N–N single bond. These ligands are well known to form dinuclear helical complexes due to the twisting of the chelating sites along the N–N single bond. The crystal structures and properties of several such complexes with the neutral N_4-donor Schiff base N,N′-bis(picolinylidene)hydrazine or its derivatives,[15–24] the dianionic deprotonated N_2O_2-donor Schiff base N,N′-bis(salicylidene)hydrazine and ligands analogous to the latter are reported.[25–29] We have tried to synthesize a double helical dinuclear copper(II) complex with the diamide N,N′-bis(picolinoyl)hydrazine (H_2diph). In the deprotonated state ($diph^{2-}$), it is potentially an N_4-donor diazine ligand. However, a hydrated tetranuclear copper(II) complex where $diph^{2-}$ acts as a planar dinucleating N_4O-donor ligand have been isolated instead of a helical complex (Figure 3.1). In this chapter, the synthesis, characterization, physical properties and X-ray structure of this tetracopper(II) species, $[Cu_4(\mu\text{-diph})_2(\mu\text{-}H_2O)_2(O_2CCH_3)_4(H_2O)_2]\cdot 4H_2O$ (**1**$\cdot 4H_2O$), are described.

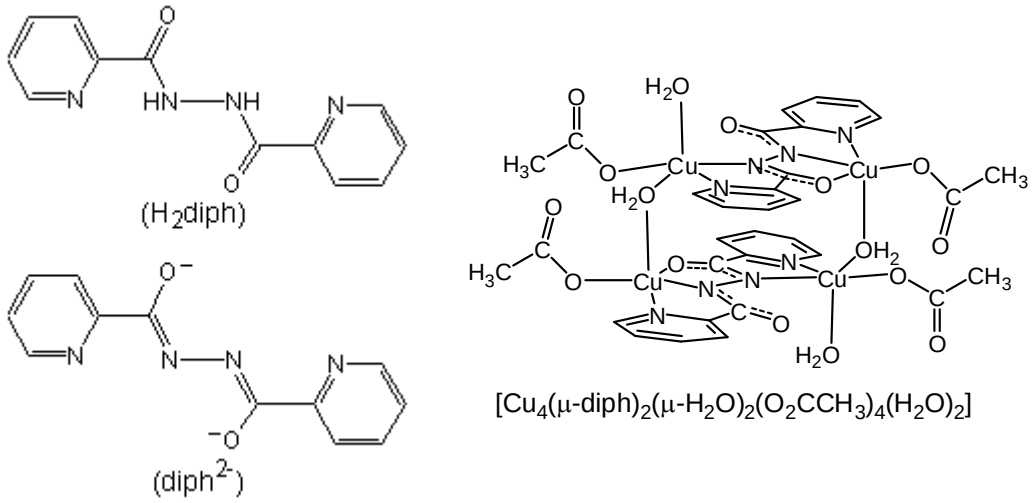

Figure 3.1.

3.3. Experimental

3.3.1. Materials

The chemicals and solvents used in this work were of analytical grade available commercially and were used without further purification.

3.3.2. Physical measurements

Elemental (C, H, N) analysis measurements were performed using a Thermo Finnigan Flash EA1112 series elemental analyzer. A Digisun DI-909 conductivity meter was used to measure the solution electrical conductivities. Magnetic susceptibilities were measured with a Sherwood Scientific balance. Diamagnetic corrections calculated from Pascal's constants[30] were used to obtain the molar paramagnetic susceptibilities. ^{1}H NMR data were obtained on a Bruker 400 MHz NMR spectrometer. A Shimadzu LCMS 2010 liquid chromatograph mass spectrometer was used for the purity verification. Infrared spectra were recorded by using KBr pellets on a Jasco-5300 FT-IR spectrophotometer. A Cary

100 Bio UV/vis spectrophotometer was used to collect the electronic spectra in solution. The solid state electronic spectrum of **1**·4H_2O was recorded by diffuse reflectance technique using $BaSO_4$ pellet on a Shimadzu UV-3600 UV-VIS-NIR spectrophotometer. A Jeol JES-FA200 spectrometer was used for the X-band EPR experiments.

3.3.3. Preparation of N,N′-bis(picolinoyl)hydrazine (H_2diph)

Hydrazine hydrate (1 ml, 1.03 g, 21 mmol) was added to ethyl-2-picolinate (6 ml, 6.71 g, 44 mmol) and heated to boiling under reflux condition for 6 h. The mixture was cooled to room temperature and H_2diph appeared as a white crystalline solid. It was collected by filtration and recrystallized from methanol. Yield: 4.1 g (80%). The identity and purity of H_2diph was confirmed by comparing its melting point, elemental analysis, LC-MS and spectroscopic (IR and ^{1}H NMR) data with that reported in literature.[31]

3.3.4. Synthesis of [Cu_4(μ-diph)$_2$(μ-H_2O)$_2$(O_2CCH_3)$_4$(H_2O)$_2$]·4H_2O (1·4H_2O)

A methanol solution (15 ml) of Cu(O_2CCH_3)$_2$·H_2O (80 mg, 0.40 mmol) was added to a methanol solution (15 ml) of H_2diph (50 mg, 0.21 mmol). The mixture was heated to boiling under reflux condition for 3 h. The green clear solution obtained was cooled to room temperature and allowed to evaporate slowly. After 2–3 days, a mixture of two crystalline materials, the green tetranuclear complex (**1**·4H_2O) and the mononuclear blue *trans*-[Cu(picolinate)$_2$]·2H_2O (**2**·4H_2O)[32] deposited were collected by filtration and treated with methanol (15 ml). Only **1**·4H_2O dissolved in methanol leaving behind the solid blue **2**·4H_2O. This mixture was filtered and the green filtrate was slowly evaporated to about 4−5 ml in air at room temperature. The pure **1**·4H_2O thus obtained was collected by filtration and dried in air. Yield: 60 mg (54%). An X-

ray quality single crystal was collected from this material. *Anal.* Calc. for $Cu_4C_{32}H_{44}N_8O_{20}$: C, 34.47; H, 3.98; N, 10.05. Found: C, 34.13; H, 3.79; N, 10.25%. $\mu_{eff.}$ (μ_B) at 298 K: 3.55. Selected IR bands (cm^{-1}): ~3375 (br), 1644 (s), 1605 (s), 1447 (s), 1348 (s), 1285 (m), 1152 (m), 1098 (w), 1050 (m), 850 (m), 775 (m), 693 (s), 627 (w), 460 (m). UV-Vis in solid state: λ (nm) = 685, 500^{sh}, 430^{sh}, 365, 280. UV-Vis in CH_3OH: λ (nm) (ε (M^{-1} cm^{-1})) = 700 (250), 490^{sh} (260), 425^{sh} (920), 360 (3170), 280 (6180). X-band EPR in powder phase at 298 and 130 K: $g_{\|}$ = 2.25 and $g_{\perp}$ = 2.08.

3.3.5. X-ray crystallography

The unit cell parameters and the intensity data at 298 K for **1**·$4H_2O$ were obtained on an Oxford Diffraction Xcalibur Gemini single crystal X-ray diffractometer using graphite monochromated Mo Kα radiation (λ = 0.71073 Å). The CrysAlisPro software[33] was used for data collection, reduction and absorption correction. The structure was solved by direct methods and refined on F^2 by full-matrix least-squares procedures. All non-hydrogen atoms were refined anisotropically. The hydrogen atoms of the water molecules were located in a difference map and refined with geometric restraints and $U_{iso}(H) = 1.5U_{iso}(O)$. The hydrogen atoms of the ligands were included in the structure factor calculation at idealized positions by using a riding model. The SHELX-97[34] programs available in the WinGx[35] package were used for structure solution and refinement. The ORTEX6a[36] and the Platon[37] packages were used for molecular graphics. Significant crystal data are listed in Table 3.1. Atomic coordinates with the isotropic thermal parameters are given in Table 3.2.

Table 3.1. Crystallographic data for $[Cu_4(\mu\text{-diph})_2(\mu\text{-}H_2O)_2(O_2CCH_3)_4(H_2O)_2]$

Empirical formula	$Cu_4C_{32}H_{44}N_8O_{20}$
Formula weight	1114.92
Crystal system	Triclinic
Space group	$P\bar{1}$
a (Å)	8.4650(12)
b (Å)	9.1494(14)
c (Å)	15.2231(19)
α (°)	88.219(11)
β (°)	85.922(11)
γ (°)	67.494(14)
V (Å^3)	1086.5(3)
Z	1
ρ (g cm^{-3})	1.704
μ (mm^{-1})	2.018
Reflections collected	7895
Reflections unique	3812
Reflections [$I \geq 2\sigma(I)$]	2899
Parameters	315
$R1$, $wR2$ [$I \geq 2\sigma(I)$] [a, b, c]	0.0380, 0.0899
$R1$, $wR2$ [all data] [b, c]	0.0523, 0.0938
Goodness-of-fit on F^2	0.954
Largest peak and hole (e Å^{-3})	0.362 and –0.639

[a]$R1 = \Sigma \| F_o | - | F_c \| / \Sigma | F_o |$. [b]$wR_2 = \{\Sigma[(F_o^2 - F_c^2)^2]\}^{1/2}$. [c]$GOF = \{\Sigma[w(F_o^2 - F_c^2)^2]/(n - p)\}^{1/2}$ where 'n' is the number of reflections and 'p' is the number of parameters refined.

Table 3.2. Atomic coordinats ($x10^4$) and equivalent isotropic displacement parameters ($Å^2 \times 10^3$) for $[Cu_4(\mu\text{-diph})_2(\mu\text{-}H_2O)_2(O_2CCH_3)_4(H_2O)_2]$

Atom	x	y	z	U(eq)
Cu(1)	2693(1)	567(1)	8399(1)	34(1)
Cu(2)	2659(1)	33(1)	11569(1)	38(1)
O(1)	2108(3)	-1380(3)	10793(2)	37(1)
O(2)	3490(3)	3070(3)	9792(2)	53(1)
O(3)	4344(3)	1612(3)	8361(2)	38(1)
O(4)	2944(3)	459(3)	7121(2)	50(1)
O(5)	1241(4)	2933(4)	6822(2)	64(1)
O(6)	235(3)	2698(3)	8486(2)	37(1)
O(7)	1937(3)	-667(3)	12666(2)	53(1)
O(8)	4387(3)	-2399(3)	13129(2)	52(1)
N(1)	2021(3)	-1298(3)	8459(2)	33(1)
N(2)	2669(3)	220(3)	9709(2)	32(1)
N(3)	2904(3)	976(3)	10456(2)	33(1)
N(4)	3068(3)	1895(4)	12005(2)	43(1)
C(1)	1732(4)	-2048(4)	7777(2)	44(1)
C(2)	1343(5)	-3373(5)	7898(3)	49(1)
C(3)	1216(4)	-3956(4)	8728(3)	47(1)
C(4)	1514(4)	-3199(4)	9439(2)	41(1)
C(5)	1900(4)	-1875(4)	9275(2)	32(1)
C(6)	2245(4)	-971(4)	9986(2)	31(1)
C(7)	3255(4)	2263(4)	10428(2)	37(1)
C(8)	3380(4)	2776(4)	11342(2)	39(1)

C(9)	3797(4)	4052(5)	11482(3)	53(1)
C(10)	3897(5)	4432(5)	12348(3)	66(1)
C(11)	3568(5)	3558(6)	13017(3)	70(1)
C(12)	3150(5)	2289(5)	12839(3)	60(1)
C(13)	2296(5)	1610(6)	6602(2)	50(1)
C(14)	2897(6)	1302(6)	5642(3)	71(1)
C(15)	2834(5)	-1615(5)	13232(2)	42(1)
C(16)	1871(5)	-1764(6)	14089(3)	68(1)
O(9)	452(4)	5570(4)	5738(2)	79(1)
O(10)	6071(5)	-5048(5)	14270(3)	105(1)

3.4. Results and discussion

3.4.1. Synthesis of $[Cu_4(\mu\text{-diph})_2(\mu\text{-}H_2O)_2(O_2CCH_3)_4(H_2O)_2]\cdot 4H_2O$ ($1\cdot 4H_2O$)

In anticipation of the neutral double helical dicopper(II) species, $[Cu_2(\mu\text{-diph})_2]$, equimolar amounts of $Cu(O_2CCH_3)_2\cdot H_2O$ and N,N′-bis(picolinoyl)hydrazine (H_2diph) were reacted in methanol. But no tractable product could be isolated. However, reaction of two mole equivalents of $Cu(O_2CCH_3)_2\cdot H_2O$ with one mole equivalent of H_2diph in the same solvent produces the green $[Cu_4(\mu\text{-diph})_2(\mu\text{-}H_2O)_2(O_2CCH_3)_4(H_2O)_2]\cdot 4H_2O$ (**1**·$4H_2O$) and the blue *trans*-[Cu(picolinate)$_2$]·$2H_2O$ (**2**·$4H_2O$). The yield of **1**·$4H_2O$ is approximately 1.4 times more than that of **2**·$4H_2O$. The former is highly soluble in methanol and ethanol, but sparingly soluble in acetonitrile and insoluble in dichloromethane, chloroform etc., while the latter is insoluble in common solvents and sparingly soluble in dimethylformamide and dimethylsulfoxide. We have established the identity of **2**·$4H_2O$ with the help of elemental analysis,

magnetic susceptibility, spectroscopic and single crystal X-ray diffraction measurements. Synthesis of **2**·4H_2O via copper(II) assisted hydrolysis of picolinonitrile and its X-ray structure have been reported in literature.[32] Thus the mononuclear complex in the present reaction is produced due to hydrolysis of a portion of H_2diph during its reaction with the copper(II) starting material. The elemental (C,H,N) analysis data for **1**·4H_2O are consistent with its molecular formula. In methanol solution, it is electrically non-conducting. The room temperature (298 K) magnetic moment (3.55 μ_B) of **1**·4H_2O in powder phase is very close to the spin-only value (3.46 μ_B) expected for a tetracopper(II) species.

3.4.2. Spectroscopic properties

In the infrared spectrum of **1**·4H_2O, the water molecules appear as a broad structured band centred at ~3375 cm^{-1}. Two overlapping strong bands are observed at 1644 and 1605 cm^{-1}. The former is attributed to the γ_{asym} stretch of the acetate[38] and the latter is likely to be associated with the diazine moiety[15–29] of $diph^{2-}$ Figure 3.2. Two more strong bands appear at 1447 and 1348 cm^{-1}. Perhaps the higher energy band is associated with the pyridine ring and the lower energy band is due to the γ_{sym} stretch of the acetate.[38]

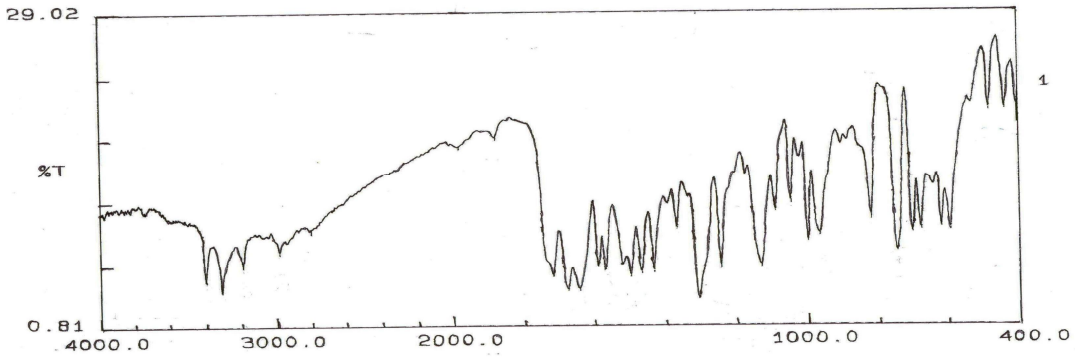

Wavelength (cm^{-1})

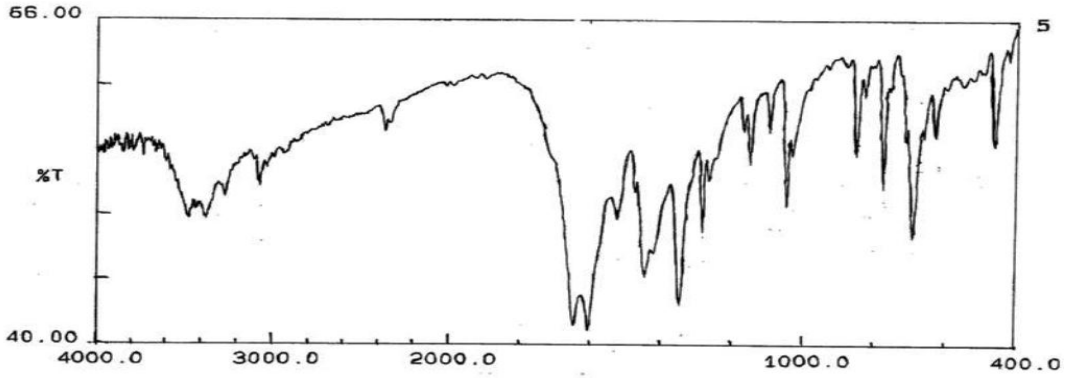

Wavelength (cm^{-1})

Figure 3.2. Infrared spectra of H_2diph (top) and $[Cu_4(\mu\text{-diph})_2(\mu\text{-}H_2O)_2(O_2CCH_3)_4(H_2O)_2]$ (bottom).

The electronic spectra of **1**·$4H_2O$ in solid state and in methanol solution display several absorptions in the 700–280 nm wavelength range (Figure 3.3, Table 3.3). The positions of the absorption maxima in solid state are very similar to that in solution except for some variations in the relative intensities of the bands. In solution, the intensities of the longer wavelength bands are comparable and significantly lower than the intensities of the following high energy bands. For copper(II) complexes similar low energy absorptions are assigned to d-d transitions and the intense high energy bands are attributed to the charge transfer and ligand centred transitions.[39–52]

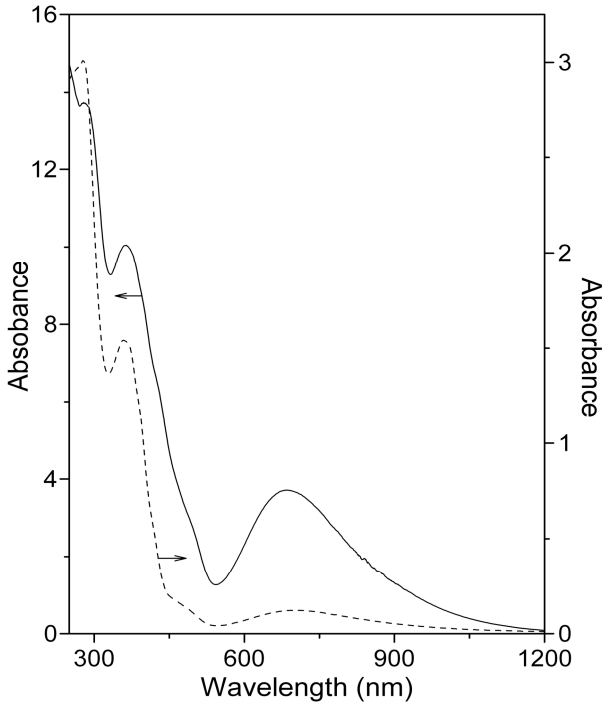

Figure 3.3. The electronic spectra of **1**·4H_2O in solid state (—) and in methanol (-----).

Table 3.3. Electronic spectral data of **1**·4H_2O

Complex	λ_{max} (nm) (ε (M^{-1} cm^{-1}))
In solid state:	685, 500^{sh}, 430^{sh}, 365, 280.
In CH_3OH:	700 (250), 490^{sh} (260), 425^{sh} (920), 360 (3170), 280 (6180).

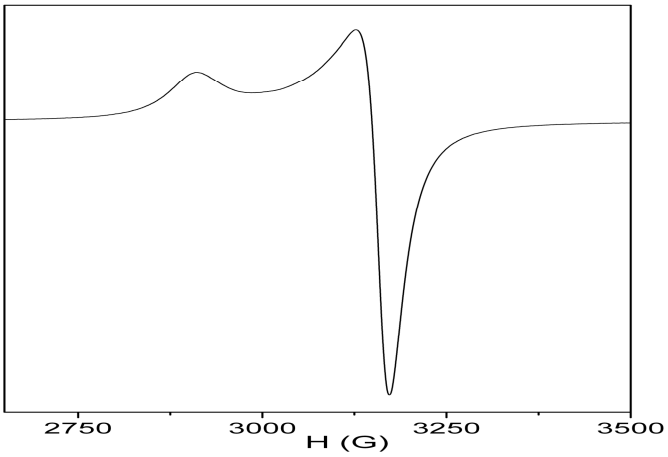

Figure 3.4. The ESR spectrum of **1**·4H_2O in powder phase at 130K.

In powder phase, **1**·4H_2O displays axial EPR spectrum with unresolved copper hyperfine structure at room (298 K) as well as at low (130 K) temperature (Figure 3.4). The $g_{\parallel}$ and $g_{\perp}$ values are 2.25 and 2.08, respectively. Such spectra are typical for copper(II) species having square based coordination geometry and the unpaired electron in the $d_{x^2-y^2}$ orbital.[45–50] These spectral features at room and low temperature indicate the absence of any significant magnetic interaction between the copper(II) centres in **1**·4H_2O. It may be noted that **1** has a rectangular {$Cu_4(\mu\text{-N–N})_2(\mu\text{-}OH_2)_2$} core, where the diazines and the water molecules are equatorial-equatorial and equatorial-apical bridging, respectively (*vide infra*). Very weak antiferromagnetic behavior is also reported for a somewhat similar tetracopper(II) complex [$Cu_4(\mu_3\text{-diph})_2(\text{imidazole})_2(NO_3)_4(H_2O)_2$] having the {$Cu_4(\mu\text{-N–N})_2(\mu\text{-N=C–O})_2$} core with equatorial-equatorial diazine and equatorial-apical iminolate bridges.[53] The frozen (130 K) solution spectrum of **1**·4H_2O can be recorded only in methanol-ethanol (1:1) mixture due to its insoluble nature in non-coordinating solvents. The spectral profile is axially

symmetric with $g_{\|} > g_{\perp}$. Although there is only one perpendicular signal ($g_{\perp}$ = 2.08), but the parallel component has two sets of copper hyperfine lines, one strong ($g_{\|}$ = 2.32 and $A_{\|}$ = 146 x 10^{-4} cm^{-1}) and one relatively weak ($g_{\|}$ = 2.35 and $A_{\|}$ = 115 x 10^{-4} cm^{-1}). Appearance of two $g_{\|}$ signals suggests that the complex is not stable in solution and dissociates to monomeric species.[47]

3.4.3. X-ray structure

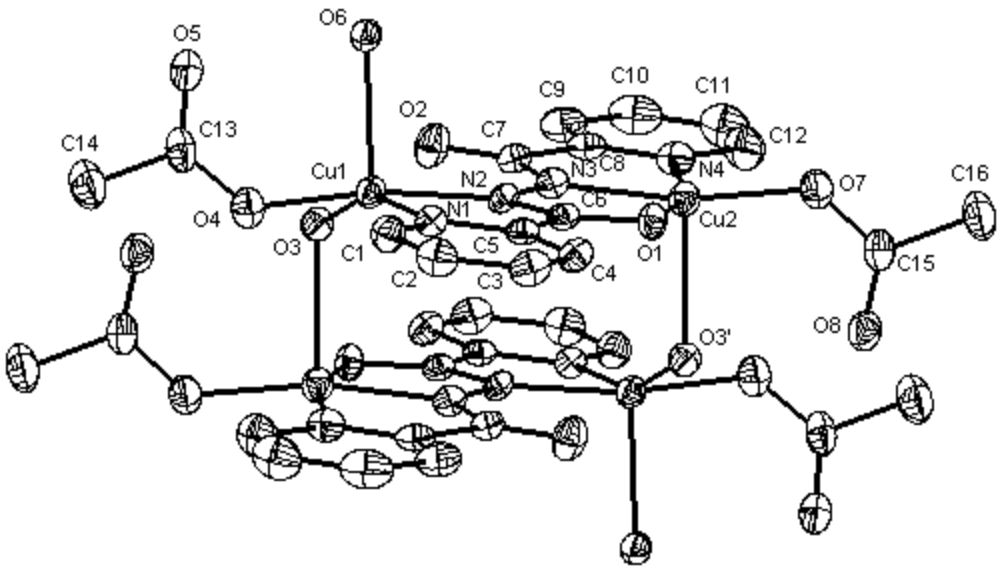

Figure 3.5. The structure of **1**·4H_2O with the atom labeling scheme. All non-hydrogen atoms are represented by their 30% probability thermal ellipsoids. Hydrogen atoms are omitted and only one symmetry related atom is labeled for clarity.

The structure of **1**·4H_2O has been determined by X-ray crystallography. The complex crystallizes in the $P\bar{1}$ space group. A perspective view of the centrosymmetric tetranuclear **1**·4H_2O is illustrated in Figure 3.5. Selected bond lengths and angles are listed in Table 3.4. The asymmetric unit contains the dicopper(II) unit {$(H_2O)_2(O_2CCH_3)$Cu(μ-diph)Cu(O_2CCH_3)} and two water molecules. Inversion symmetry related two such dicopper(II) units form the tetranuclear **1**·4H_2O with a rectangular {Cu_4(μ-N–N)$_2$(μ-$OH_2)_2$} core. In this core, the diazine bridges are along the length (Cu···Cu, 4.834(1) Å) and the water molecules are along the width (Cu···Cu, 3.762(1) Å). In the planar bridging diph^{2-} moiety, the dihedral angle between the two *trans* oriented *ortho*-$C_5H_5NC(O^-)$=N– fragments (mean deviations 0.02 Å) is 2.5(1)^o. Thus there is no twisting along the N–N single bond. It acts as N_2-donor to the first metal centre (Cu1), while N_2O-donor to the second metal centre (Cu2). The same coordination mode of diph^{2-} in copper(II) complexes has been observed before.[53,54] In the diiminolate (–(O^-)C=N–N=C(O^-)–) fragment of diph^{2-}, the two C=N bond lengths (C6–N2, 1.320(4) Å; C7–N3, 1.319(4) Å) are comparable, whereas one of the two C–O bond lengths (C6–O1, 1.284(4) Å) is significantly longer than the other one (C7–O2, 1.250(4) Å). It may be noted that O1 is coordinated to Cu2 and the corresponding iminolate-N (N2) is coordinated to Cu1, while O2 is uncoordinated and the corresponding iminolate-N (N3) is coordinated to Cu2 (Figure 3.5). The Cu1−N2 bond length (2.009(3) Å) is also significantly longer than the Cu2−N3 bond length (1.911(3) Å). Thus the varying degree of charge delocalization in the two iminolates due to their bridging (CuN=COCu) and non-bridging (CuN=CO) modes is the primary reason for the differences in the C–O and Cu−N(imine) bond lengths. Overall the N=C and the C–O bond lengths in diph^{2-} are consistent with the iminolate (–N=C(O^-)–) form of the amide functionalities.[50–55] The Cu–N(pyridine), Cu–N(imine), Cu–O(acetate) and Cu–O(iminolate) bond lengths are comparable with the bond lengths reported for copper(II) complexes having

the same coordinating atoms.[16–18,20,45–47,49–57] The equatorial Cu–OH_2 bond length is unexceptional[57] and as commonly observed significantly shorter than the apical Cu–OH_2 bond length (Table 3.4). The Cu1···O5 (3.165(3) Å) and Cu2···O8 (3.227(3) Å) distances are just above the distance (3.0 Å) considered to be interactive[56] and hence reflect the monodentate coordination mode of the acetates. The intra-acetate bond lengths are consistent with their monodentate character.

The metal centres in **1** are in slightly distorted square-pyramidal N_2O_3 coordination spheres. In the case of Cu1, the square-base is formed by the pyridine-N, the imine-N, the actetate-O and a water-O (mean deviation 0.14 Å) and the second water-O occupies the apical position. In the case of Cu2, the pyridine-N, the imine-N, the iminolate-O and the actetate-O form the square-base (mean deviation 0.03 Å) and the apical site is satisfied by the water-O that is already equatorially coordinated to Cu1. Both Cu1 and Cu2 are displaced from the basal plane towards the apical O-atom by 0.30(1) and 0.16(1) Å, respectively. The degree of distortion from square-pyramidal to trigonal-bipyramidal geometry can be gauged from the τ value defined as $(\beta-\alpha)/60$, where β is the larger and α is the smaller *trans* bond angle in the basal plane.[48] The τ is 0 for the ideal square-pyramid and 1 for the ideal trigonal-bipyramid. The values of τ are 0.24 and 0.12 for Cu1 and Cu2, respectively. Thus there is a small distortion from square-pyramidal geometry for Cu2 where $diph^{2-}$ is tridentate, while the distortion is doubled for Cu1 where it is bidentate.

Table 3.4. Selected bond lengths (Å) and angles (°) for **1**·4H_2O [a]

Cu(1)–N(1)	1.993(3)	Cu(2)–N(3)	1.911(3)
Cu(1)–N(2)	2.009(3)	Cu(2)–N(4)	2.005(3)
Cu(1)–O(3)	1.969(2)	Cu(2)–O(1)	1.980(2)
Cu(1)–O(4)	1.944(3)	Cu(2)–O(7)	1.914(3)
Cu(1)–O(6)	2.240(2)	Cu(2)–O(3)′	2.412(2)
N(1)–Cu(1)–N(2)	80.91(11)	N(3)–Cu(2)–N(4)	81.58(12)
N(1)–Cu(1)–O(3)	154.31(10)	N(3)–Cu(2)–O(1)	80.77(10)
N(1)–Cu(1)–O(4)	90.95(11)	N(3)–Cu(2)–O(7)	168.55(11)
N(1)–Cu(1)–O(6)	105.80(9)	N(3)–Cu(2)–O(3)′	95.69(9)
N(2)–Cu(1)–O(3)	95.31(10)	N(4)–Cu(2)–O(1)	161.58(11)
N(2)–Cu(1)–O(4)	168.85(11)	N(4)–Cu(2)–O(7)	98.81(12)
N(2)–Cu(1)–O(6)	93.20(9)	N(4)–Cu(2)–O(3)′	90.74(10)
O(3)–Cu(1–O(4)	88.72(10)	O(7)–Cu(2)–O(1)	97.45(10)
O(3)–Cu(1)–O(6)	99.76(9)	O(1)–Cu(2)–O(3)′	96.20(9)
O(4)–Cu(1)–O(6)	96.36(10)	O(7)–Cu(2)–O(3)′	95.75(9)

[a] Symmetry transformation used to generate the equivalent atom: –x+1, –y, –z+2

3.4.4. Hydrogen bonding:

Both equatorial and apical water molecules are involved in strong intra and intermolecular hydrogen bonds (Table 3.5). The uncoordinated iminolate-O (O2) of the $diph^{2-}$ and the acetate-O (O5) atoms act as acceptors for the equatorial and apical water molecules, respectively in the intramolecular interactions (Figure 3.7). The lattice water molecules are also strongly hydrogen bonded to the acetate

O-atoms (O5 and O8) that are not coordinated to the metal centres (Figure 3.5). The uncoordinated iminolate-O (O2) is also involved in an intermolecular hydrogen bond with the apical water hydrogen molecules to produce a ladder type structure (Figure 3.7a). The parallel ladders are again connected by intermolecular hydrogen bonds involving the uncoordinated water molecules and uncoordinated acetate-O (O5 and O8). These two types of intermolecular hydrogen bonding interactions are approximately diagonal to each other. As a result a two-dimensional sheet structure of **1**·4H_2O is produced (Figure 3.7b)

Table 3.5. Hydrogen bonding parameters (Å and ^{o}) for **1**·4H_2O

D–H···A	d (D–H)	d (H···A)	d (D···A)	< (DHA)
Intramolecular				
O3–H···O2	0.96(1)	1.61(2)	2.503(3)	153(3)
O6–H···O5	0.95(1)	1.73(2)	2.643(4)	158(3)
Intermolecular				
O9–H···O5	0.96(1)	1.84(2)	2.768(4)	163(4)
O10–H···O8	0.97(1)	1.99(3)	2.893(5)	153(5)

Symmetry transformations used to generate equivalent atoms: #1 -x+1,-y,-z+2

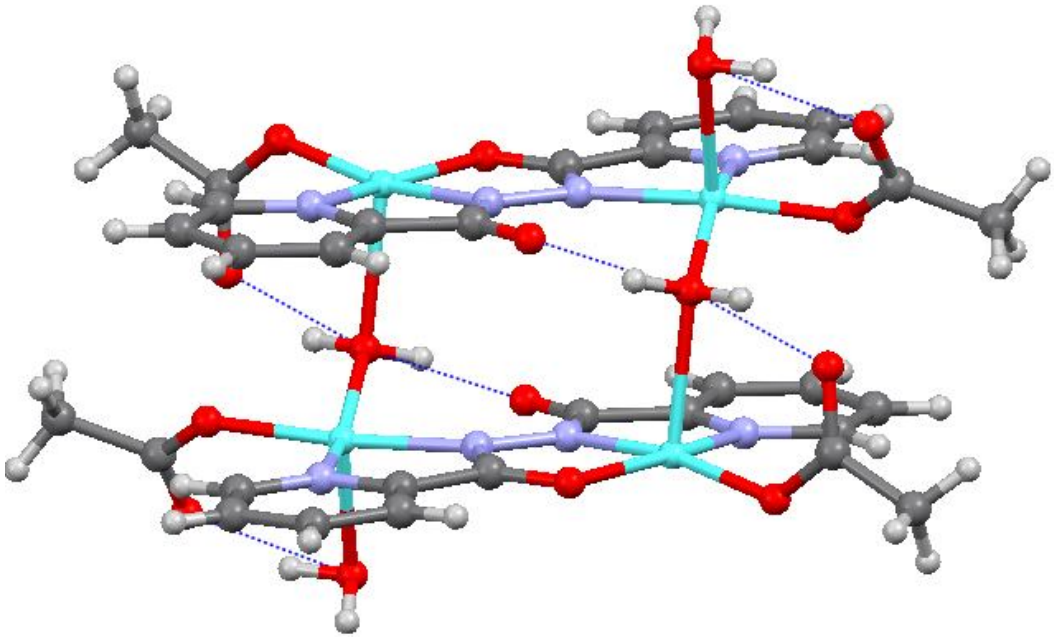

Figure 3.6. Intramolecular hydrogen bonding in $[Cu_4(\mu\text{-diph})_2(\mu\text{-}H_2O)_2(O_2CCH_3)_4(H_2O)_2]$

a)

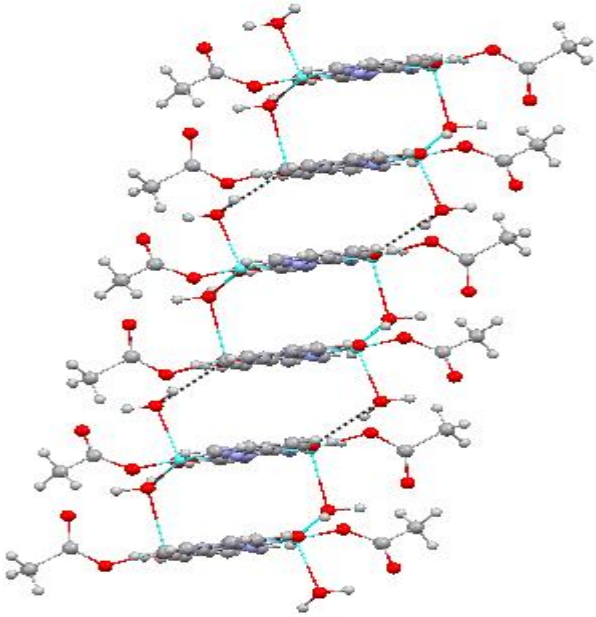

b)

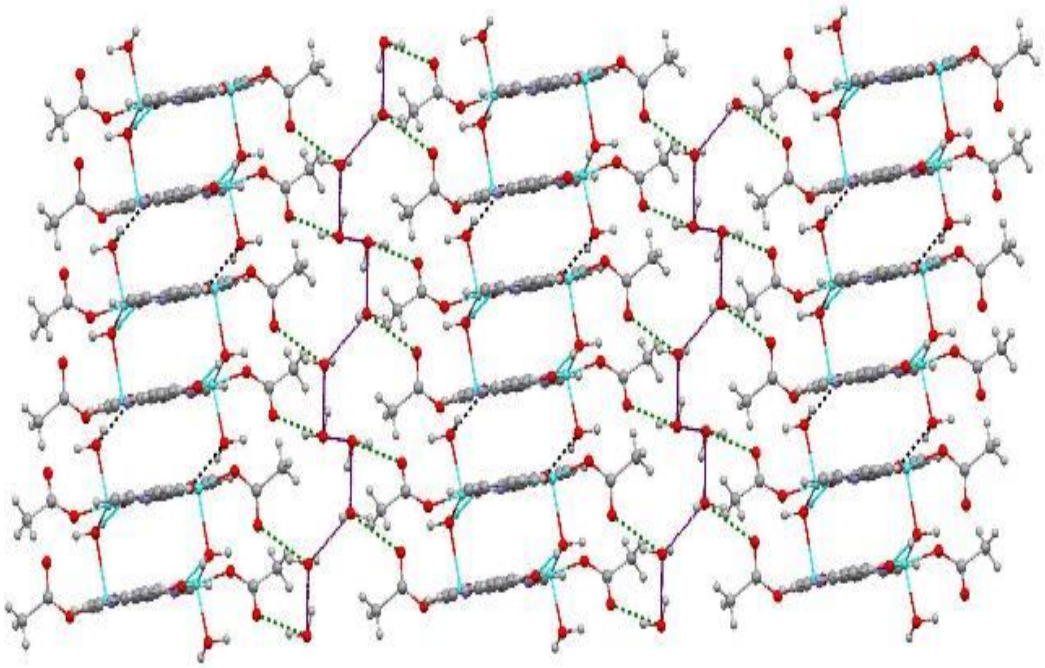

Figure 3.7. Intremolecular hydrogen bond assisted (a) one-dimensional ladder type arrangement of **1** and (b) two-dimensional sheet structure of **1**·$4H_2O$.

3.5. Conclusion

In methanol, reaction of $Cu(O_2CCH_3)_2{\cdot}H_2O$ with N,N′-bis(picolinoyl)hydrazine (H_2diph) in 2:1 mole ratio produces $[Cu_4(\mu\text{-diph})_2(\mu\text{-}H_2O)_2(O_2CCH_3)_4(H_2O)_2]{\cdot}4H_2O$ (**1**·$4H_2O$) and *trans*-[Cu(picolinate)$_2$]·$2H_2O$ (**2**·$4H_2O$)[32]. No significant spin-exchange between the metal centres in **1**·$4H_2O$ is indicated by its spin-only magnetic moment (3.55 μ_B) at 298 K and the powder EPR spectrum characterized by axial g tensor with $g_{\|} > g_{\perp}$ at 298 and 130 K. X-ray structure of **1**·$4H_2O$ reveals slightly distorted square-pyramidal N_2O_3 coordination sphere of two types around the metal centres and a rectangular $\{Cu_4(\mu\text{-N–N})_2(\mu\text{-}OH_2)_2\}$ core assembled by the diazine fragments of the two diph^{2-} and two water molecules. The diazine fragments are along the length (Cu···Cu, 4.834(1) Å) and the water molecules are along the width (Cu···Cu, 3.762(1) Å). We are currently involved in exploring the coordination chemistry of H_2diph and analogous systems with various 3d metal ions.

3.6. References

1. J.–M. Lehn, A. Rigault, J. Siegel, J. Harrowfield, B. Chevrier, D. Moras, *Proc. Natl. Acad. Sci*., U.S.A., **1987**, *84*, 2565.
2. E.C. Constable, *Prog. Inorg. Chem*., **1994**, *42*, 67.
3. J.-M. Lehn, *Supramolecular Chemistry*., VCH, Weinheim., **1995**.
4. C. Piguet, G. Bernardinelli, G. Hopfgartner, *Chem. Rev*., **1997**, *97*, 2005.
5. A. Williams, *Chem.–Eur. J*., **1997**, *3*, 15.
6. M. Albrecht, *Chem. Rev*., **2001**, *101*, 3457.
7. I. Meistermann, V. Moreno, M.J. Prieto, E. Molderheim, E. Sletten, S. Khalid, M. Rodger, J. Perberdy, C.J. Isaac, A. Rodger, M.J. Hannon, *Proc. Natl. Acad. Sci*., U.S.A., **2002**, *99*, 5069.
8. J.L. Serrano, T. Sierra, *Coord. Chem. Rev*., **2003**, *242*, 73.
9. B. Kesanli, W. Lin, *Coord. Chem. Rev*., **2003**, *246*, 305.
10. M.J. Hannon, L.J. Childs, *Supramol. Chem*., **2004**, *16*, 7.
11. C. Piguet, M. Borkovec, J. Hamacek, K. Zeckert, *Coord. Chem. Rev*., **2005**, *249*, 705.
12. V. Amendola, L. Fabbrizzi, F. Foti, M. Licchelli, C. Mangano, P. Pallavicini, A. Poggi, D. Sacchi, A. Taglietti, *Coord. Chem. Rev*., **2006**, *250*, 273.
13. C.R.K. Glasson, L.F. Lindoy, G.V. Meehan, *Coord. Chem. Rev*., **2008**, *252*, 940.
14. X.–D. Zheng, T.–B. Lu, *Cryst. Eng. Comm*., **2010**, *12*, 324.
15. P.D.W. Boyd, M. Gerloch, G.M. Sheldrick, *J. Chem. Soc., Dalton Trans*., **1974**, 1097.
16. C.J. O'Connor, R.J. Romananch, D.M. Robertson, E.E. Eduok, F.R. Fronczek, *Inorg. Chem*., **1983**, *22*, 449.

17. Z. Xu, L.K. Thompson, D.O. Miller, *Inorg. Chem.*, **1997**, *36*, 3985.
18. L.K. Thompson, Z. Xu, A.E. Goeta, J.A.K. Howard, H.J. Clase, D.O. Miller, *Inorg. Chem.*, **1998**, *37*, 3217.
19. Z. Xu, L.K. Thompson, D.O. Miller, H.J. Clase, J.A.K. Howard, A.E. Goeta, *Inorg. Chem.*, **1998**, *37*, 3620.
20. Z. Xu, L.K. Thompson, C.J. Matthews, D.O. Miller, A.E. Goeta, C. Wilson, J.A.K. Howard, M. Ohba, H. Okawa, *J. Chem. Soc., Dalton Trans.*, **2000**, 69.
21. G. Dong, D. Chun-ying, F. Chen-jie, M. Qing-jin, *J. Chem. Soc., Dalton Trans.*, **2002**, 834.
22. J. Hamblin, A. Jackson, N.W. Alcock, M.J. Hannon, J. *Chem. Soc., Dalton Trans.*, **2002**, 1635.
23. G. Dong, P. Ke-liang, D. Chun-ying, H. Cheng, M. Qing-jin, *Inorg. Chem.*, **2002**, *41*, 5978.
24. P.V. Bernhardt, P. Chin, D.R. Richardson, *J. Chem. Soc., Dalton Trans.*, **2004**, 3342.
25. J. Saroja, V. Manivannan, P. Chakraborty, S. Pal, *Inorg. Chem.*, **1995**, *34*, 3099.
26. M. Hong, G. Dong, D. Chun-ying, L. Yu-ting, M. Qing-jin, *J. Chem. Soc., Dalton Trans.*, **2002**, 3422.
27. M. Hong, F. Chen-jie, D. Chun-ying, L. Yu-ting, M. Qing-jin, *J. Chem. Soc., Dalton Trans.*, **2003**, 1229.
28. S.G. Sreerama, S. Pal, *Inorg. Chem.*, **2005**, *44*, 6299.
29. S.G. Sreerama, A. Mukhopadhyay, S. Pal, *Polyhedron.*, **2007**, *26*, 4101.
30. W.E. Hatfield, in: E.A. Boudreaux, L.N. Mulay (Eds.), *Theory and Applications of Molecular Paramagnetism.*, Wiley, New York, **1976**, p. 491.
31. H. Zhao, T.R. Burke, Jr., *Tetrahedron.*, **1997**, *53*, 4219.

32. P. Segl'a, M. Jamnický, M. Koman, J. Šima, T. Glowiak, *Polyhedron*., **1998**, *17*, 4525.
33. CrysAlisPro version 1.171.33, Oxford Diffraction Ltd., Abingdon, Oxfordshire, UK, **2007**.
34. G.M. Sheldrick, SADABS, *Program for Area Detector Absorption Correction*, University of Göttingen, Göttingen, Germany, **1997**.
35. L.J. Farrugia, *J. Appl. Crystallogr*., **1999**, *32*, 837-838.
36. P. McArdle, *J. Appl. Crystallogr*., **1995**, *28*, 65.
37. A.L. Spek, Platon, *A Multipurpose Crystallographic Tool*, Utrecht University, Utrecht, The Netherlands, **2002**.
38. K. Nakamoto, *Infrared and Raman Spectra of Inorganic and Coordination Compounds*, Wiley, New York, **1986**, p. 233.
39. A. Taha, *Spectrochim. Acta A.*, **2003**,*59*, 1611.
40. A.K. Patra, M. Nethaji, A.R. Chakravarty, *Dalton Trans*., **2005**, 2798.
41. P. Sarmah, R.K. Barman, P. Purkayastha, S.J. Bora, P. Phukan, B.K. Das, *Indian J. Chem. Sect. A.*, **2009**, *48*, 637.
42. Z. Lu, T. Ladrak, O. Roubeau, J. van der Toorn, S. J. Teat, C. Massera, P. Gamez, J. Reedijk, *Dalton Trans*., **2009**, 3559.
43. A. Paulovicova, U. El-Ayaan, K. Shibayama, T. Morita, Y. Fukuda, *Eur. J. Inorg. Chem*., **2001**, 2641.
44. C.P. Pradeep, P.S. Zacharias, S.K. Das, *J. Chem. Sci*., **2005**, *117*, 133.
45. T. Ghosh, S. Das, S. Pal, *Polyhedron*., **2010**, *29*, 3074.
46. S. Maloth, S. Pal, *Polyhedron*., **2010**, *29*, 3257.
47. M.M. Whittaker, W.R. Duncan, J.W. Whittaker, *Inorg. Chem*., **1996**, *35*, 382.
48. A.W. Addison, T.N. Rao, J. Reedijk, J. van Rijn, G.C. Verschoor, *J. Chem. Soc., Dalton Trans.*, **1984**, 1349.
49. Z. Liu, C. Duan, Y. Tian, X. You, *Inorg. Chem*., **1996**, *35*, 2253.

50. T. Ghosh, A. Mukhopadhyay, K.S.C. Dargaiah, S. Pal, *Struct. Chem*., **2010**, *21*, 147.
51. S.N. Pal, J. Pushparaju, N.R. Sangeetha, S. Pal, *Trans. Met. Chem*., **2000**, *25*, 528.
52. T. Ghosh, S. Pal, *Inorg. Chim. Acta.*, **2010**, *363*, 3632.
53. X.–H. Bu, H. Liu, M. Du, L. Zhang, Y.–M. Guo, M. Shionoya, J. Ribas, *Inorg. Chem*., **2002**, *41*, 1855.
54. M. Lagrenée, S. Sueur, J.P. Wignacourt, *Acta Crystallogr., Sect. C*., **1991**, *47*, 1158.
55. S. Roy, T.N. Mandal, A.K. Barik, S. Gupta, M.S.E. Fallah, J. Tercero, R.J. Butcher, S.K. Kar, *Dalton Trans*., **2009**, 8215.
56. B.K. Koo, *Bull. Korean Chem. Soc*., **2001**, *22*, 113.
57. L. Li, N.N. Murthy, J. Telser, L.N. Zakharov, G.P.A. Yap, A.L. Rheingold, K.D. Karlin, S.E. Rokita, *Inorg. Chem*., **2006**, *45*, 7144.

Chapter 4

Dicopper(II) complexes with 2-hydroxy-5-methylbenzene-1,3-dicarbaldehyde bis(benzoylhydrazone)

4.1. Abstract

The reaction of $Cu(O_2CCH_3)_2 \cdot H_2O$ and 2-hydroxy-5-methyl benzene-1,3-dicarbaldehyde bis(benzoylhydrazone) (H_3L) in methanol affords a dinuclear complex having the general formula $[Cu_2(\mu\text{-}L)(\mu\text{-}OCH_3)]$ (**1**). On the other hand the reaction of $Cu(ClO_4) \cdot 6H_2O$ and H_3L in presence of KOH in methanol affords two dinuclear complexes. These are **1** and $[Cu_2(\mu\text{-}HL)(\mu\text{-}OCH_3)(H_2O)]ClO_4 \cdot CH_3OH \cdot H_2O$ (**2**). In the solid state, the complex **1** dimerises through two pair of weak reciprocal equatorial-apical bridges involving the iminolate-O and methoxo-O atoms and complex **2** dimerises through a pair of weak reciprocal equatorial-apical bridges involving only methoxo-O atom. Each metal centre is in NO_4 square pyramidal coordination sphere. The two metal centers in **1** and **2** are bridged through an endogenous phenolate and exogenous methoxo oxygen atoms. Each complex has been characterized by elemental analysis, magnetic and various spectroscopic (IR, UV-Vis and EPR) measurements. In the crystal lattice of **2**, the uncoordinated water and methanol molecules and perchlorate participate in intermolecular hydrogen bonding and produce a three dimensional network. Variable temperature magnetic susceptibility measurements reveal the presence of an antiferromagnetic interaction (J = -42.28(3) cm^{-1}) between the Cu(II) centers in $[Cu_2(\mu\text{-}L)(\mu\text{-}OCH_3)]$ (**1**).

4.2. Introduction

The dinucleating Schiff base, 2-hydroxy-5-methyl benzene-1,3-dicarbaldehyde was first developed by Robson[1] and Ōkawa[2] in 1970. A related dithiosemicarbazone was used by Hoskins *et al.*[3] for the synthesis of dinuclear copper(II) and nickel(II) complexes. This type of ligand is known to form binuclear complexes where metal ions are bridged by two different groups, such as the endogenous phenolic oxygen and an exogenous group such as hydroxide, alkoxide, halide, pseudohalide, carboxylate, or pyrazolate ion. Latter complexes of this ligand were extensively used for the study of spin-exchange interaction[4] and for modeling of the active site of type-III copper proteins.[5-7]

In chapters 2 and 3, we have described the chemistry of mononuclear and dinuclear Cu(II) complexes. In this chapter, we are reporting two new dinuclear copper(II) complexes with the pentadentate dinucleating N_2O_3 donor Robson type Schiff base (2-hydroxy-5-methylbenzene-1,3-dicarbaldehyde bis(benzoylhydrazone)) (H_3L), derived from one mole equivalent of 2-hydroxy-5-methylbenzene-1,3-dicarbaldehyde and two mole equivalents of benzoylhydrazone. In the following sections, syntheses, characterization and physical properties of these three complexes have been described. The single crystal structures of these complex molecules have been determined.

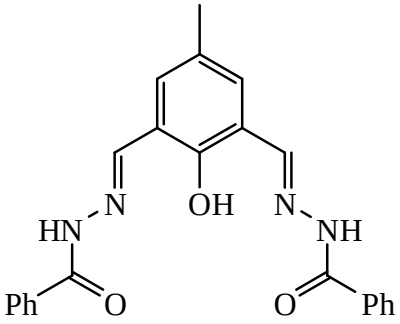

(H_3L)

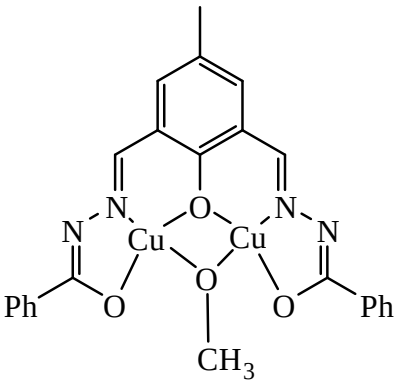

[$Cu_2(\mu\text{-}L)(\mu\text{-}OCH_3)$]

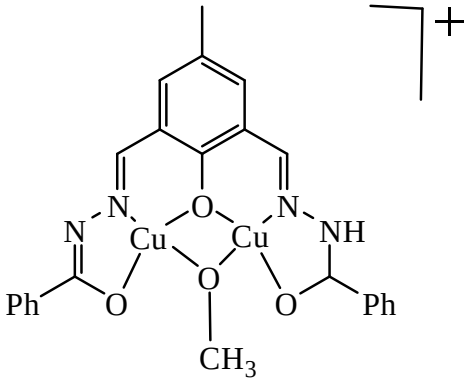

$[Cu_2(\mu\text{-}L)(\mu\text{-}OCH_3)]^+$

Figure 4.1.

4.3. Experimental section

4.3.1. Materials

Pentadentate N_2O_3 donor dinucleating Schiff base (H_3L) was obtained in good yield 82% (198 mg) by reacting two mole equivalents of benzoylhydrazone (166 mg, 1.2 mmol) and one mole equivalent of 2-hydroxy-5-methyl benzene-1,3-dicarbaldehyde (100 mg, 0.6mmol) in methanol. All other chemicals and solvents used in this work were of analytical grade available commercially and were used without further purification.

4.3.2. Physical measurements

Elemental (C, H, N) analysis measurements were performed using a Thermo Finnigan Flash EA1112 series elemental analyzer. A Digisun DI-909 conductivity meter was used to measure the solution electrical conductivities. Magnetic susceptibilities were measured with a Sherwood Scientific balance. Diamagnetic corrections calculated from Pascal's constants[8] were used to obtain the molar paramagnetic susceptibilities. A Shimadzu LCMS 2010 liquid

chromatograph mass spectrometer was used for the purity verification. Infrared spectra were recorded by using KBr pellets on a Jasco-5300 FT-IR spectrophotometer. A Cary 100 Bio UV/Vis spectrophotometer was used to collect the electronic spectra in solution. A Jeol JES-FA200 spectrometer was used for the X-band EPR experiments. Variable temperature magnetic susceptibility measurements in the temperature range 4-300 K were performed using a Quantum Design VSM-SQUID. X-ray powder diffraction patterns were collected on a Philips PW-3710 diffractometer using Cu-Kα radiation (λ = 1.54184 Å).

4.3.3. Synthesis of [Cu_2 (μ-L) (μ- OCH_3)] (1)

A methanol solution (10 ml) of $Cu(O_2CCH_3)_2 \cdot 1H_2O$ (50 mg, 0.25 mmol) was added to a suspension of H_3L (50 mg, 0.125 mmol) in methanol (15 ml). Immediately the color of the reaction mixture became green, this reaction mixture was refluxed for 3 h. After cooling to room temperature it was allowed to evaporate slowly. The complex separated as green crystalline material was collected by filtration, washed with little ice-cold methanol and finally dried in air. The yield was 66% (46 mg). Anal. Calcd. for $Cu_2C_{24}H_{20}N_4O_4$ (555.24): C, 51.87; H, 3.63; N, 10.09. Found: C, 51.76; H, 3.68; N, 10.15%. μ_{eff}: $2 \cdot 10\mu_B$. UV-Vis in CH_3OH solution: λ (nm) (10^{-2} x ε (M^{-1} cm^{-1})) = 255^{sh} (172), 338 (255), 402^{sh} (114), 430 (86), 652 (15).

4.3.4. [Cu_2(μ-HL)(μ-OCH_3)(H_2O)]$ClO_4 \cdot CH_3OH \cdot H_2O$ (2)

A methanol solution (15 ml) of $Cu(ClO_4) \cdot 6H_2O$ (93 mg, 0.25 mmol) was added to a methanol solution (15 ml) of H_3L (50 mg, 0.125 mmol) and KOH (14 mg, 0.249 mmol). The mixture was heated to reflux for 3 h. After cooling to room temperature complex **1** obtained as precipitate was filtered and the green colored filtrate was allowed to evaporate slowly. After 2-3 days crystalline material of the

complex **2** was collected by filtration, washed with ice cold methanol and finally dried in air. The yield was 49% (40 mg). Anal. Calcd. for $Cu_2C_{25}H_{29}N_4O_{11}Cl_1$: C, 41.45; H, 4.04; N, 7.74. Found: C, 41.36; H, 4.48; N, 7.75%. μ_{eff}: 2·20μ_B. UV-Vis in CH_3CN solution: λ (nm) (10^{-2} x ε (M^{-1} cm^{-1})) = 256 (274), 279 (201), 336 (268), 396 (131), 418^{sh} (112), 651 (13).

4.3.6. X-ray crystallography

Single crystals of **1** were grown by slow evaporation of its solution. Crystals of **2** were collected directly from the reaction mixture. The unit cell parameters and the intensity data at 298 K for complex **2** was obtained on an Oxford Difrraction Xcalibur Gemini single crystal X-ray diffractometer using graphite monochromated Mo Kα radiation (λ = 0.71073 Å). The crysAlispro software[9] was used for data collection, reduction and absorption correction. In case of Complex **1** the unit cell parameters and the intensity data were obtained at 100 K on a Bruker-Nonius SMART APEX CCD single crystal diffractometer, equipped with a graphite monochromator and a Mo Kα fine-focus sealed tube (λ = 0.71073 Å) operated at 2.0 kW. The detector was placed at a distance of 6.0 cm from the crystal. The SMART software was used for data acquisition and the SAINT-Plus software was used for data extraction.[10] An absorption correction was performed with the help of SADABS program.[11] Both complexes crystallize in the triclinic $P\bar{1}$ space group. Each of the two structures was solved by direct methods and refined on F^2 by full-matrix least-squares procedures. All non-hydrogen atoms were refined anisotropically. Hydrogen atoms were included in the structure factor calculations at idealized positions by using a riding model. The SHELX-97[12] programs available in the WinGx[13] package were used for structure solution and refinement. The ORTEX6a[14] and Platon[15] packages were used for molecular graphics. Significant crystallographic data are summarized in

Table 4.1. Atomic coordinates for **1** and **2** are listed in tables 4.2 and 4.3, respectively.

Table 4.1. Crystallographic data for **1** and **2**.

Complex	**1**	**2**
Chemical formula	$Cu_2C_{24}H_{20}N_4O_4$	$Cu_2C_{25}H_{29}N_4O_{11}Cl_1$
Formula weight	555.52	724.05
Crystal system	Triclinic	Triclinic
Space group	$P\bar{1}$	$P\bar{1}$
Temperature (K)	100	298
a (Å)	8.3167(17)	8.3910(17)
b (Å)	9.3072(19)	12.101(2)
c (Å)	14.745(3)	15.059(3)
α (°)	79.53(3)	88.27(3)
β (°)	80.95(3)	86.40(3)
γ (°)	81.84(3)	74.44(3)
V (Å^3)	1100.8(4)	1470.0(5)
Z	2	2
ρ (g cm^3)	1.676	1.636
μ (mm^{-1})	1.973	1.603
Reflections collected	10642	9767
Reflections unique	3859	5157
Reflections ($I \geq 2\sigma(I)$)	2997	4220
Parameters	309	410
$R1$, $wR2$ ($I \geq 2\sigma(I)$)	0.0377, 0.0930	0.0400, 0.1075
$R1$, $wR2$ (all data)	0.0517, 0.0989	0.0512, 0.1110
GOF (F^2)	1.039	1.067
Largest peak and hole (e Å^{-3})	0.442, − 0.252	1.023, –0.583

Table 4.2. Atomic coordinates (x 10^4) and equivalent isotropic displacement parameters ($Å^2$x 10^3) for [Cu_2(μ-L)(μ-OCH_3)] (**1**).

Atom	x	y	z	U(eq)
Cu(1)	3244(1)	4832(1)	9688(1)	45(1)
Cu(2)	5356(1)	6708(1)	8331(1)	44(1)
O(1)	1960(3)	4599(2)	10906(2)	47(1)
O(2)	4391(3)	4935(2)	8432(1)	46(1)
O(3)	6217(3)	8534(2)	8099(2)	48(1)
O(4)	4374(3)	6524(2)	9616(1)	43(1)
N(1)	944(3)	2863(3)	10278(2)	52(1)
N(2)	2090(3)	3301(3)	9527(2)	46(1)
N(3)	6212(3)	6696(3)	7056(2)	40(1)
N(4)	7048(3)	7885(3)	6641(2)	41(1)
C(1)	-215(4)	4057(4)	12529(2)	50(1)
C(2)	-1229(5)	3713(4)	13354(3)	60(1)
C(3)	-2174(5)	2603(4)	13469(3)	63(1)
C(4)	-2136(5)	1824(4)	12761(3)	66(1)
C(5)	-1119(4)	2149(4)	11936(2)	53(1)
C(6)	-146(4)	3271(3)	11812(2)	44(1)
C(7)	980(4)	3603(4)	10944(2)	43(1)
C(8)	2268(4)	2641(4)	8820(2)	51(1)
C(9)	3347(4)	2989(3)	7963(2)	42(1)

C(10)	3339(4)	2148(4)	7273(2)	48(1)
C(11)	4246(4)	2407(3)	6403(2)	43(1)
C(12)	5161(4)	3570(3)	6222(2)	43(1)
C(13)	5220(4)	4469(3)	6879(2)	40(1)
C(14)	4325(4)	4142(3)	7772(2)	40(1)
C(15)	6138(4)	5697(3)	6568(2)	42(1)
C(16)	6968(4)	8752(3)	7256(2)	40(1)
C(17)	7820(4)	10079(3)	6981(2)	39(1)
C(18)	8551(4)	10487(4)	6081(2)	49(1)
C(19)	9372(4)	11714(4)	5846(3)	57(1)
C(20)	9469(4)	12527(4)	6515(3)	60(1)
C(21)	8730(5)	12143(4)	7416(3)	61(1)
C(22)	7918(4)	10917(4)	7646(2)	49(1)
C(23)	4231(5)	1439(4)	5689(2)	54(1)
C(24)	3697(5)	7750(4)	10064(3)	61(1)

Table 4.3. Atomic coordinates (x 10^4) and equivalent isotropic displacement parameters (Å^{2}x 10^3) for $[Cu_2(\mu\text{-HL})(\mu\text{-}OCH_3)(H_2O)]ClO_4 \cdot CH_3OH \cdot H_2O$ (**2**).

Atom	x	y	z	U(eq)
Cu(1)	6210(1)	4539(1)	3298(1)	11(1)
Cu(2)	6855(1)	5093(1)	5111(1)	11(1)
O(1)	4735(3)	4973(2)	2327(2)	14(1)
O(2)	7589(3)	3874(2)	4257(2)	13(1)
O(3)	6470(3)	6339(2)	5929(2)	14(1)
O(4)	5244(3)	5660(2)	4214(2)	12(1)
O(5)	8071(3)	5458(2)	2700(2)	16(1)
N(1)	6207(4)	3234(3)	1839(2)	14(1)
N(2)	7019(3)	3148(2)	2618(2)	12(1)
N(3)	8731(3)	4476(3)	5804(2)	13(1)
N(4)	8880(3)	5190(3)	6491(2)	13(1)
C(1)	2709(5)	5424(4)	932(3)	21(1)
C(2)	1724(5)	5663(4)	212(3)	28(1)
C(3)	1990(5)	4900(4)	-478(3)	29(1)
C(4)	3238(5)	3890(4)	-461(3)	30(1)
C(5)	4255(5)	3630(4)	254(2)	21(1)
C(6)	3992(4)	4406(3)	953(2)	14(1)
C(7)	5014(4)	4218(3)	1739(2)	13(1)
C(8)	8096(4)	2205(3)	2823(2)	13(1)

C(9)	9022(4)	2056(3)	3625(2)	12(1)
C(10)	10245(4)	1010(3)	3705(2)	15(1)
C(11)	11282(4)	781(3)	4409(2)	16(1)
C(12)	11081(4)	1618(3)	5048(2)	17(1)
C(13)	9856(4)	2670(3)	5016(2)	13(1)
C(14)	8799(4)	2888(3)	4295(2)	12(1)
C(15)	9806(4)	3482(3)	5716(2)	14(1)
C(16)	7635(4)	6134(3)	6486(2)	12(1)
C(17)	7541(4)	7015(3)	7168(2)	14(1)
C(18)	8606(5)	6824(3)	7869(2)	17(1)
C(19)	8482(5)	7667(4)	8495(3)	24(1)
C(20)	7282(5)	8708(4)	8440(3)	26(1)
C(21)	6222(5)	8898(3)	7746(3)	24(1)
C(22)	6344(4)	8071(3)	7112(3)	18(1)
C(23)	12613(5)	-336(3)	4465(3)	22(1)
C(24)	4655(5)	6854(3)	4026(3)	25(1)
Cl	8195(2)	8550(1)	2113(1)	41(1)
O(6)	9775(6)	7781(5)	2095(6)	151(4)
O(7)	8119(8)	9507(4)	2622(3)	96(2)
O(8)	7719(7)	8944(4)	1248(3)	79(2)
O(9)	7085(5)	7940(3)	2494(3)	56(1)
O(10)	7819(5)	1505(4)	8991(3)	62(1)
C(25)	6548(8)	1733(5)	8373(4)	63(2)
O(11)	7509(4)	1340(2)	792(2)	31(1)

Table 4.4. Selected bond lengths (Å) and angles (^{o}) for [Cu_2(μ-L)(μ-OCH_3)] (**1**).

Cu(1)-N(2)	1.895(3)	Cu(1)-O(2)	1.938(2)
Cu(1)-Cu(2)	2.9379(12)	Cu(2)-O(3)	1.891(2)
Cu(2)-N(3)	1.904(3)	Cu(2)-O(2)	1.908(2)
Cu(2)-O(4)	1.929(2)	N(2)-Cu(1)-O(4)	169.51(10)
N(2)-Cu(1)-O(1)	82.68(10)	O(4)-Cu(1)-O(1)	105.61(9)
N(2)-Cu(1)-O(2)	91.57(10)	O(4)-Cu(1)-O(2)	79.99(9)
O(1)-Cu(1)-O(2)	174.16(8)	N(2)-Cu(1)-Cu(2)	130.49(8)
O(4)-Cu(1)-Cu(2)	40.38(6)	O(1)-Cu(1)-Cu(2)	145.60(7)
O(2)-Cu(1)-Cu(2)	39.80(6)	O(3)-Cu(2)-N(3)	82.45(10)
O(3)-Cu(2)-O(2)	173.40(9)	N(3)-Cu(2)-O(2)	92.81(10)
O(3)-Cu(2)-O(4)	104.04(9)	N(3)-Cu(2)-O(4)	173.44(9)
O(2)-Cu(2)-O(4)	80.64(9)	O(3)-Cu(2)-Cu(1)	143.48(7)
N(3)-Cu(2)-Cu(1)	133.17(8)	O(2)-Cu(2)-Cu(1)	40.56(6)

Table 4.5. Selected bond lengths [Å] and angles [°] for $[Cu_2(\mu\text{-HL})(\mu\text{-}OCH_3)(H_2O)]ClO_4 \cdot CH_3OH \cdot H_2O$.[a]

Cu(1)-O(2)	1.927(2)	Cu(1)-O(1)	1.944(2)
Cu(1)-O(5)	2.276(3)	Cu(1)-Cu(2)	2.9468(9)
Cu(2)-N(3)	1.911(3)	Cu(2)-O(3)	1.923(3)
Cu(2)-O(2)	1.933(2)	Cu(2)-O(4)	1.949(2)
Cu(2)-O(4)#1	2.355(3)	O(4)-Cu(2)#1	2.355(2)
O(2)-Cu(1)-N(2)	91.04(11)	O(2)-Cu(1)-O(4)	80.64(10)
N(2)-Cu(1)-O(4)	164.87(11)	O(2)-Cu(1)-O(1)	170.73(10)
N(2)-Cu(1)-O(1)	82.31(11)	O(4)-Cu(1)-O(1)	104.35(10)
O(2)-Cu(1)-O(5)	93.06(10)	N(2)-Cu(1)-O(5)	96.79(11)
O(4)-Cu(1)-O(5)	96.27(10)	O(1)-Cu(1)-O(5)	94.14(10)
O(2)-Cu(1)-Cu(2)	40.30(7)	N(2)-Cu(1)-Cu(2)	131.18(9)
O(4)-Cu(1)-Cu(2)	40.87(7)	O(1)-Cu(1)-Cu(2)	145.22(7)
O(5)-Cu(1)-Cu(2)	90.99(7)	N(3)-Cu(2)-O(3)	82.57(11)
N(3)-Cu(2)-O(2)	91.89(11)	O(3)-Cu(2)-O(2)	170.94(10)
N(3)-Cu(2)-O(4)	169.24(11)	O(3)-Cu(2)-O(4)	104.11(10)
O(2)-Cu(2)-O(4)	80.37(10)	O(3)-Cu(2)-O(4)#1	94.15(10)
O(2)-Cu(2)-O(4)#1	94.18(10)	O(4)-Cu(2)-O(4)#1	83.64(10)
N(3)-Cu(2)-Cu(1)	130.27(9)	O(3)-Cu(2)-Cu(1)	142.53(8)
O(2)-Cu(2)-Cu(1)	40.15(7)	O(4)-Cu(2)-Cu(1)	40.75(7)
O(4)#1-Cu(2)-Cu(1)	93.67 (6)		

a = Symmetry transformations used to generate equivalent atoms:
#1 -x+1,-y+1,-z+1

4.4. Results and Discussion

4.4.1. Syntheses and characterization

The complexes **1** and **2** have been synthesized in moderate to good yield by reacting one mole equivalent of binucleating pentadentate N_2O_3 donor Schiff base H_3L (2-hydroxy-5-methyl benzene-1,3-dicarbaldehydebis(benzoylhydrazone)) with two mole equivalents of $Cu(O_2CCH_3)_2 \cdot H_2O$ (for **1**) and $Cu(ClO_4)_2 \cdot 6H_2O$ (for **2**) in methanol. The elemental analysis data are satisfactory with the empirical molecular formulas of the complexes. The molar conductivity Λ_M (146 Ω^{-1} cm^2 mol^{-1}) of the complex **2** in acetonitrile is within the range expected for a 1:1 electrolyte.[16] This value indicates that the perchlorate is outside the coordination sphere. The effective magnetic moments of **1** and **2** at room temperature (298 K) are within 2.10-2.22 μ_B .

4.4.2. Spectroscopic properties

The infrared spectra of H_3L and complexes **1** and **2** were collected in KBr pellets. The spectra are shown in Figure 4.2. The free ligand H_3L shows υ(OH) and υ(NH) at 3431 cm^{-1} and 3213 cm^{-1}, respectively. The υ(C=O) stretching vibration is observed 1651 cm^{-1} and υ(C=N) stretching vibration is observed 1550 cm^{-1}. The complexes display these bands at ~ 1600 cm^{-1} and ~ 1550 cm^{-1}, respectively.[17,18] A weak band at 3580 cm^{-1} observed for **2** is possibly due to the coordinated water molecules.[19] The strong and broad band centered at 1080 cm^{-1} and the sharp and strong band at 623 cm^{-1} observed for **2** are typical for the perchlorate counterion.

a) Ligand H_3L

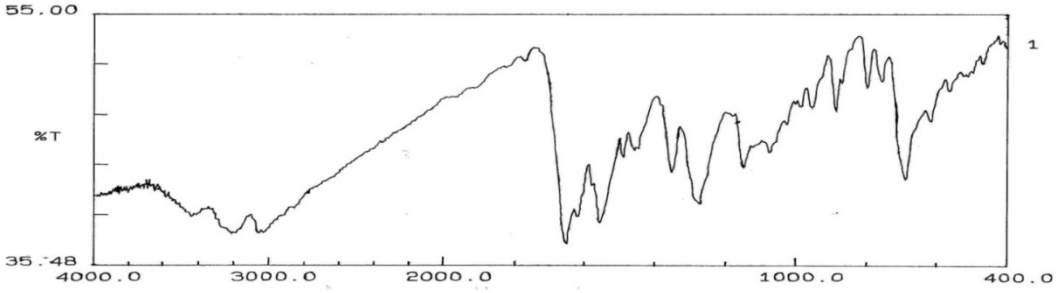

Wavelength (nm)

b) Complex **1**

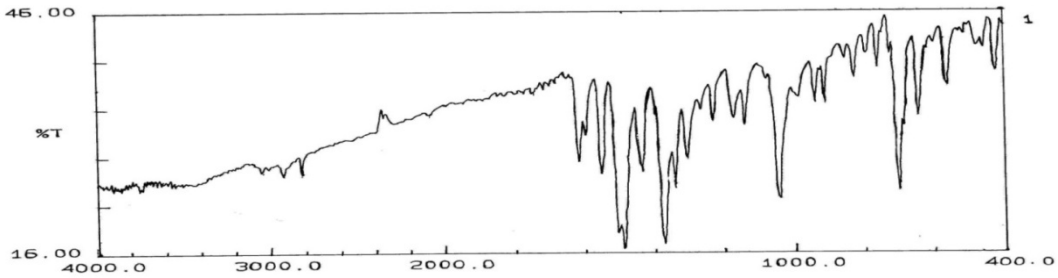

Wavelength (nm)

c) Complex **2**

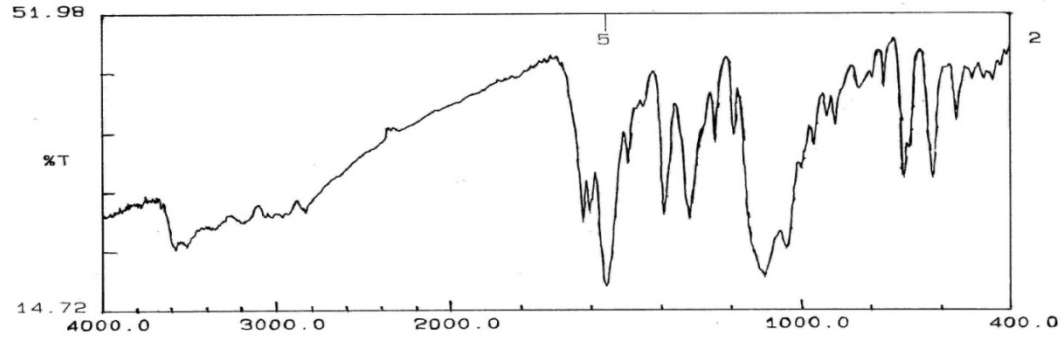

Wavelength (nm)

Figure 4. 2. Infrared spectra of (a) H_3L, (b) **1** and (c) **2**.

The electronic spectra of **1** and **2** were recorded using their methanol solutions. The spectra are displayed in Figures 4.3 and 4.4. The spectral profiles of the two complexes are very similar and display a weak band in the range 651-667 nm corresponding to the d-d transition.[20-25] The remaining bands below 500 nm are likely to be associated with charge transfer and intra ligand transitions.[26]

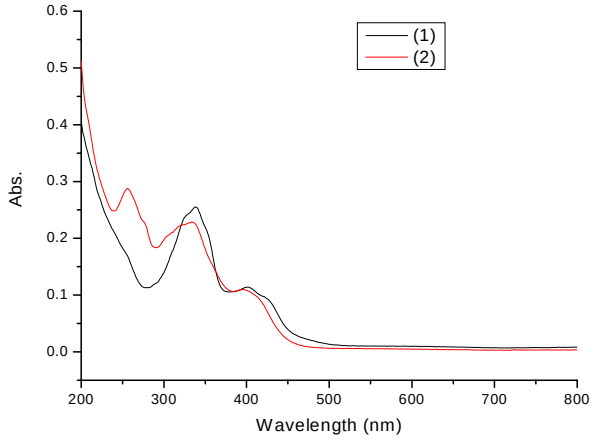

Figure 4.3. The electronic spectra of **1** and 2 in methanol.

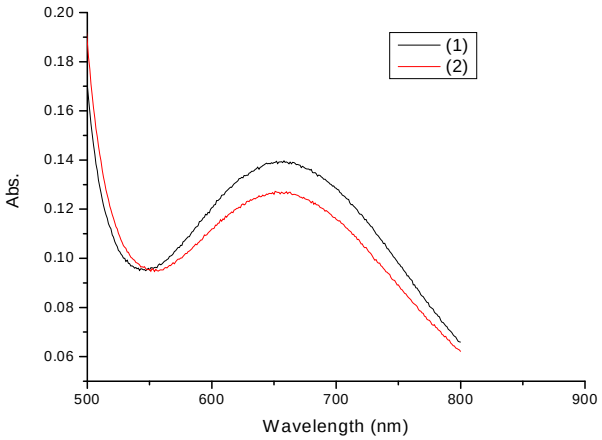

Figure 4.4. The d-d transitions observed for **1** and **2**.

Both complexes **1** and **2** are EPR silent (Figure 4.5), in their polycrystalline state as well as in 1:1 acetonitrile-toluene mixture, due to the presence of strong antiferromagnetic interaction between the Cu(II) centers.

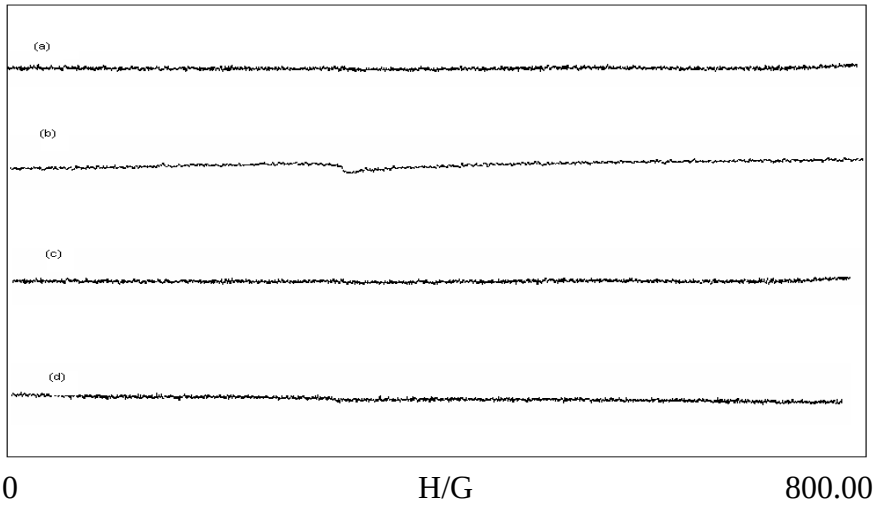

Figure 4.5. X-band EPR spectrum of **1**; (a) in polycrystalline sample at 298 K. (b) in polycrystalline phase at 120 K, (c) in acetonitrile-toluene (1:1) at 298 K using flat cell and (d) in frozen acetonitrile-toluene (1:1) at 120 K.

4.4.3. Cryomagnetic behavior of $[Cu_2(\mu\text{-}L)(\mu\text{-}OCH_3)]$ (**1**).

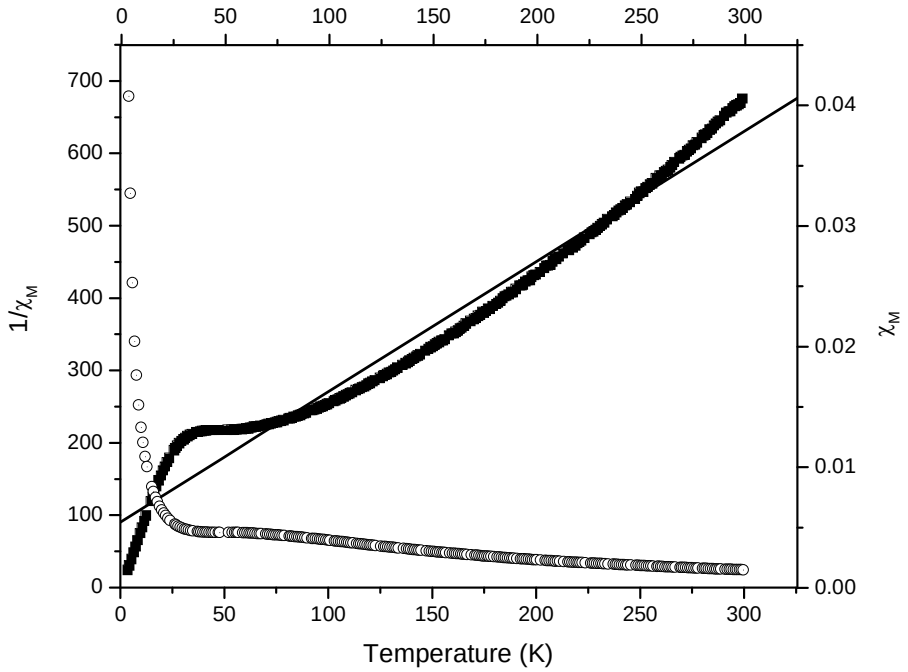

Figure 4.6. χ_M (○) and $1/\chi_M$ (■) of $[Cu_2(\mu\text{-}L)(\mu\text{-}OCH_3)]$ (**1**) as functions of temperature. The solid line represents the fitting of the data using Curie-Weiss law.

Temperature dependent magnetic susceptibility measurements of $[Cu_2(\mu\text{-}L)(\mu\text{-}OCH_3)]$ (**1**) have been performed (Figure 4.6). The complex **1** shows an antiferromagnetic behavior. The data were fit with the Curie-Weiss law, $\chi_M = C/(T-\theta)$. The fit provides the Weiss constant θ as –50.32 K and Curie constant C as 0.556 emu/g Oe. From Curie constant C, effective magnetic moment (μ_{eff}) of

$[Cu_2(\mu\text{-}L)(\mu\text{-}OCH_3)]$ can be evaluated by using the $\mu_{eff}^2 = 3Ck/\mu_B^2N$ equation where k is the Boltzmann constant, μ_B is the Bohr magneton and *N* is the Avogadro's number. From the above expression μ_{eff} is calculated as 2.10 μ_B per two copper. The spin only magnetic momentum of Cu^{+2} ion can be estimated using the equation $\mu_{eff} = \mu_S = 2[S(S+1)]^{1/2}$ since Cu^{+2}, a d^9 system, has no orbital moment ($L = 0$) contribution. The value calculated is 2.45 μ_B. The difference in the experimental value and the calculated value for two copper centers, is due to antiferromagnetic super exchange through phenolate oxygen (O2) and methoxo (O4) bridges.

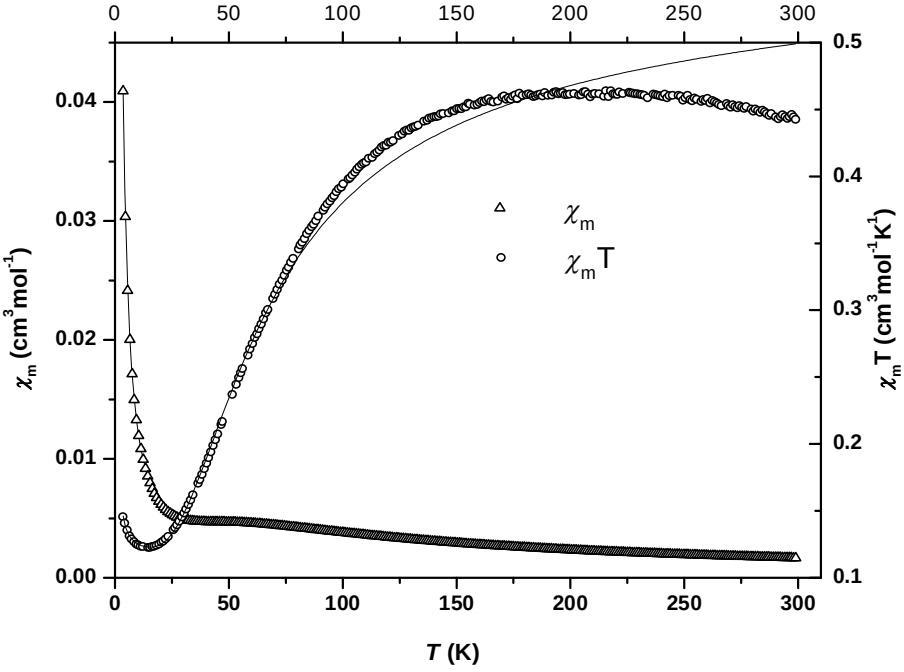

Figure 4.7. χ_M (○) and $1/\chi_M$ (■) of $[Cu_2(\mu\text{-}L)(\mu\text{-}OCH_3)]$ (**1**) as functions of temperature. The solid line represents the quality of the data fitting using the Bleaney–Bowers equation.

The data were also analyzed (Figure 4.7) using Bleaney-Bowers expression.[27] The parameters used are: χ in the paramagnetic susceptibility per molecule after correction for diamagnetism, p is the paramagnetic impurities, g_i is the average g factor, –2J is the singlet–triplet energy separation and Nα is the temperature independent paramagnetism (TIP). TIP is assumed to be 60 x10^{-6} cm^3 mol^{-1} for Cu(II) dimers.[28] The optimized values for the parameters are g = 2.37, J = -42.28 (3) cm^{-1} and Nα = 60 x 10^{-6}.

4.4.4. Powder X-ray diffraction of complexes 1 and 2.

The phase purity of **1** and **2** bulk samples were confirmed by comparing the experimental powder X-ray diffraction patterns with those simulated from the single crystal data using Mercury 2.4 software. The experimental and simulated diffraction patterns are shown in Figure 4.8. The very similar experimental and simulated powder X-ray diffraction patterns indicate the homogeneous nature of the complex **1**, where as in the complex **2**, a slight difference between experimental and simulated patterns is attributed to loss of uncoordinated solvent molecules (methanol and water).

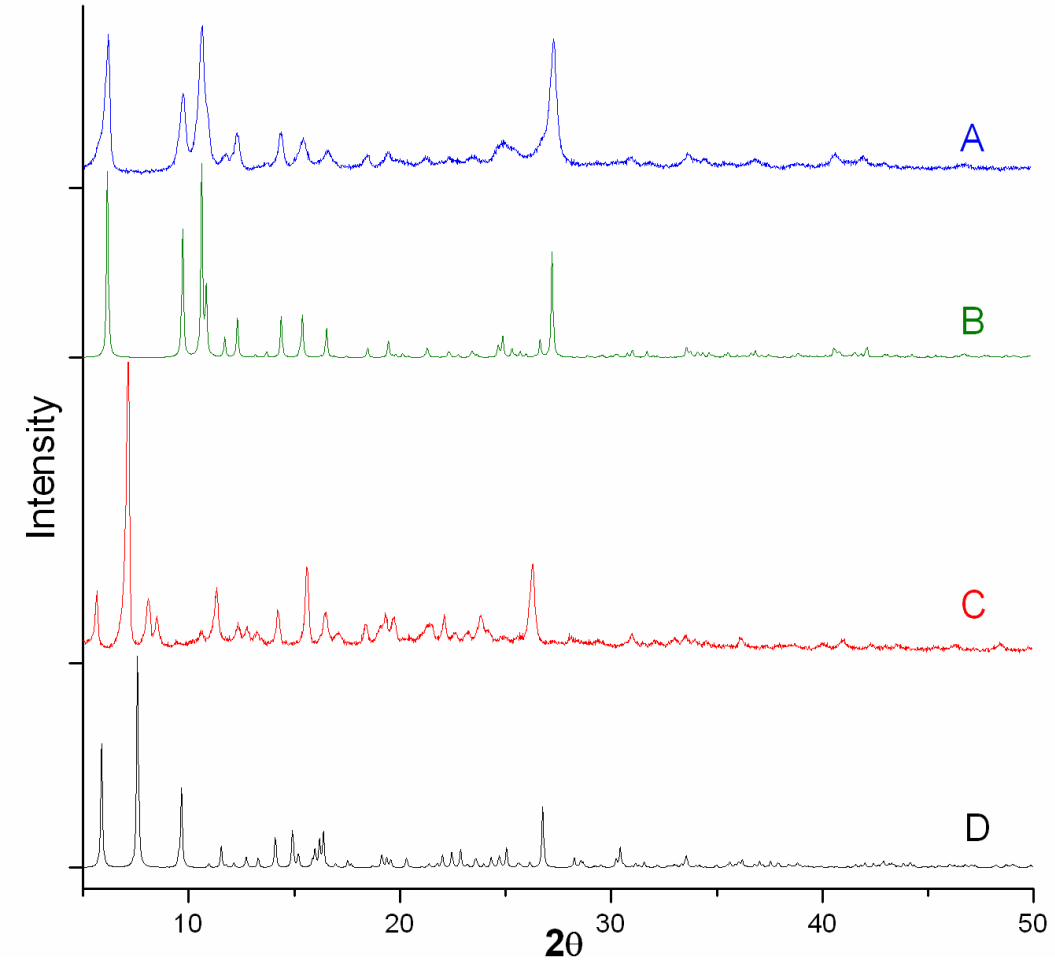

Figure 4.8. Powder X-ray diffraction patterns of **1** (curve A experimental and curve B simulated) and **2** (curve C experimental and curve D simulated).

4.4.5. Structural description of complexes **1** and **2**

The structures of complexes **1** and **2** were determined by X-ray structural analysis using single crystals obtained directly from reaction mixture. Important

bond lengths and angles are given in Tables 4.4 and 4.5. The ORTEP drawings of **1** and **2** with the atom numbering schemes are shown in Figures 4.9 and 4.10.

The asymmetric unit of **1** contains a single complex molecule (Figure 4.9) while that of **2** contains one dinuclear complex cation, the counter anion perchlorate, one water and one methanol molecule (Figure 4.10). The two copper centers are symmetrically coordinated in **1** and unsymmetrically coordinated in **2** with pentadentate N_2O_3 donor ligand, to form two six membered and two five membered fused chelating rings. Each Cu(II) center is in a square-plane formed by N-imine, O-iminolato, O-phenolato, O-methoxo donor atoms. The two copper(II) centers of each of **1** and **2** are bridged by an endogenous phenolate-O and an exogenous methoxo-O atom, to form a four membered Cu_2O_2 butterfly core. The complex **1** dimerises through two pairs of weak reciprocal equatorial-apical bridges involving the iminolate-O and methoxo-O atoms and complex **2** dimerises via a pair of weak reciprocal equatorial-apical bridges involving methoxo-O atom to produce corresponding dimer of dimer form in their solid state (Figures 4.11 and 4.12). Each of the copper centers in **1** and **2** are in distorted square pyramidal geometry. The water molecule satisfies the fifth coordination site of second Cu(II) center of **2**, which does not participate in bridging of dimers. The ligand is in tribasic form (L^{3-}) in **1,** while in **2** it is in dibasic form (HL^{2-}). The same thing was confirmed by its IR spectral studies (Section 4.4.2) as well as its single crystal X-ray structural analysis. The arms of the ligand in **2** are unsymmetrical because of its dibasic form (HL^{2-}), which makes the two Cu(II) centers and their bonding parameters different in **2**. The bond distances Cu1-O1 and Cu1-N2 of protonated arm are significantly longer than same set of bond distances Cu2-O3 and Cu2-N3 of the deprotonated arm. The longer bond distance C7-N and shorter bond distance C7-O1 of protonated arm compared to bond distance C16-N4 and C16-O3 of deprotonated arm, also

supports the existence of dibasic (HL^{2-}) form in complex $[Cu_2(\mu\text{-}HL)(\mu\text{-}OCH_3)(H_2O)]ClO_4{\cdot}CH_3OH{\cdot}H_2O$ (**2**). These bond distances are listed in Table 4.6

Table 4.6. Bond distances involwing two unsymmetrical arms in **2**.

Protonated amide (Arm 1)		Deprotonated amide (Arm 2)	
Cu1-O1	1.944(2)	Cu2-O3	1.923(3)
Cu1-O2	1.927(2)	Cu2-O2	1.933(2)
Cu1-O4	1.944(2)	Cu2-O4	1.949(2)
Cu1-N2	1.935(3)	Cu2-N3	1.911(3)
N1-N2	1.382(4)	N3-N4	1.400(4)
C7-N1	1.346(5)	C16-N4	1.325(5)
C7-O1	1.257(4)	C16-O3	1.296(4)

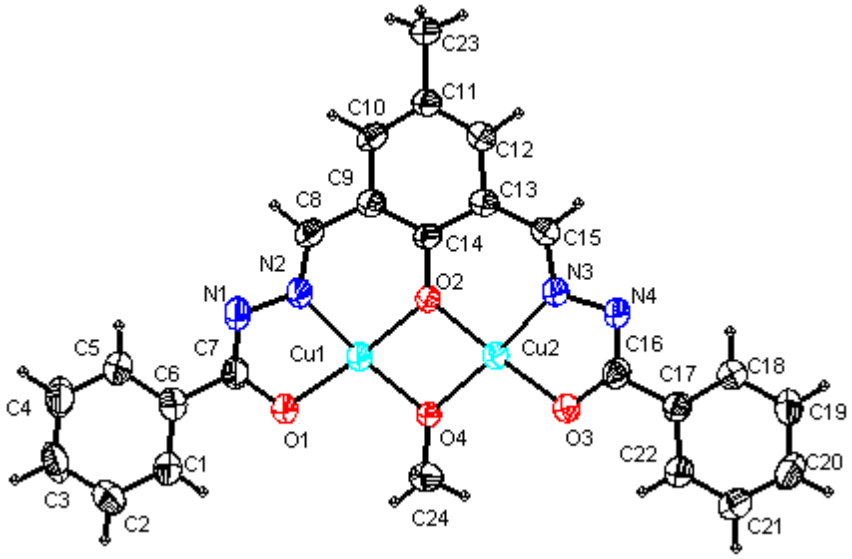

Figure.4.9. Ortep representation of $[Cu_2(\mu\text{-}L)(\mu\text{-}\ OCH_3)]$ (**1**) with their atom labeling scheme.

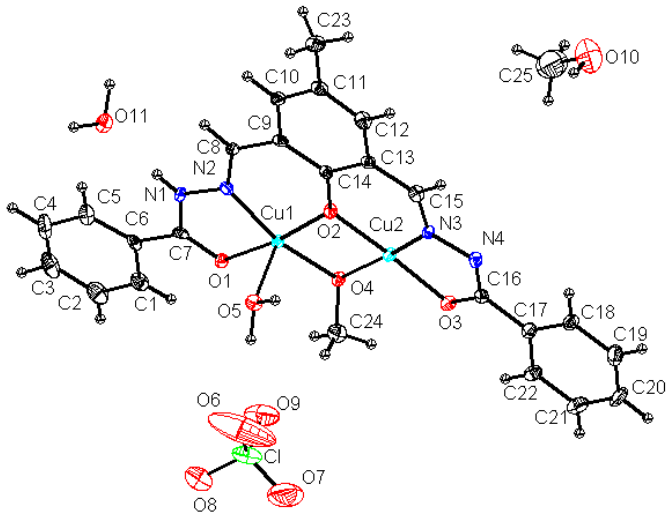

Figure.4.10. Ortep representation of $[Cu_2(\mu\text{-}HL)(\mu\text{-}OCH_3)(H_2O)]ClO_4{\cdot}CH3OH{\cdot}H_2O$ (**2**) with their atom labeling scheme.

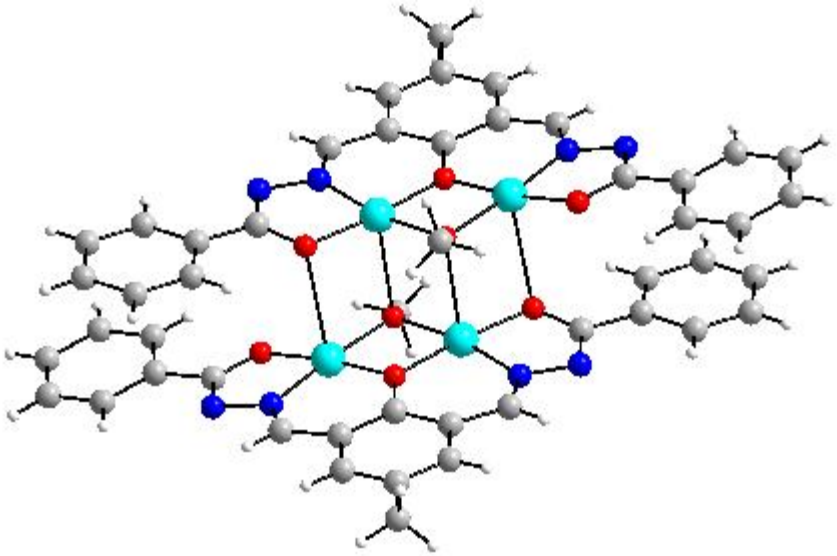

Figure.4.11. Dimer of dimer structure of [Cu_2(μ-L)(μ- OCH_3)] (**1**).

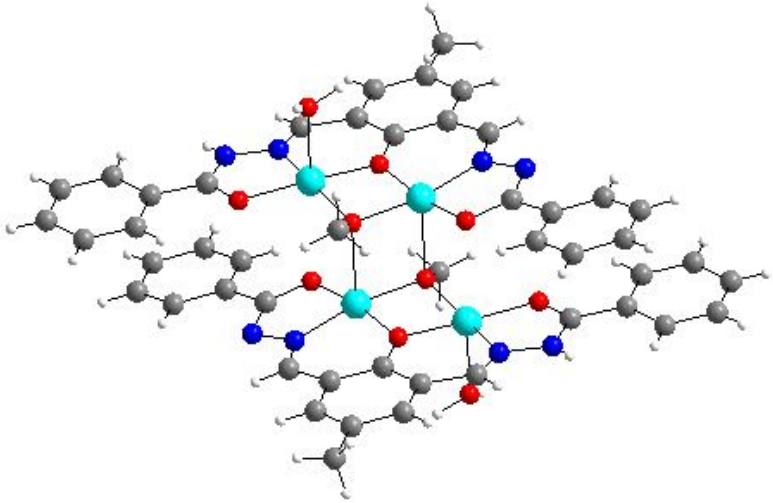

Figure.4.12. Dimer of dimer representation of [Cu_2(μ-HL)(μ-OCH_3)(H_2O)]ClO_4·CH_3OH·H_2O complex (counter ion and solvent molecules are excluded for clarity).

4.4.6. Supramolecular structure of 2.

In complex $[Cu_2(\mu\text{-HL})(\mu\text{-OCH}_3)(H_2O)]ClO_4\cdot CH_3OH\cdot H_2O$ (**2**), the solvent molecules trapped in the crystal lattice and the counter perchlorate ion plays important roles to built the corresponding supramolecular structures and forms a six membered molecular ring with the help of inter molecular hydrogen bonding interactions (Table 4.7).

Table 4.7. Hydrogen bonds in $[Cu_2(\mu\text{-HL})(\mu\text{-OCH}_3)(H_2O)]ClO_4\cdot CH_3OH\cdot H_2O$ (**2**) [Å and °].

D-H...A	d(D-H)	d(H...A)	d(D...A)	<(DHA)
N(1)-H(2A)...O(11)	0.75(5)	2.03(5)	2.755(4)	163(5)
O(5)-H(5A)...O(9)	0.958(10)	1.964(14)	2.906(4)	167(3)
O(5)-H(5B)...N(4)#2	0.958(10)	1.875(14)	2.811(4)	165(3)
O(10)-H(10A)...O(6)#2	0.979(10)	1.868(17)	2.815(6)	162(3)
O(11)-H(11A)...O(10)#3	0.987(10)	2.04(4)	2.715(5)	124(4)
O(11)-H(11B)...O(8)#4	0.965(10)	1.965(14)	2.920(5)	170(4)

Symmetry transformations used to generate equivalent atoms:
#1 -x+1,-y+1,-z+1 #2 -x+2,-y+1,-z+1 #3 x, y, z-1
#4 x, y-1, z

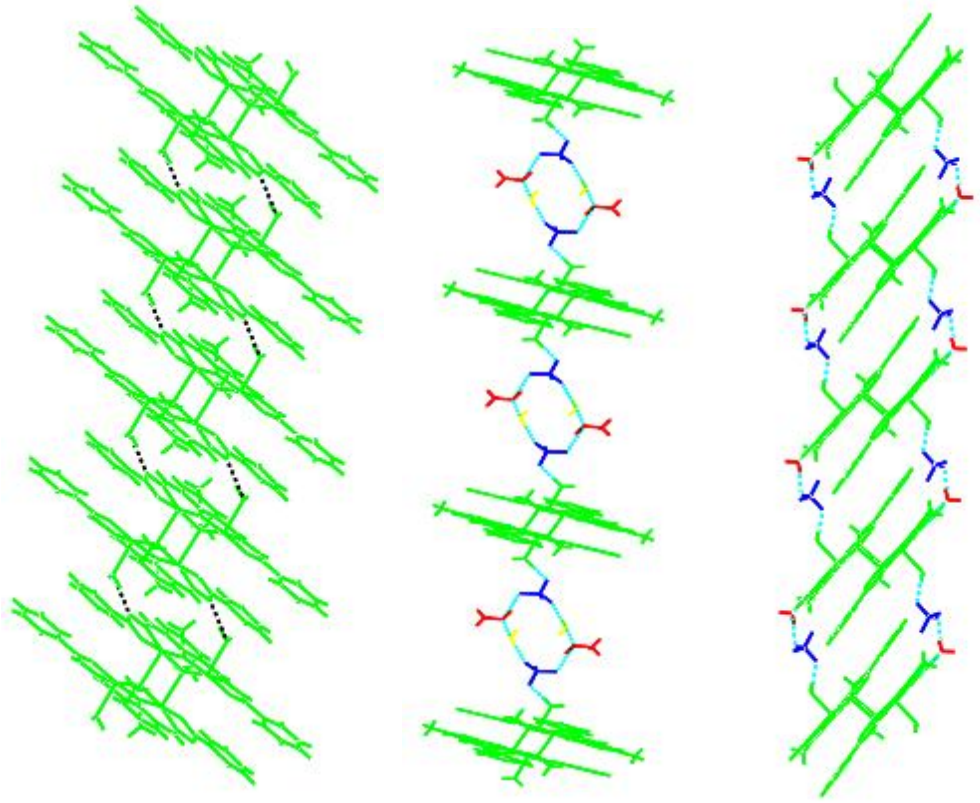

(a) **(b)** **(c)**

Figure 4.13. One dimensional self-assembly of **2** assisted by three different intermolecular hydrogen bonding.

(a)

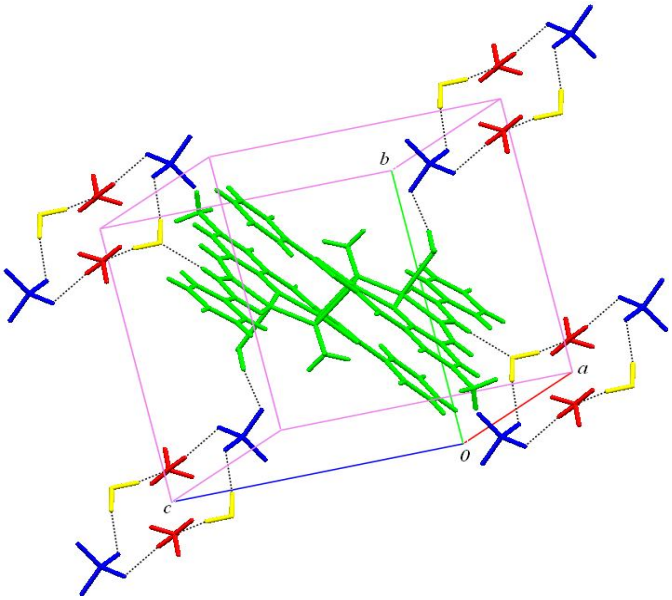

(b)

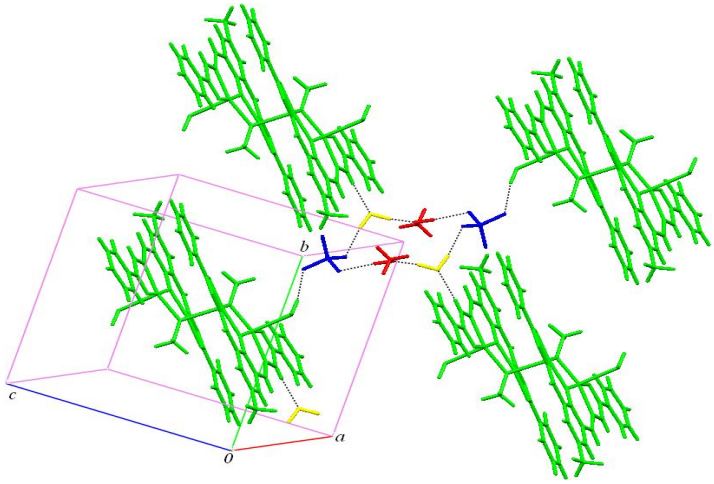

Figure 4.14. (a) primary and (b) secondary building blocks for three dimensional frame work (assistated by hydrogen bonding) of complex **2**.

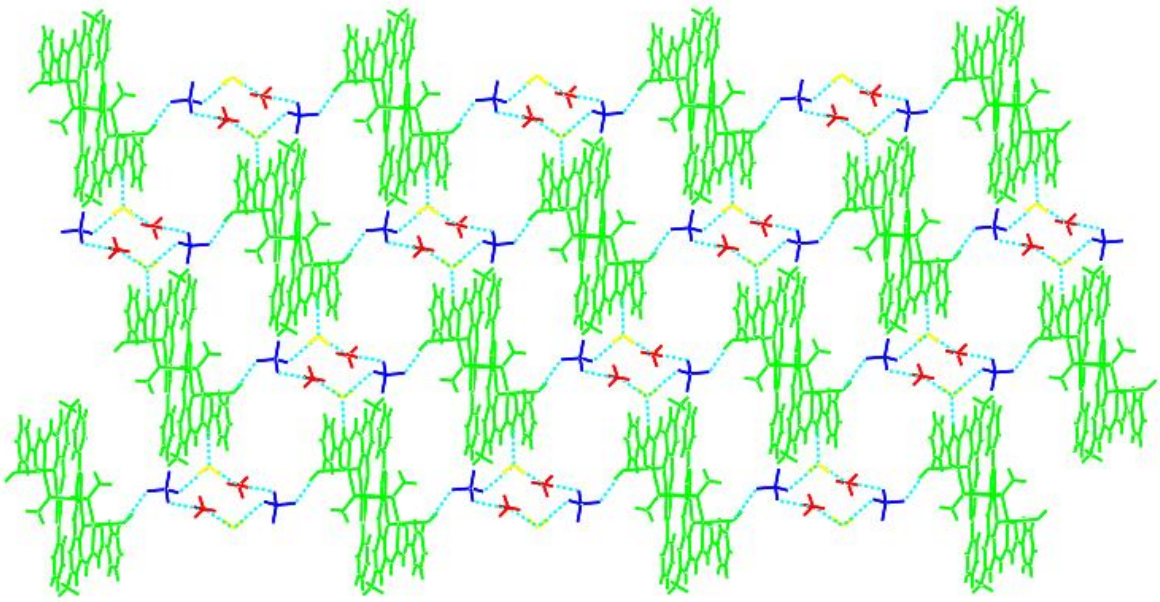

(a)

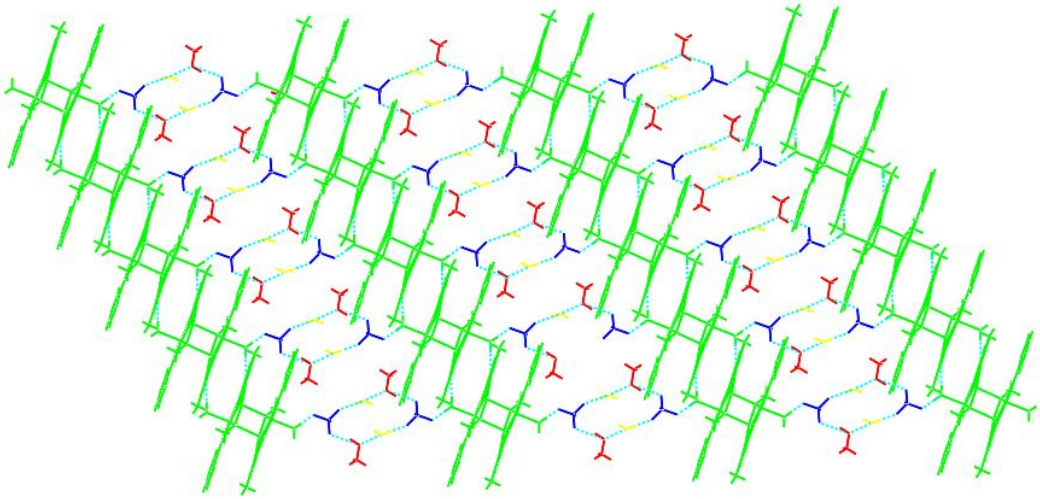

(b)

Figure 4.15. 2d layers of $[Cu_2(\mu\text{-}HL)(\mu\text{-}OCH_3)(H_2O)]ClO_4{\cdot}CH_3OH{\cdot}H_2O$ (**2**)**.**

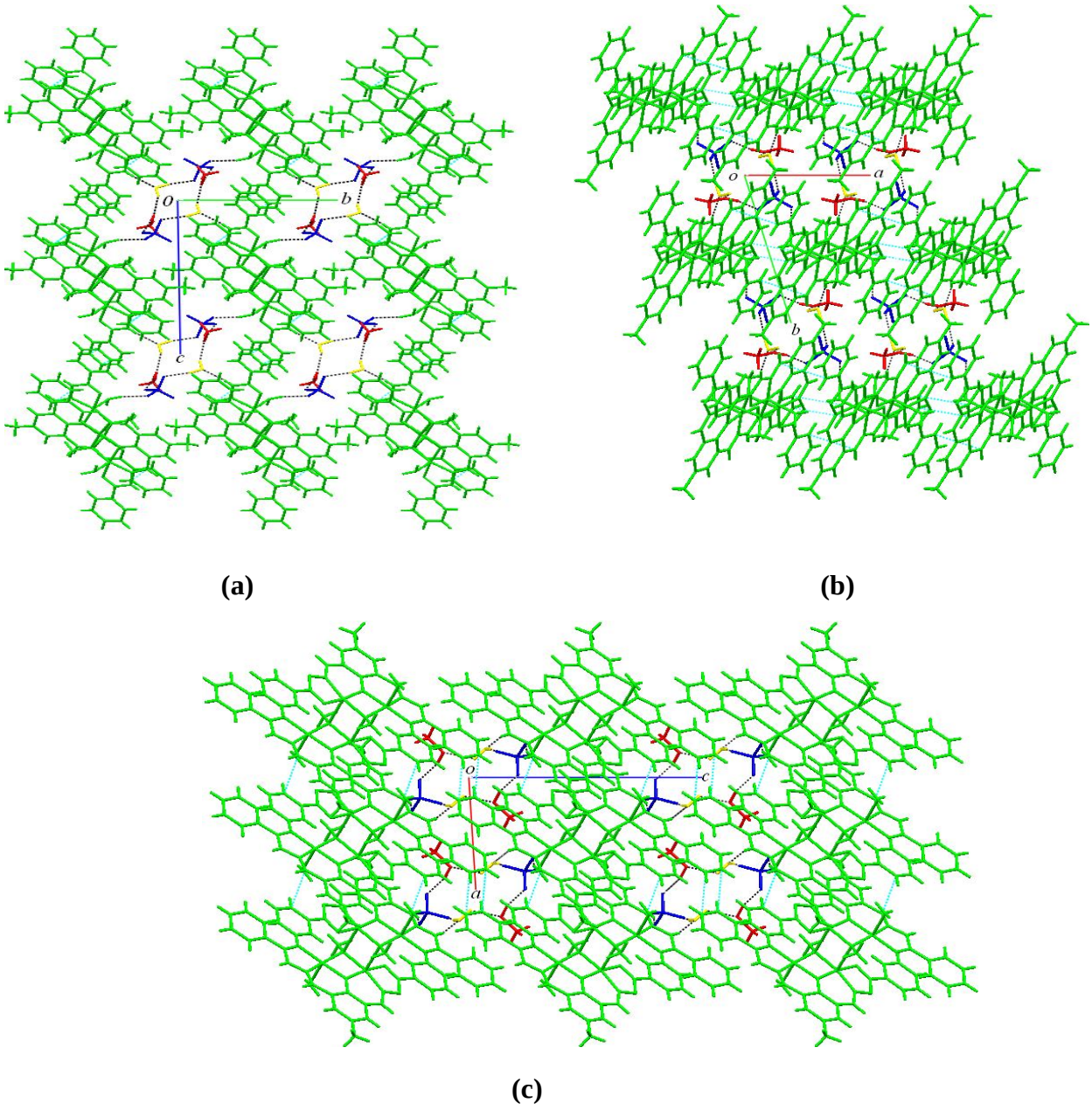

Figure 4.16. Three dimensional networks of **2** (a) along *a* axis (b) along *c* axis and (c) along *b* axis.

The inter molecular hydrogen bonding between apically coordinated water molecule and amidate-N (O(5)-H(5B)...N(4)#2) leads to a one dimensional chain running along one of the crystallographic axis. The hydrogen bonding (O(5)-H(5A)...O(9)) between two apically coordinated water molecule and two perchlorate ions in the six membered molecular cycle assembles a one dimensional chain like structure (Figure 4.13). The repeating units in one dimensional chain consists two molecules of **2** and inversely connected through inter molecular hydrogen bonding using the sequence of apically coordinated water molecule (O(5)-H(5A)...O(9)), counter perchlorate ion (O(11)-H(11B)...O(8)#4), lattice water molecule (N(1)-H(2A)...O(11)) and amide N-H (Figure 4.13).

As shown in Figure 4.14(a) and (b), each of the complex molecule is connected to four numbers of six membered molecular cycle and vice versa leading to formation of two dimensional layers (Figure 4.15) and finally three dimensional networks (Figure 4.16).

4.5. Conclusion

The complexes $[Cu_2(\mu\text{-}L)(\mu\text{-}OCH_3)]$ (**1**) and $[Cu_2(\mu\text{-}HL)(\mu\text{-}OCH_3)(H_2O)]ClO_4{\cdot}CH_3OH{\cdot}H_2O$ (**2**) were synthesized in moderate to good yields and characterized by elemental analysis, single crystal X-ray analysis and various spectroscopic methods. Cryomagnetic measurement of **1** reveals that the Cu(II) centers in complex **1** are antiferromagnetically coupled due to super exchange via endogenous phenolate-O and exogenous methoxo-O bridges. The molecular structures of **1** and **2** reveal that each Cu(II) center is in distorted square pyramidal geometry. The supramolecular structures of **2** assisted by various intermolecular hydrogen bonding were briefly discussed.

4.6. References

1. R. Robson, *Inorg. Nucl. Chem. Lett*, **1970**, *6*, 125; *Aust. J. Chem*., **1970**, *23*, 2217.
2. (a) H. Ōkawa, *Bull. Chem. Soc. Jpn*., **1970**, *43*, 3019. (b) H. Ōkawa, S. Kida, *ibid*., **1971**, *44*, 1172. (c) H. Ōkawa, S. Kida, Y. Muto, T. Tokii, *ibid*., **1972**, *45*, 2480. (c) H. Ōkawa, T. Tokii, Y. Nonaka, Y. Muto, S. Kida, *ibid*., **1973**, *46*, 1462. (d) H. Ōkawa, I. Ando, S. Kida, *ibid*., **1974**, *47*, 3041.
3. B. F. Hoskins, R. Robson, H. Schaap, *Inorg. Nucl. Chem. Lett*., **1972**, *8*, 21.
4. (a) D. J. Hodgson, *Prog. Inorg. Chem*., **1975**, *19*, 173. (b) C. J. O'Connor, *ibid*., **1982**, *29*,203. (c) M. Melnic, *Coord. Chem. Rev*., **1982**, *42*,259. (d) K. S. Murray, in *'Biological and Inorganic Copper Chemistry,' eds*. K. D. Karlin, J. Zubieta, *Adenine Press*, *New York*., **1987**, *2*, 161. (e) E. Sinn, *ibid*., p. 195. (f) P. Zanello, S. Tarnbririni, P. A. Vigato, G. A. Mazzocchin., *Coord. Chem. Rev*., **1987**, *77*, 165.
5. (a) T. N. Sorrel, D. L. Jameson, C. J. O'Connor, *Inorg. Chem*., **1980**, *23*, 190. (b) T. N. Sorrell, *Tetrahedron*., **1989**, *45*, 3.
6. P. Iliopoulos, K. S. Murray, R. Robson, J. Wilson, G. A. Williams, *J. Chem. Soc., Dalton Trans*., **1987**, 1585.
7. (a) T. Mallah, 0. Kahn, J. Gouteron, S. Jeannin, Y. Jeannin, C. J. O'Connor, *Inorg. Chem*., **1987**, *26*, 1375. (b) P. Guerriero, U. Casellato, D. Ajo, S. Sitran, P. A. Vigato, R. Graziani, *Inorg. Chim. Acta*., **1988**, *142*,305.

8. W.E. Hatfield, in: E.A. Boudreaux, L.N. Mulay (Eds.), *Theory and Applications of Molecular Paramagnetism*, Wiley, New York., **1976**, p. 491.
9. CrysAlisPro version 1.171.33, Oxford Diffraction Ltd., Abingdon, Oxfordshire, UK, **2007**.
10. SMART version 5.630 and SAINT-plus version 6.45, Bruker-Nonius Analytical X-ray Systems Inc., Madison, WI, USA, **2003**.
11. G.M. Sheldrick, SADABS, Program for Area Detector Absorption Correction, University of Göttingen, Göttingen, Germany, **1997**.
12. G.M. Sheldrick, XHELX-97, Structure Determination Software, University of Göttingen, Göttingen, Germany, **1997**.
13. L.J. Farrugia, J. Appl. Crystallogr., **1999**, *32*, 837-838.
14. P. McArdle, J. Appl. Crystallogr., **1995**, *28*, 65.
15. A.L. Spek, Platon, A Multipurpose Crystallographic Tool, Utrecht University, Utrecht, The Netherlands, **2002**.
16. W. J. Geary, *Coord. Chem. Rev.*, **1971**, *7*, 81−122.
17. K. Nakamoto, *Infrared and Raman Spectra of Inorganic and Coordination Compounds*, Wiley, New York, **1977**, p. 227.
18. K. Nakamoto, *Infrared and Raman Spectra of Inorganic and Coordination Compounds*, Wiley, New York, **1977**, p. 316
19. L. El Sayed, M. F. Iskander, J. *Inorg. Nucl. Chem.*, **1971**, *33*, 435.
20. D. Reinen, Friebel, *Inorg. Chem.*, **1984**, *23*, 741.
21. S. Karunakaran, M. Kandaswamy, *J. Chem. Soc., Dalton Trans.*, **1994**, 1595.

22. H. Okawa, J. Nishio, M. Ohba, Tadokoro, S. Kida, D. E. Fenton, *Inorg. Chem*., **1993**, *32*, 2949.

23. (a) S. Sujatha, T. M. Rajendiran, R. Kannappan, R. Venkatesan, P. Sambasiva Rao, *Indian Acad. Sci. (Chem. Sci.)*, **2000**, *112*, 1. (b) S. Karthikeyan , T. M. Rajendiran, R. Kannappan, R. Mahalakshmy, R. Venkatesan, P. Sambasiva Rao, *Indian Acad. Sci. (Chem. Sci.),* **2001**, *113*, 245.

24. (a) T. M. Rajendiran, R. Venkatesan, P. Sambasiva Rao, M. Kandaswamy, *Polyhedron*, **1998**, *17*, 3427. (b) T. M. Rajendiran, R. Kannappan, R. Venkatesan, P. Sambasiva Rao, M. Kandaswamy, *Polyhedron*, **1999**, *18*, 3085.

25. R. Kannappan, T. M. Rajendiran, R. Mahalakshmy, R. Venkatesan, P. Sambasiva Rao, *Indian Acad. Sci. (Chem. Sci.),* **2003**, *115*, 1.

26. (a) A. Taha, *Spectrochim. Acta A*., **2003**,*59*, 1611. (b) A.K. Patra, M. Nethaji, A.R. Chakravarty, *Dalton Trans*., **2005**, 2798. (c) P. Sarmah, R.K. Barman, P. Purkayastha, S.J. Bora, P. Phukan, B.K. Das, *Indian J. Chem. Sect. A*., **2009**, *48*, 637. (d) Z. Lu, T. Ladrak, O. Roubeau, J. van der Toorn, S. J. Teat, C. Massera, P. Gamez, J. Reedijk, *Dalton Trans*., **2009**, 3559. (e) A. Paulovicova, U. El-Ayaan, K. Shibayama, T. Morita, Y. Fukuda, *Eur. J. Inorg. Chem*., **2001**, 2641. (f) C.P. Pradeep, P.S. Zacharias, S.K. Das, *J. Chem. Sci*., **2005**, *117*, 133. (g) T. Ghosh, S. Das, S. Pal, *Polyhedron*., **2010**, *29*, 3074. (h) S. Maloth, S. Pal, *Polyhedron*., **2010**, *29*, 3257. (h) M. M. Whittaker, W.R. Duncan, J.W. Whittaker, *Inorg. Chem*., **1996**, *35*, 382. (i) A.W. Addison, T.N. Rao, J. Reedijk, J. van Rijn, G.C. Verschoor, *J. Chem. Soc., Dalton Trans.*, **1984**, 1349. (j) Z. Liu, C. Duan, Y. Tian, X.

You, *Inorg. Chem*., **1996**, *35*, 2253. (k) T. Ghosh, A. Mukhopadhyay, K.S.C. Dargaiah, S. Pal, *Struct. Chem*., **2010**, *21*, 147. (l) S.N. Pal, J. Pushparaju, N.R. Sangeetha, S. Pal, *Trans. Met. Chem*., **2000**, *25*, 528. (m) T. Ghosh, S. Pal, *Inorg. Chim. Acta*., **2010**, *363*, 3632.

27. B. Bleany, K. D. Bowers, *Proc. R. Soc. London*, **1952**, *A214*, 415.

28. L. K. Thompson, N. D. Donald, E. William, J. Fred Banks, R. M. Buchanan, Hsiu-Rougchay, R. J. Webb, D. N. Hendrickson, *Inorg. Chem*., **1990**, *29*, 1058.

Chapter 5

A Pentacobalt(III) Complex with a paramagnetic Octahedral Metal Center Exhibiting Thermal Spin Transition

5.1. Abstract

Synthesis, characterization, X-ray structure and properties of a pentanuclear Co(III) complex [{L(O_2CCH_3)$Co_2O(OCH_3)_2$}$_2$Co](ClO_4)$_3$ (**1**) (L^- = 2,6-bis((3-aminopropylimino)methyl)-4-methylphenola-te) are described. The central paramagnetic Co(III) in **1** has a distorted octahedral O_6 environment assembled by two μ_3-oxo and four μ_2-methoxo groups from the two diamagnetic {L(O_2CCH_3)$Co_2O(OCH_3)_2$} units. The μ_{eff} of **1** is temperature dependent.

5.2. Introduction

Spin crossover complexes are of considerable contemporary interest not only for the intricacies required in designing such systems but also for their potential applications as molecular materials in various devices that utilize their physical property changes associated with the high-spin (hs) to low-spin (ls) transition process.[1–3] The spin crossover is expected to occur for octahedral complexes of d^4–d^7 metal ions. The majority of the octahedral spin crossover complexes reported in literature are of Fe(III) (d^5), Fe(II) (d^6), and Co(II) (d^7). Unlike the large number and variety of magnetically uncoupled Fe(II) complexes, only one type of complex containing octahedral Co(III) another d^6 metal ion is known to exhibit spin crossover phenomenon. This species is [{η^5-

$CpCo(R_2PO)_3\}_2Co]^+$ where the central Co(III) that shows the spin transition is coordinated to two *facial* O_3-donor diamagnetic $\{\eta^5$-$CpCo(R_2PO)_3\}^-$ units ($Cp^- = C_5H_5^-$).[4] The primary reason for this scarcity is the very low Δ_o at the quintet-singlet crossing point in Co(III) than that in Fe(II). As a result fluoride a very weak ligand provides the only known high-spin Co(III) complexes $[CoF_6]^{3-}$ and $[CoF_3(H_2O)_3]$,[5,6] while except for $\{\eta^5$-$CpCo(R_2PO)_3\}^-$ remaining all ligands or combination of ligands reported so far provide exclusively low-spin hexacoordinated Co(III) complexes.[7] The ligand field strength of $\{\eta^5$-$CpCo(R_2PO)_3\}^-$ unit can be tuned by changing R and it is just about sufficient to provide the critical Δ_o needed for the spin crossover phenomenon to occur in the Co(III) complex formed by two such units. A few unusual tetra- and pentacoordinated Co(III) complexes with S = 1 spin state are reported in literature.[8] These are: (a) a pseudotetrahedral neutral imido complex with tris(3-^{t}Bu-5-Me-pyrazolyl)borate,[8a,b] (b) monoanionic square-planar complexes with a tetradentate $N(amidate)_2O(alkoxide)_2$-donor ligand[8c] and with bidentate $N(amidate)_2$-donor biuret and related ligands,[8d] and (c) presumably square-pyramidal species with halide and dianionic deprotonated N_4-donor Schiff bases derived from *o*-aminobenzaldehyde and various diamines.[8e] It may be noted that the pseudo-tetrahedral and the square-pyramidal species show the thermal spin crossover behavior. In our attempt to prepare a dinuclear Co(III) complex with the pentadentate Schiff base 2,6-bis((3-aminopropylimino)methyl)-4-methylphenol (HL), we have isolated a novel paramagnetic pentanuclear Co(III) species $[\{L(O_2CCH_3)Co_2O(OCH_3)_2\}_2Co]^{3+}$ (Chart 1), where metal centers in the $\{L(O_2CCH_3)Co_2O(OCH_3)_2\}$ fragments are diamagnetic, while the central Co(III) is paramagnetic and shows thermal spin transition phenomenon. In this chapter,

we describe synthesis, characterization, crystal structure, spectral properties, and magnetic behavior of the triperchlorate salt of this complex cation.

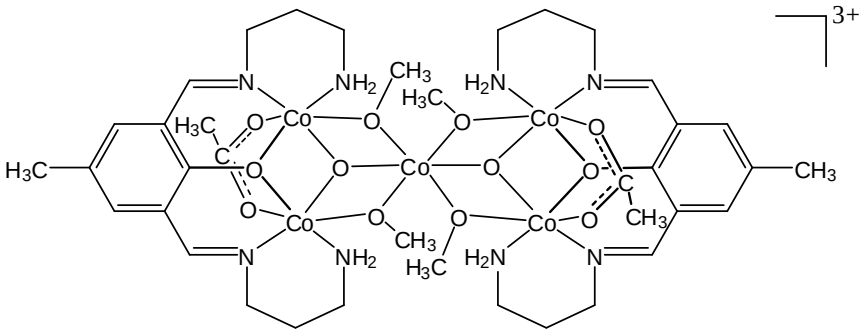

Chart 1. $[\{L(O_2CCH_3)Co_2O(OCH_3)_2\}_2Co]^{3+}$($L^-$=2,6-bis((3aminopropylimino)methyl)-4-methylphenolate)

5.3. Experimental section

5.3.1. Materials

All chemicals and solvents used in this work are of reagent grade and used as received without further purification.

5.3.2. Physical measurement

A Thermo Finnigan Flash EA1112 series elemental analyzer was used for the elemental (C, H, N) analysis measurement. The mass spectrum was collected on a Bruker Maxis HRMS (ESI-TOF analyzer) spectrometer. Solution electrical conductivity was measured with the help of a Digisun DI-909 conductivity meter.

The infrared spectrum was recorded on a Thermo Scientific Nicolet 380 FT-IR spectrometer. A Shimadzu UV-3600 UV-VIS-NIR spectrophotometer was used to collect the electronic spectrum. Variable temperature magnetic susceptibility measurements with a powdered sample of the complex at a magnetic field of 10 kG were performed on a Quantum Design MPMS XL-5 Squid magnetometer. A Jeol JES-FA200 and Bruker-ER073 spectrometers. For the liquid helium temperature EPR measurements, a temperature controller supplied from Oxford instruments (ITC 503S) was used.

5.3.3. Synthesis of $[\{L(O_2CCH_3)Co_2O(OCH_3)_2\}_2Co](ClO_4)_3$ (1)

1,3-diaminopropane (0.05 ml, 44 mg, 0.6 mmol) was added to a solution of 2,6-diformyl-4-methyl-phenol (50 mg, 0.3 mmol) in methanol (10 ml) and the mixture was refluxed for 1 h. It was cooled to room temperature and a methanol solution (10 ml) of $Co(O_2CCH_3)_2{\cdot}4H_2O$ (187 mg, 0.75 mmol) was added followed by stirring at room temperature in air for about ½ h. The initial yellow color of the mixture turned to dark brown. A methanol solution (5 ml) of $NaClO_4{\cdot}H_2O$ (85 mg, 0.6 mmol) was added to this brown solution and stirring was continued for an additional ½ h followed by refluxing for 6 h. After cooling to room temperature the brown solution was filtered and allowed to evaporate in air. A crystalline material deposited in about 2−3 days was collected by filtration and dried in air. This material was then recrystallized from a 30 ml mixture of acetonitrile-toluene (1:1). The recrystallized product was dried in air, powdered and then stored in vacuum. The yield was 175 mg (41%). The dark green powder of the complex thus obtained was used for elemental analysis, spectroscopic and magnetic

susceptibility measurements. Anal. Calcd. for $Co_5C_{38}H_{64}N_8O_{24}Cl_3$: C, 32.17; H, 4.55; N, 7.90. Found: C, 32.25; H, 4.48; N, 7.81. UV-Vis data in CH3CN (λ_{max} (nm) (10^{-4} x ε (M^{-1} cm^{-1}))): 365 (1.9), 305sh (3.4), 250sh (9.1), 213 (13.2).

5. 3.4. X-ray Crystallography

Single crystals of the complex obtained from acetonitrile-toluene (1:1) solution as $1.C_6H_5CH_3$. Determination of the unit cell parameters and the collection of the intensity data at 100 K were performed on a Bruker-Nonius SMART APEX CCD single crystal diffractometer. The data were collected using graphite monochromated Mo $K\alpha$ radiation (λ = 0.71073 Å). The SMART (version 5.630) and SAINT-Plus (version 6.45) programs[9] were used for data acquisition and data extraction, respectively. The absorption corrections were performed using the SADABS program.[10] The structure was solved by direct method and refined on F^2 by full-matrix least-squares procedures. The non-hydrogen atoms were refined using anisotropic thermal parameters. The hydrogen atoms were included in the structure factor calculation at idealized positions by using a riding model. Structure solution and refinement were performed using the SHELX-97 programs[11] available in the WinGX package.[12] The Ortex6a,[13] Platon[14] and Mercury[15] packages were used for molecular graphics. Significant crystallographic data are summarized in Table 5.1. Atomic coordinates and equivalent isotropic displacement parameters for **(1)** is provided in Table 5.2.

Table 5.1. Crystallographic data for $[\{L(O_2CCH_3)Co_2O(OCH_3)_2\}_2Co](ClO_4)_3.C_6H_5CH_3$.

Empirical formula	$Co_5C_{45}H_{72}Cl_3N_8O_{24}$
Formula weight	1510.13
Crystal system	Monoclinic
Space group	P21/n
a (Å)	17.095(2)
b (Å)	16.640(2)
c (Å)	21.531(3)
α (^{o})	90
β (^{o})	85.922(11)
γ (^{o})	99.744(2)
V (Å^3)	1086.5(3)
Z	4
ρ (g cm^{-3})	1.662
μ (mm^{-1})	1.563
Reflections collected	57220
Reflections unique	10645
Reflections [$I \geq 2\sigma(I)$]	9123
Parameters	766
$R1$, $wR2$ [$I \geq 2\sigma(I)$] [a, b, c]	0.0440, 0.1294
$R1$, $wR2$ [all data] [b, c]	0.0511, 0.1355
Goodness-of-fit on F^2	1.067
Largest peak and hole (e Å^{-3})	1.068 and –0.668

[a]$R1 = \Sigma \| F_o | - | F_c \| / \Sigma | F_o |$. [b]$wR_2 = \{\Sigma[(F_o^2 - F_c^2)^2]\}^{1/2}$. [c]GOF = $\{\Sigma[w(F_o^2 - F_c^2)^2]/(n - p)\}^{1/2}$ where 'n' is the number of reflections and 'p' is the number of parameters refined.

Table 5.2. Atomic coordinates ($x10^4$) and equivalent isotropic displacement parameters ($Å^2 \times 10^3$) for $[\{L(O_2CCH_3)Co_2O(OCH_3)_2\}_2Co](ClO_4)_3 . C_6H_5CH_3$.

Atom	x	y	z	U(eq)
Co(1)	6321(1)	1657(1)	428(1)	33(1)
Co(2)	7059(1)	2284(1)	1577(1)	36(1)
Co(3)	8998(1)	2270(1)	114(1)	39(1)
Co(4)	7988(1)	3181(1)	-772(1)	37(1)
Co(5)	7531(1)	2843(1)	427(1)	34(1)
O(1)	5999(1)	2272(1)	1100(1)	35(1)
O(2)	9049(1)	3288(1)	-305(1)	41(1)
O(3)	7353(1)	1879(1)	840(1)	35(1)
O(4)	7916(1)	2313(1)	-229(1)	35(1)
O(5)	6287(1)	702(1)	918(1)	40(1)
O(6)	6891(1)	1216(1)	1853(1)	41(1)
O(7)	9189(2)	1714(2)	-625(1)	49(1)
O(8)	8397(1)	2472(2)	-1349(1)	45(1)
O(9)	6461(1)	2626(1)	-8(1)	36(1)
O(10)	7283(1)	3286(1)	1212(1)	39(1)
O(11)	8648(1)	2791(1)	807(1)	40(1)
O(12)	7569(1)	3754(1)	-136(1)	39(1)
N(1)	6806(2)	1037(2)	-167(1)	41(1)
N(2)	5241(2)	1493(2)	12(1)	41(1)

N(3)	6689(2)	2691(2)	2325(1)	45(1)
N(4)	8155(2)	2184(2)	1965(1)	46(1)
N(5)	8808(2)	1236(2)	473(2)	49(1)
N(6)	10124(2)	2292(2)	446(2)	51(1)
N(7)	8101(2)	4107(2)	-1294(1)	43(1)
N(8)	6936(2)	2919(2)	-1202(1)	40(1)
C(1)	6398(2)	797(2)	-802(2)	53(1)
C(2)	5544(2)	580(3)	-817(2)	60(1)
C(3)	5063(2)	1294(3)	-665(2)	56(1)
C(4)	4654(2)	1543(2)	311(2)	45(1)
C(5)	4699(2)	1714(2)	977(2)	43(1)
C(6)	4027(2)	1537(2)	1236(2)	52(1)
C(7)	3991(3)	1669(3)	1863(2)	60(1)
C(8)	4651(2)	2008(3)	2229(2)	57(1)
C(9)	5336(2)	2203(2)	1991(2)	48(1)
C(10)	5365(2)	2058(2)	1354(2)	39(1)
C(11)	5979(2)	2584(2)	2414(2)	50(1)
C(12)	7221(3)	3121(3)	2825(2)	63(1)
C(13)	8006(3)	2689(3)	3013(2)	63(1)
C(14)	8512(3)	2696(3)	2503(2)	62(1)
C(15)	3242(3)	1479(4)	2118(3)	85(2)
C(16)	9326(3)	874(3)	1012(2)	71(1)
C(17)	10204(3)	955(3)	957(3)	74(1)
C(18)	10466(2)	1824(3)	1012(2)	69(1)

C(19)	10617(2)	2687(3)	180(2)	58(1)
C(20)	10430(2)	3205(2)	-370(2)	50(1)
C(21)	11053(2)	3444(3)	-675(2)	57(1)
C(22)	10950(2)	3956(2)	-1182(2)	53(1)
C(23)	10196(2)	4249(2)	-1386(2)	51(1)
C(24)	9547(2)	4018(2)	-1112(2)	47(1)
C(25)	9659(2)	3488(2)	-596(2)	44(1)
C(26)	8781(2)	4363(2)	-1375(2)	50(1)
C(27)	7409(2)	4570(2)	-1607(2)	56(1)
C(28)	6755(2)	4050(3)	-1954(2)	55(1)
C(29)	6370(2)	3539(2)	-1513(2)	51(1)
C(30)	11630(2)	4196(3)	-1515(2)	63(1)
C(31)	6586(2)	654(2)	1498(2)	41(1)
C(32)	6567(3)	-152(2)	1800(2)	65(1)
C(33)	8844(2)	1882(2)	-1179(2)	48(1)
C(34)	8986(3)	1307(3)	-1690(2)	79(1)
C(35)	5847(2)	3222(2)	-58(2)	46(1)
C(36)	6786(2)	3964(2)	1269(2)	54(1)
C(37)	9078(2)	3475(2)	1088(2)	53(1)
C(38)	7859(2)	4534(2)	49(2)	53(1)
Cl(1)	6122(1)	1345(1)	-2567(1)	87(1)
O(13)	6835(4)	1602(7)	-2263(3)	225(5)
O(14)	5615(5)	1833(5)	-2335(4)	209(4)
O(15)	6031(7)	589(4)	-2379(3)	252(5)

O(16)	6063(3)	1339(3)	-3223(2)	123(2)
Cl(2)	7901(1)	-1016(1)	232(1)	83(1)
O(17)	8206(5)	-355(4)	-51(5)	227(4)
O(18)	7204(4)	-800(6)	355(4)	235(4)
O(19)	8475(4)	-1351(5)	658(3)	185(3)
O(20)	7789(4)	-1530(4)	-298(4)	184(3)
Cl(3)	5694(1)	5320(1)	2269(1)	86(1)
O(21)	5478(4)	5294(5)	1608(2)	171(3)
O(22)	6494(3)	5482(3)	2442(3)	159(3)
O(23)	5264(3)	5926(5)	2496(3)	172(3)
O(24)	5544(6)	4558(5)	2479(4)	228(4)
C(39)	4184(5)	4358(5)	541(6)	134(3)
C(40)	4147(5)	4324(5)	-142(5)	131(3)
C(41)	3717(5)	3762(6)	-477(5)	130(3)
C(42)	3310(6)	3242(7)	-244(6)	154(4)
C(43)	3267(6)	3234(5)	383(6)	143(4)
C(44)	3727(7)	3800(6)	799(5)	151(4)
C(45)	3713(9)	3739(6)	1450(5)	240(8)

5.4. Results and discussion

5.4.1. Synthesis and characterization

In methanol, the reaction of 2,6-diformyl-4-methyl-phenol, 1,3-diaminopropane, $Co(O_2CCH_3)_2{\cdot}4H_2O$, and $NaClO_4{\cdot}H_2O$ in 2:4:5:4 mole ratio in air produces $[\{L(O_2CCH_3)Co_2O(OCH_3)_2\}_2Co](ClO_4)_3$ (**1**). The recrystallized (from 1:1 CH_3CN-$C_6H_5CH_3$) product was dried, powdered, stored in vacuum, and then used for all measurements. The elemental analysis data support the molecular formula of **1**. The molar conductivity Λ_M (380 Ω^{-1} cm^2 mol^{-1}) of the complex in acetonitrile is within the range expected for a 1:3 electrolyte.[16]

5.4.2. Spectroscopic properties

The positive ion ESI mass spectrum of **1** (Figure 5.1) shows three characteristic peaks with the expected isotropic patterns at *m/z* = 373.03, 609.03, and 1316.99 for the triply charged complex cation, one perclhorate containing doubly charged, and two perchlorate containing monopositive ion pairs, respectively.

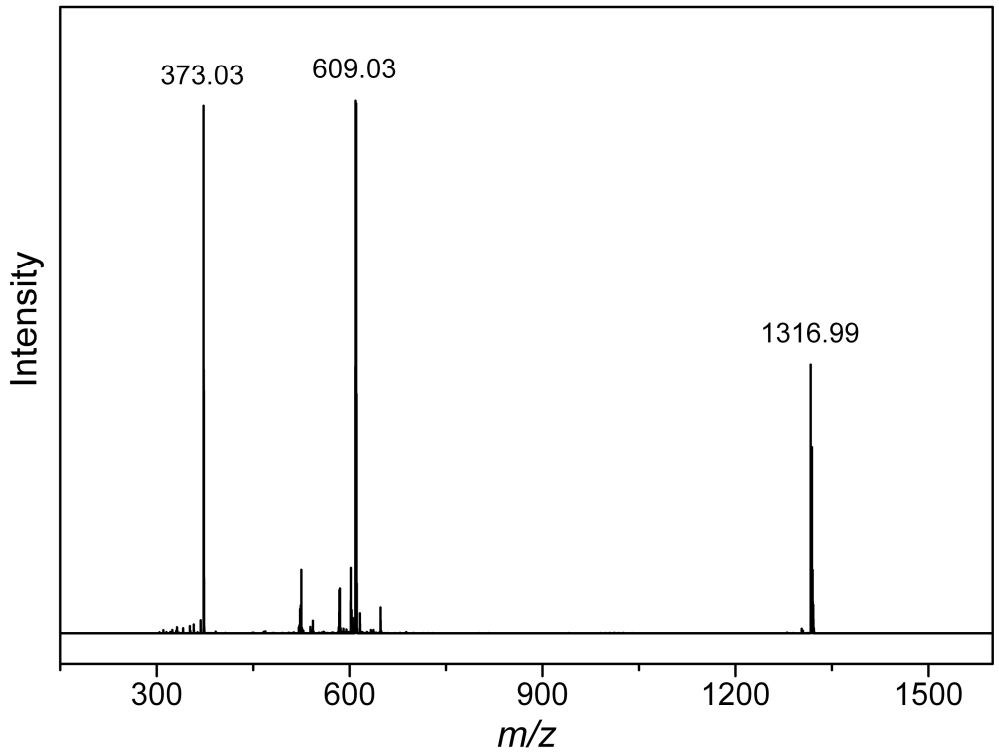

Figure 5.1. ESI mass spectrum of **1** in acetonitrile.

The infrared spectrum of **1** was collected in KBr pellet (Figure 5.2). In the higher wavenumber range, the spectrum shows two closely spaced bands at 3600 and 3540 cm^{-1} and a group of bands in the range 3260−2820 cm^{-1} due to the NH_2 and the C−H vibrations, respectively. The C=N stretching is located at 1640 cm^{-1}.[17] The strong band at 1580 cm^{-1} is attributed to the bridging acetate asymmetric stretch. The band at 1470 cm^{-1} that overlaps with the following broad and strong band centered at 1460 cm^{-1} is possibly due to the symmetric stretch of the bridging acetate. The very strong and broad band centered at 1080 cm^{-1} and

the sharp and strong band at 623 cm^{-1} are typical of the perchlorate counteranion in **1**.

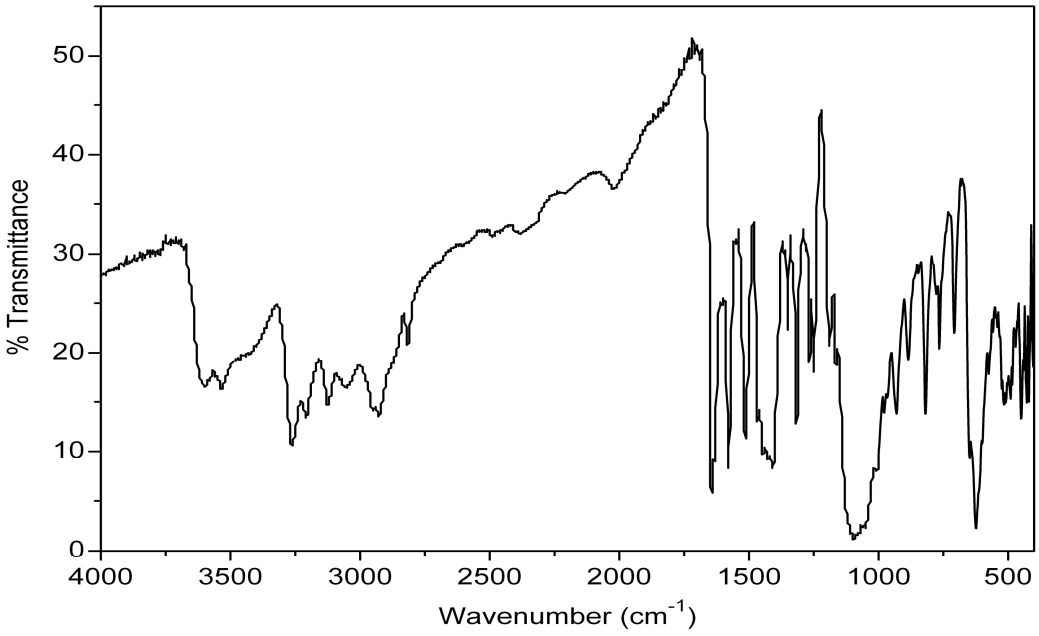

Figure 5.2. Infrared spectrum of $[\{L(O_2CCH_3)Co_2O(OCH_3)_2\}_2Co](ClO_4)_3$ (**1**) in KBr disk.

The electronic spectrum of **1** in acetonitrile displays multiple bands in the range 400−200 nm (Figure 5.3). All the absorptions are very intense. The extinction coefficients (ε) are in the order of 10^4 to 10^5 M^{-1} cm^{-1}. Thus these bands are likely to be due to primarily ligand to metal charge transfer and ligand centered transitions.[18]

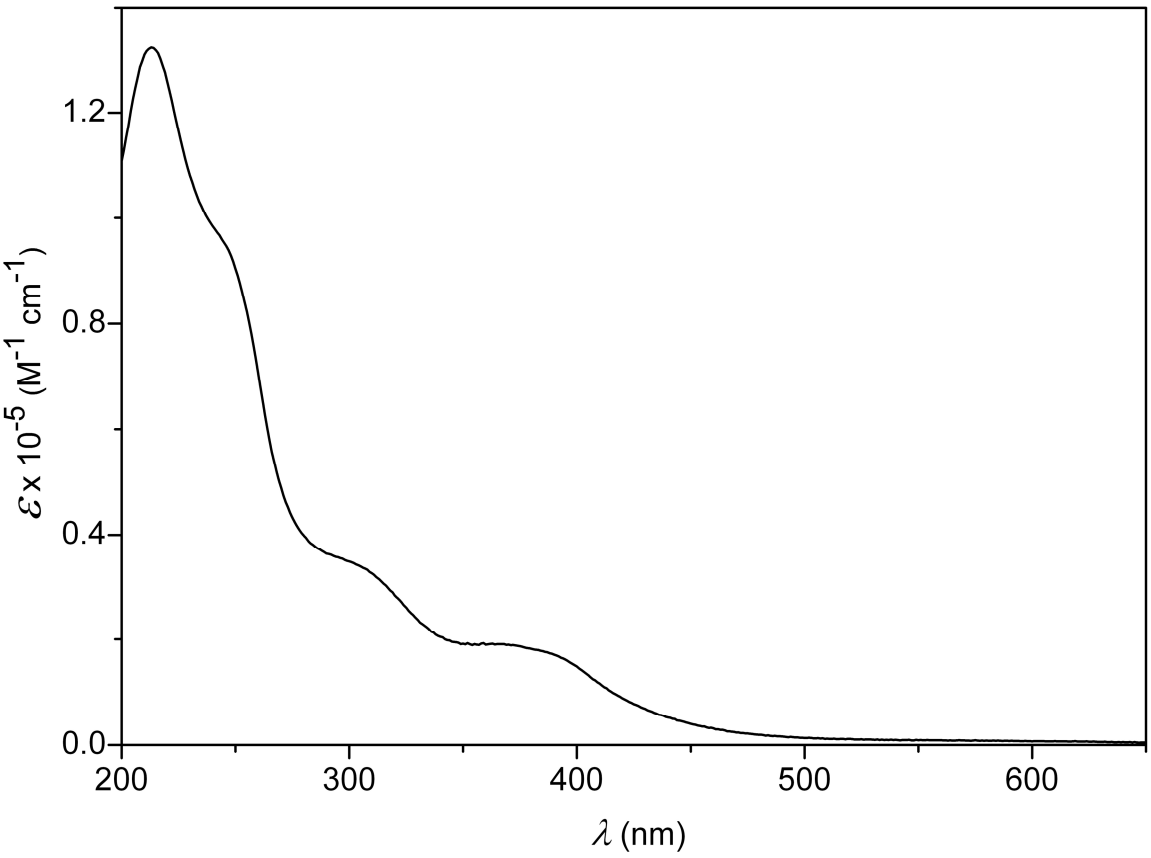

Figure 5.3. Electronic spectrum of [{$L(O_2CCH_3)Co_2O(OCH_3)_2\}_2Co](ClO_4)_3$ (**1**) acetonitrile.

5.4.3. Cryomagnetic behavior of (1) [{$L(O_2CCH_3)Co_2O(OCH_3)_2\}_2Co](ClO_4)_3$

The magnetic susceptibility measurements in the temperature range 2−300 K was performed using a powdered sample of **1**. A diamagnetic correction of

-652×10^{-6} cm^3 mol^{-1} calculated from Pascal's constants[19] was applied to obtain the molar paramagnetic susceptibilities (χ_M). The effective magnetic moment (μ_{eff}) as a function of temperature is shown in Figure 5.4. The continuous rise of the μ_{eff} vs. T curve with the increase of temperature indicates a gradual conversion of the spin state. The μ_{eff} values are 0.57 and 2.27 μ_B at 2 and 300 K, respectively. The EPR silence (Figure 5.5) of **1** in frozen solution at 77 as well as 4 K rules out the possibility of the observed magnetic moment due to low-spin Co(II). Thus the spin crossover is incomplete and the S = 2 state is at way above the room temperature. The super imposable μ_{eff} vs. T curves obtained from the data collected first by increasing the temperature from low to high and then decreasing the temperature from high to low indicate the absence of any thermal hysteresis in the temperature range 2−300 K. The gradual spin change and the lack of thermal hysteresis suggest a non-cooperative spin crossover process in **1**.[4b,20] The profile of the curve does not indicate existence of the intermediate S = 1 spin state as observed in a complex of metal-metal bonded Co_3^{7+} unit.[20] Assuming the magnetic moment of the high-spin (S = 2) species as 5.4 μ_B[4b] the equilibrium constant K (= hs/ls) at 300 K for the quintet-singlet transformation process of **1** has been calculated[21] as 0.22. Thus at room temperature the spin state composition of **1** is 18 % high-spin (S = 2) and 82 % low-spin (S = 0).

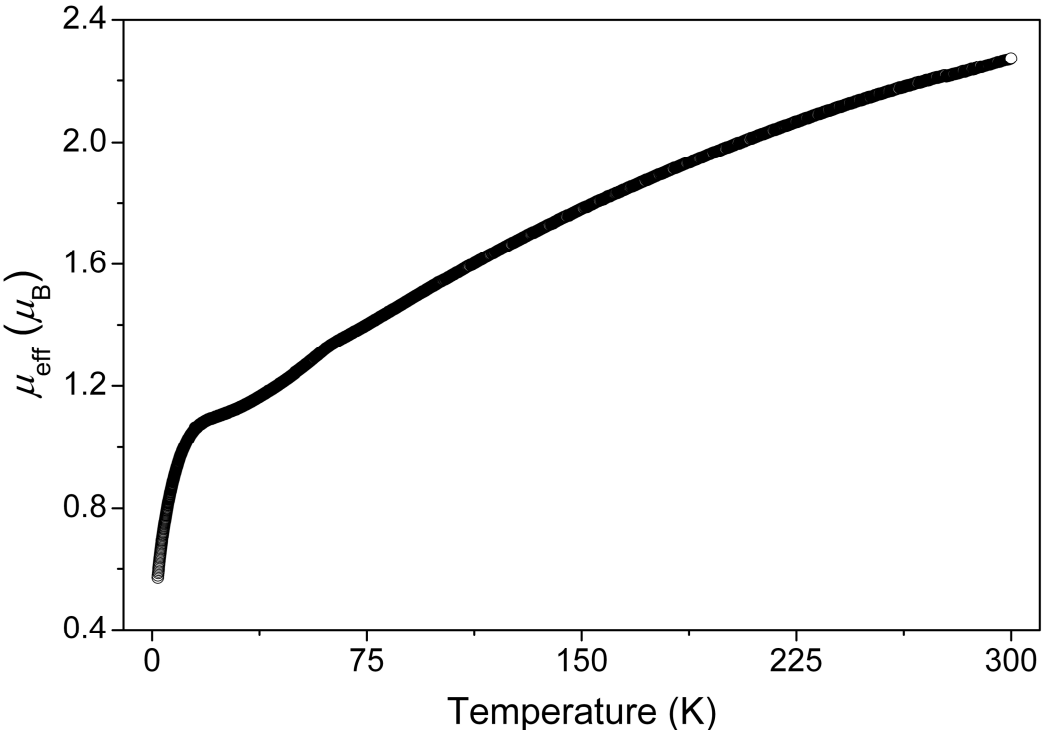

Figure 5.4. Effective magnetic moment (μ_{eff}) of **1** as a function of temperature.

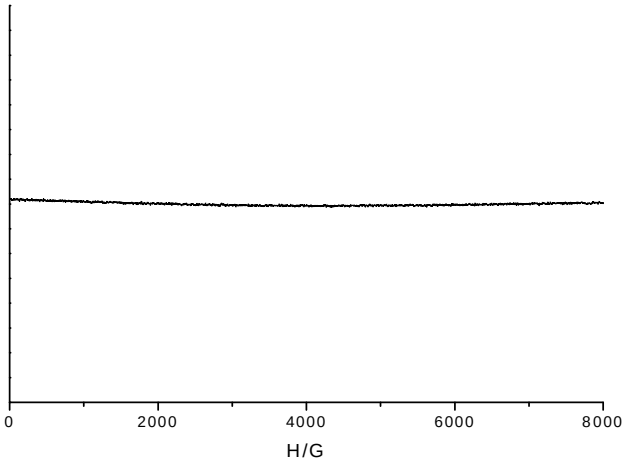

Figure 5.5. EPR spectrum of **1** in acetonitrile-toluene (1:1) solution at 77 K.

5.4.4. Powder X-ray diffraction of complex 1

The powder X-ray diffraction patterns of the sample used for all physical measurements such as CHN analysis, spectroscopy and magnetic susceptibility was compared with the powder X-ray diffraction pattern obtained by simulation of the single crystal data using Mercury 2.4 software. The experimental (A) and simulated (B) diffraction patterns are shown in Figure 5.6. The difference in the experimental and the simulated patterns indicate that the loss of lattice toluene molecule in the powder sample.

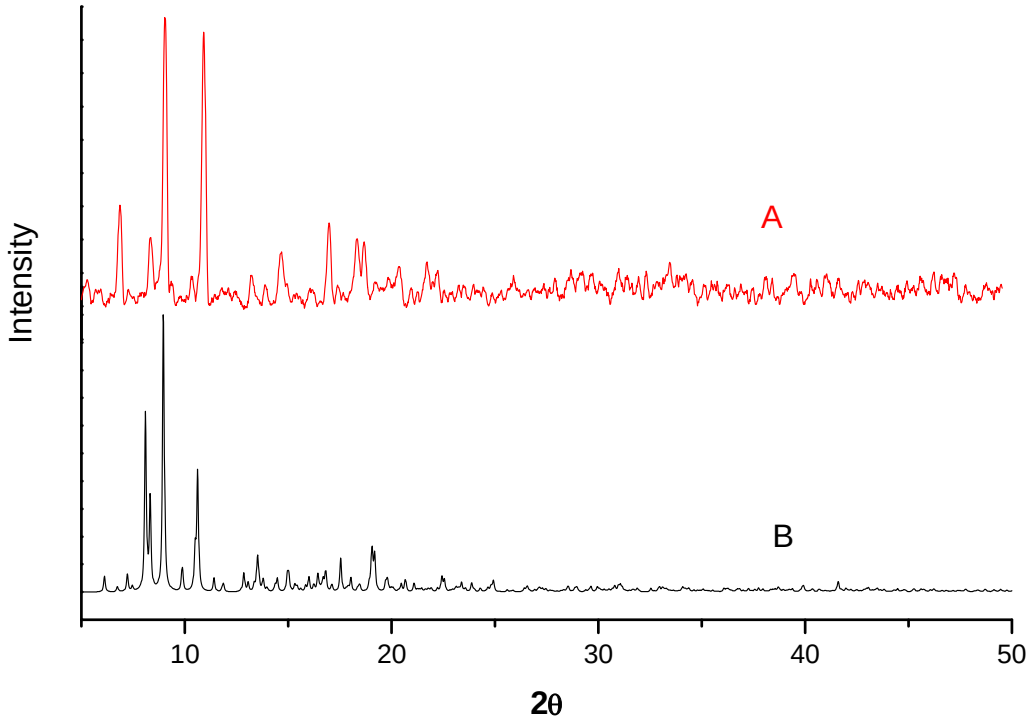

Figure 5.6. Powder X-ray diffraction patterns of **1** (curve A experimental and curve B simulated)

5.4.5. Structural description of (1) $[\{L(O_2CCH_3)Co_2O(OCH_3)_2\}_2Co](ClO_4)_3$

The molecular structure of **1** has been determined by X-ray crystallography. Single crystals of the complex were grown by slow evaporation of its acetonitrile-toluene (1:1) solution. The complex crystallizes as $\mathbf{1}\cdot C_6H_5CH_3$. The unit cell determination and the data collection were performed at 100 K. The structure of $[\{L(O_2CCH_3)Co_2O(OCH_3)_2\}_2Co]^{3+}$ is depicted in Figure 5.7 and the bond lengths involving the metal centers are listed in Table 5.3. In each dinuclear $\{L(O_2CCH_3)Co_2O(OCH_3)_2\}$ unit, the metal centers are in distorted octahedral N_2O_4 coordination spheres. The L^- coordinates to two Co(III) ions via the bridging phenolate-O, two amine-N, and two imine-N atoms and form four fused six-membered chelate rings. An acetate and an oxo group provide additional bridges between the two metal centers. The sixth coordination site of each Co(III) is satisfied by a methoxo group. The facially disposed O-atoms of the oxo and the two methoxo groups from the two $\{L(O_2CCH_3)Co_2O(OCH_3)_2\}$ units create a distorted octahedral O_6 coordination sphere around the central metal center Co(5) (Chart 1, Figure 5.7). In each terminal dinuclear unit, two edge shared N_2O_4 octahedra host the two metal centers. On the other hand, the central O_6 octahedron shares two pairs of opposite edges with the four terminal N_2O_4 octahedra. Both the $\{Co_3(\mu_3\text{-}O)\}$ fragments are pyramidal. The sums of the three Co−O−Co bond angles for $\{Co_3(\mu_3\text{-}O(3))\}$ and $\{Co_3(\mu_3\text{-}O(4))\}$ are 295.7(1) and 296.7(1)^o, respectively. The five metal centers are not coplanar. The dihedral angle between the plane formed by Co(1), Co(2), and Co(5) and the plane formed by Co(3), Co(4), and Co(5) is 72.41(2)^o. The Co···Co distances (2.7828(7) and 2.7931(6) Å) in the two dinuclear units are significantly shorter than the distances

(2.8581(7)−2.8843(7) Å) between the central Co(5) and Co(1)−Co(4). All the bond parameters in the two $\{L(O_2CCH_3)Co_2O(OCH_3)_2\}$ units are comparable. The μ_3-oxo to Co(1)−Co(5) bond lengths (1.870(2)−1.882(2) Å) are also very similar. However, Co(5) to four μ_2-methoxo O-atoms (O(9)−O(12)) bond lengths (1.942(2)−1.955(2) Å) are significantly longer than the bond lengths (1.901(2)−1.910(2) Å) involving Co(1)−Co(4) and the corresponding μ_2-methoxo group. This variation is very likely due to the disparity between the spin state of Co(5) and that of Co(1)−Co(4) (*vide infra*). Overall the metal to coordinating atom bond lengths in **1** (Table 5.3) are within the ranges reported for Co(III) complexes having the same coordinating atoms.[22]

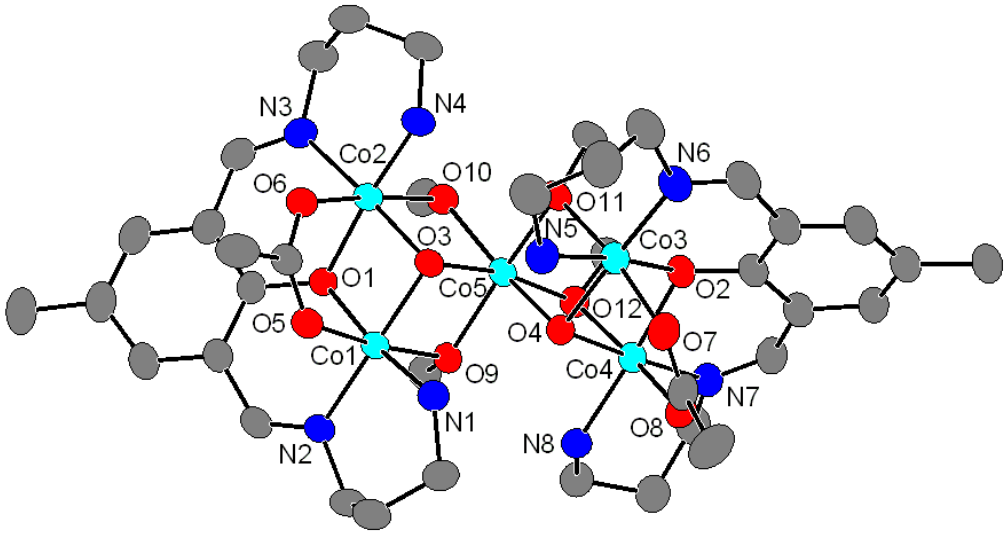

Figure 5.7. Structure of $[\{L(O_2CCH_3)Co_2O(OCH_3)_2\}_2Co]^{3+}$ (thermal ellipsoids are at 40% probability). Hydrogen atoms are omitted and carbon atoms are not labeled for clarity.

Table 5.3. Selected Bond Lengths (Å) in $[\{L(O_2CCH_3)Co_2O(OCH_3)_2\}_2Co](ClO_4)_3 \cdot C_6H_5CH_3$ (1. $C_6H_5CH_3$)

Co(1)−O(1)	1.926(2)	Co(3)−O(11)	1.907(2)
Co(1)−O(3)	1.872(2)	Co(3)−N(5)	1.936(3)
Co(1)−O(5)	1.914(2)	Co(3)−N(6)	1.937(3)
Co(1)−O(9)	1.901(2)	Co(4)−O(2)	1.929(2)
Co(1)−N(1)	1.937(3)	Co(4)−O(4)	1.876(2)
Co(1)−N(2)	1.929(3)	Co(4)−O(8)	1.927(2)
Co(2)−O(1)	1.926(2)	Co(4)−O(12)	1.906(2)
Co(2)−O(3)	1.870(2)	Co(4)−N(7)	1.936(3)
Co(2)−O(6)	1.911(2)	Co(4)−N(8)	1.929(3)
Co(2)−O(10)	1.910(2)	Co(5)−O(3)	1.882(2)
Co(2)−N(3)	1.949(3)	Co(5)−O(4)	1.876(2)
Co(2)−N(4)	1.925(3)	Co(5)−O(9)	1.942(2)
Co(3)−O(2)	1.927(2)	Co(5)−O(10)	1.955(2)
Co(3)−O(4)	1.873(2)	Co(5)−O(11)	1.948(2)
Co(3)−O(7)	1.916(3)	Co(5)−O(12)	1.950(2)

5.5. Conclusion

We have synthesized and characterized a rare high-spin Co(III) containing pentanuclear complex $[\{L(O_2CCH_3)Co_2O(OCH_3)_2\}_2Co](ClO_4)_3$ **(1)**. To the best of our knowledge, after $[CoF_6]^{3-}$, $[CoF_3(H_2O)_3]$, and $[\{\eta^5\text{-}CpCo(R_2PO)_3\}_2Co]^+$, **1** is the fourth example for paramagnetic octahedral magnetically uncoupled Co(III) species. In the first two examples, the ligand-field strengths (Δ_o) of F_6 and F_3O_3 coordination spheres are very weak and provides only high-spin Co(III), while in the third example and in **1**, the O_6 environment created by two *facial* O_3-donor units ($\{\eta^5\text{-}CpCo(R_2PO)_3\}^+$ and $\{L(O_2CCH_3)Co_2O(OCH_3)_2\}$, respectively) has the critical Δ_o needed for the central Co(III) to be in the spin crossover zone. Currently we are trying to synthesize complexes analogous to **1** in various alcohols (ROH) and examine the effect of different alkoxo groups (RO^-) of the terminal dinuclear units on the spin state of the central metal ion.

5.6. References

1. *Topics in Current Chemistry*; P. Gütlich, H. A. Goodwin, Eds.; Springer-Verlag: Berlin, **2004**, *Vols. 233–235*, Chapters on “Spin Crossover in Transition Metal Compounds I–III”.
2. (a) P. Gütlich, Y. Garcia, H. A. Goodwin, *Chem. Soc. Rev.*, **2000**, *29*, 419−427. (b) J. A. Real, A. B. Gaspar, M. Muñoz, *Dalton Trans.*, **2005**, 2062−2079. (c) A. Bousseksou, G. Molnár, J. A. Real, K. Tanaka, *Coord. Chem. Rev.*, **2007**, *251*, 1822−1833. (d) M. A. Halcrow, *Polyhedron*., **2007**, *27*, 3523−3576. (e) K. S. Murray, *Eur. J. Inorg. Chem.*, **2008**, 3101−3121. (f) J. Olguín, S. Brooker, *Coord. Chem. Rev.*, **2011**, *255*, 203−240. (g) S. Hayami, Y. Komatsu, T. Shimizu, H. Kamihata, Y. H. Lee, *Coord. Chem. Rev.*, **2011**, *255*, 1981−1990.
3. (a) C. Atmani, F. E. Hajj, S. Benmansour, M. Marchivie, S. Triki, F. Conan, V. Patinec, H. Handel, G. Dupouy, C. J. Gómez-Garcia, *Coord. Chem. Rev.*, **2010**, *254*, 1559−1569. (b) M. A. Halcrow, *Chem. Soc. Rev.*, **2011**, *40*, 4119−4142.
4. (a) W. Kläui, J. Chem. Soc., *Chem. Commun.*, **1979**, 700. (b) W. Kläui, W. Eberspach, P. Gütlich, *Inorg. Chem.*, **1987**, *26*, 3977−3982.
5. (a) J. T. Grey, Jr. *J. Am. Chem. Soc.*, **1946**, *68*, 605−608. (b) R. Hoppe, *Recl. Trav. Chim. Pays-Bas* **1956**, *75*, 569−575.
6. H. C. Clark, B. Cox, A. G. Sharpe, *J. Chem. Soc.*, **1957**, 4132−4133.
7. (a) C. E. Housecroft, *Coord. Chem. Rev.*, **1990**, *98*, 123-250. (b) M. B. Davies, *Coord. Chem. Rev.*, **1993**, *124*, 107-181. (c) M. B. Davies, *Coord. Chem. Rev.*, **1996**, *152*, 1−85. (d) M. B. Davies, *Coord. Chem. Rev.*, **1998**,

169, 237−361. (e) F. A. Cotton, G. Wilkinson, C. A. Murillo, M. Bochmann, *Advanced Inorganic Chemistry*; 6th edn, Wiley: Singapore, 2004, p 824.

8. (a) D. T. Shay, G. P. A.Yap, L. N. Zakharov, A. L. Rheingold, K. H. Theopold, *Angew. Chem. Int. Ed.*, **2005**, *44*, 1508–1510. (b) Corrigendum: D. T. Shay, G. P. A.Yap, L. N. Zakharov, A. L. Rheingold, K. H. Theopold, *Angew. Chem. Int. Ed.*, **2006**, *45*, 7870. (c) T. J. Collins, T. G. Richmond, B. D. Santarsiero, B. G. R. T. Treco, *J. Am. Chem. Soc.*, **1986**, *108*, 2088−2090. (d) P. J. M. W. L. Birker, J. J. Bour, J. J. Steggerda, *Inorg. Chem.*, **1973**, *12*, 1254−1259. (e) M. Gerloch, *J. Chem. Soc., Chem. Commun.*, **1971**, 1149−1150.
9. Bruker-Nonius Analytical X-ray Systems Inc., Madison, WI, USA, **2003.**
10. G. M. Sheldrick, *SADABS: Program for Area Detector Absorption Correction*; University of Göttingen: Germany, **1997.**
11. G. M. Sheldrick, *SHELX97: Structure Determination Software*; University of Göttingen: Germany, **1997.**
12. L. J. Farrugia, *J. Appl. Crystallogr.*, **1999**, *32*, 837−838.
13. P. McArdle, *J. Appl. Crystallogr.*, **1995**, *28*, 65.
14. A. L. Spek, *PLATON:* A Multipurpose Crystallographic Tool, Utrecht University: The Netherlands, **2002.**
15. C. F. Macrae, I. J. Bruno, J. A. Chisholm, P. R. Edgington, P. McCabe, E. Pidcock, L. Rodriguez-Monge, R. Taylor, J. van de Streek, P. A. Wood, **J. Appl. Cryst., 2008**, *41*, 466−470.
16. Geary, W. J. *Coord. Chem. Rev.*, **1971**, *7*, 81−122.

17. (a) F. Hueso-Ureña, N. A. Illán-Cabeza, M. N. Moreno-Carretero, J. M. Martínez-Martos, M. J. Ramírez-Expósito, *J. Inorg. Biochem.,* **2003**, *94*, 326−334. (b) Z. –L. Wang, Q. –H. Luo, C. –Y. Duan, C. –Y. Shen, Y. –Z. Li, *Dalton Trans.,* **2004**, 1104−1111.

18 (a) R. J. de Oliveira, P. Brown, G. B. Correia, S. E. Rogers, R. Heenan, I. Grillo, A. Galembeck, J. Eastoe, *Langmuir.,* **2011**, *27*, 9277−9284. (b) J. Chakraborty, R. K. B. Singh, B. Samanta, C. R. Choudhury, S. K. Dey, P. Talukder, M. J. Borah, S. *Z.* Mitra, *Naturfor.,* **2006**, *61b*, 1209−1216.

19. G. A. Bain, J. F. Berry, *J. Chem. Edu.,* **2008**, *85*, 532−536.

20. R. Clérac, F. A. Cotton, K. R. Dunbar, T. Lu, C. A. Murillo, X. Wang, *J. Am. Chem. Soc.,* **2000**, *122*, 2272−2278.

21. T. Iizuka, M. Kotani, *Biochim. Biophys. Acta.,* **1969**, *181*, 275−286.

22. (a) J. K. Beattie, J. A. Klepetko, A. F. Masters, P. Turner, *Polyhedron.,* **2003**, *22*, 947−965. (b) Y. Wang, J. Yu, Q. Pan, Y. Du, Y. Zou, R. Xu, *Inorg. Chem.,* **2004**, *43*, 559−565. (c) A. M. Goforth, R. E. Hipp, M. D. Smith, L. Jr. Peterson, H. –C. zur Loye, *Acta Cryst. Sect. E.,* **2005**, *61*, m1531−m1533. (d) J. Luo, N. P. Rath, L. M. Mirica, *Inorg. Chem.,* **2011**, *50*, 6152−6157. (e) S. Paul, W. Wing-Tak, D. Ray, *Inorg. Chim. Acta.,* **2011**, *372*, 160−167. (f) M. Salehi, R. Kia, A. Khaleghian, *J. Coord. Chem.,* **2012**, *65*, 3007−3018.

List of Publications

Thesis work

1. Copper(II) complexes with 2-[(2-pyridin-2-yl-ethylimino)-methyl]-phenol and its substituted derivatives: Syntheses, physical properties and structures.
   S. Maloth and S. Pal
   Polyhedron., **2010**, *29*, 3257.

2. A tetracopper(II) complex with N,N'-bis(picolinoyl)hydrazine.
   S. Maloth and S. Pal
   Inorg. Chemica. Acta., **2011**, *372*, 407.

3. A Pentacobalt(III) Complex with a paramagnetic Octahedral Metal Center Exhibiting Thermal Spin Transition.
   S. Maloth and S. Pal
   Inorg. Chem., under revision

4. Dicopper(II) complexes with 2-hydroxy-5-methylbenzene-1,3 dicarbaldehyde bis(benzoylhydrazone)
   S. Maloth and S. Pal
   (To be submitted)

Other work:

5. Nickel(II) Coordination Polymers-4-Bipyridine-Connected Six- and Four-Fold Metal-Succinate Helices and Their Corresponding Chiral and Achiral Networks.
   S. Das, **S. Maloth** and S. Pal
   Eur. J. Inorg Chem., **2011**, *27*, 4270.

6. Dioxomolybdenum(VI) complexes with 2-((2-(pyridin-2-yl)hydrazono)methyl)phenol and its derivatives.
   S. K. Kurapati, U. Ugandar, **S. Maloth** and S. Pal
   Polyhedron, **2012**, *42*, 161.

7. Pentacobalt(III) complexes with 2-hydroxy-5-methylbenzene-1,3 dicarbaldehyde bis(benzoylhydrazone) and its substituted derivatives: Syntheses, physical properties and structures.
   S. Maloth and S. Pal
   (Manuscript under preparation)

8. Crystal structures and magnetic properties of Dinuclear Manganese(II) and Cobalt(II) complexes with 2-hydroxy-5-methylbenzene-1,3 dicarbaldehyde bis(benzoylhydrazone).
   S. Maloth and S. Pal
   (Manuscript under prepareation)

Posters and Presentations

1. Di- and Tetranuclear Cu(II) and Ni(II) Complexes: Syntheses, Structures and Properties

   Poster Presentation

   Modern Trends in Inorganic Chemistry, 2009 (MTIC-XIII, 2009), IISc-Bangalore.

2. Dicopper(II) and Dinickel(II) complexes: Synthesis, structure and properties.

   Poster Presentation

   Chemfest-2010, University of Hyderabad, Hyderabad.

3. Chiral and Achiral Networks Formed by 4,4′-Bipyridine Connected Six- and Four-fold Nickel(II)-succinate Helices.

   Poster Presentation

   3rd Asian Conference on Coordination Chemistry, 2011 (ACCC-3), 2011), Indian Habitat Center, New Delhi.

4. Chiral and Achiral Networks Formed by 4,4′-Bipyridine Connected Six- and Four-fold Nickel(II)-succinate Helices.

   Oral and Poster Presentation.

   Chemfest-2012, University of Hyderabad, Hyderabad.